Visualizing Light Cones in Space-Time

Elmabrouk, Tarig

Award date:
2013

Awarding institution:
Coventry University

Visualizing Light Cones in Space-Time

By

T Elmabrouk

September 2013

Visualizing Light Cones in Space-Time

Tarig Elmabrouk

Applied Mathematics Research Centre

September 2013

A thesis submitted in partial fulfillment of the requirement of the degree of Doctor of Philosophy at Coventry University.

Acknowledgements

Foremost, I would like to express my sincere gratitude to my advisor Dr Robert Low for the continuous support of my study and research, for his patience, motivation, enthusiasm, and immense knowledge. His guidance helped me in all the time of research and writing of this thesis. I could not have imagined having a better advisor and mentor for my Ph.D. study.

I express my gratitude to my parents and my wife, for their continued support and encouragement.

DECLARATION

I hereby declare that this Ph.D. thesis entitled 'Visualizing Light Cones in Space-Time' has been compiled by me under the supervision of Dr. Robert Low , Department of Mathematics and Control Engineering Coventry University. This thesis has not been submitted anywhere for any award .

Abstract

Although introductory courses in special relativity give an introduction to the causal structure of Minkowski space, it is common for causal structure in general space-times to be regarded as an advanced topic, and omitted from introductory courses in general relativity, although the related topic of gravitational lensing is often included.

Here a numerical approach to visualizing the light cones in exterior Schwarzschild space taking advantage of the symmetries of Schwarzschild space and the conformal invariance of null geodesics is formulated, and used to make some of these ideas more accessible.

By means of the Matlab software developed, a user is able to produce figures showing how light cones develop in Schwarzschild space, starting from an arbitrary point and developing for any length of time. The user can then interact with the figure, changing their point of view, or zooming in or out, to investigate them.

This approach is then generalised, using the symbolic manipulation facility of Matlab, to allow the user to specify a metric as well as an initial point and time of development. Finally, the software is demonstrated with a selection of metrics.

Contents

Chapter 1

Introduction

In this thesis we will develop an approach to visualizing light cones in space-time by using Matlab to integrate the geodesic equations and produce three dimensional plots which can be manipulated, and demonstrate the approach by considering some particular space-times of interest. The aim of this project has been to develop the code, which will be made generally available for students of general relativity to use to improve their understanding of null geodesics and light cones, and instructors to use as an education aid in teaching such students, and to carry out some sample investigations using it.

In very brief outline, the thesis consists of a review of the relevant aspects of differential geometry, followed by descriptions and sample applications of Matlab code both in the special case of Schwarzschild space-time and in more general space-times, and concludes with some suggestions for further work in this area.

In more detail, we have:

Chapter 2: Geometric Background

In the second chapter we will provide a brief review of the areas of differential geometry relevant to this project. We will first consider the basic structure of manifolds, vectors and vector fields, and associated structures. Next, we re-

view the general case of semi-Riemannian manifolds, and the Levi-Civita connection , quickly specialising to Lorentz manifolds. We pay particular attention to geodesics and more specifically to null geodesics, and the sense in which they are conformally invariant, before recalling the notion of a Jacobi field. Finally we review the notion of causal structure, and the relationships between the null geodesics and causal structure.

Chapter 3: Static Space-Times

In this chapter we review the notions of stationary and static space-time. We will use the conformal invariance of null geodesics to motivate a conformal transformation which takes a general static space-time to a useful special form, which we will use to provide a basis for the numerical approach to visualizing light cones.

Chapter 4: Light Cones and Causal Structure for Schwarzschild Space-Time

Next we will describe a Matlab code which solves the null geodesic equations for Schwarschild space-time numerically, and enable a visualization of the light cones in Schwarzschild space, which helps us to understand the causal structure of Schwarzchild space-time. This code allows the user to specify the initial point of the light cone, the time for which it develops, and the number of null geodesics used to construct the light cone, or subset of the light cone.

We will show how this code can be used to investigate both the full light cones of points, and the structure of interesting subsets of the light cones, including individual null geodesics. The visualisation of the light cones will be carried out with one dimension suppressed, so that we can consider the full space-time development of the light cones. Finally, we describe a companion Matlab code which can be used to give an animated view of the development of the wave front in three spatial dimensions. Most of the material in this chapter can be

adapted with very little effort to work in Octave, a free program which is very similar in functionality to Matlab.

Chapter 5 : Matlab for General Metrics

In this chapter we will see how to use the symbolic manipulation facility in Matlab to extend the previous work to allow the user to investigate a (2+1) dimensional static metric of his or her choice rather than working with a predetermined metric. This can be done in either polar or Cartesian background coordinates. We also check that the code gives the expected results in the cases of Minkowski space-time and Schwarzschild space-time.

The code here consists of two parts, a program which the user provides the metric to, and which computes the required connection coefficients and writes a Matlab function which the second program uses to integrate the null geodesic equations. As in the Schwarzchild space-time case, the user can then specify the various parameters for the light cone, or part of the light cone, to be considered.

We believe that it should be possible to convert this code to Octave also, but the syntax of symbolic manipulation is rather different in Octave, and we expect that it would require a considerable amount of effort.

Chapter 6: Applications

In this chapter we demonstrate the use of the Matlab code described in the previous chapter to investigate the development of the light cones in some particular metrics.

In turn, we will look at: a simple metric which has a region of positive curvature near the origin, which acts as a gravitational lens; then we will consider the Reissner-Nordstrom metric, for various values of the charge; a space-time considered by Ayon-Beato and Garcia [32] which gives a different description

of a charged black hole in which space-time is not coupled to standard electromagnetic theory, but one which results in a non-singular space-time; and a non-spherically symmetric gravitational lens is our last example.

Chapter 7: Conclusions and Further Work

We provide a brief summary of what has been done, and the strengths and weaknesses of this approach, and suggest various ways in which this work might be continued or extended.

Chapter 2

Geometric Background

In this chapter we will provide a brief review of the areas of differential geometry relevant to this project. This will mostly consist of establishing definitions, notation and terminology, leaving proofs to the literature. In turn, we will consider semi-Riemannian manifolds, quickly specialising to Lorentz manifolds, and then to geodesics, causal structure, and the relationships between the null geodesics and causal structure.

2.1 Semi-Riemannian Manifolds

In special relativity we model space-time as $\mathbb{R}^4$, with coordinates (t, x, y, z), where t is a time coordinate and (x, y, z) are three space coordinates. If U and V are the vectors connecting two pairs of points in $\mathbb{R}^4$, then U has components (U^t, U^x, U^y, U^z) given by the differences in the t, x, y, and z components respectively, and similarly for V. We then define the inner product $\langle U, V \rangle$ by

$$\langle U, V \rangle = -U^t V^t + U^x V^x + U^y V^y + U^z V^z \tag{2.1}$$

We call $\mathbb{R}^4$ equipped with this structure Minkowski space, and denote it by $\mathbb{M}$: in this context, it is standard to refer to points as events in space-time [1].

This mathematical object works well for considering situations in which gravitation is negligible. However, we wish also to consider situations in which gravitational effects are significant, so we need an appropriate generalisation of $\mathbb{M}$. We need our generalization to look similar to $\mathbb{M}$ over sufficiently small regions of space-time, but it must be allowed to differ significantly over large regions, and in a way which can be used to describe gravitational phenomena. The appropriate object in this case is a Lorentz manifold. Lorentz manifolds are a special case of semi-Riemannian manifolds, and so we now give a brief review of semi-Riemannian geometry before specialising to the case of Lorentz geometry[2].

Recall that a manifold is a separable Hausdorff space in which some neighbourhood of each point admits a local Cartesian coordinate system. That is, for each point x, there is an open subset of the manifold containing x, say U, such that there is a homomorphism $f : U \to R^n$ from U to an open subset of R^n(d-dimensional Euclidean space). n is called the dimension of the manifold. The mapping f is called a local chart at x. The collection of all charts at all points of the manifold is called an atlas. The separability condition ensures that the atlas will need at most a countably infinite number of charts[3][4].

We obtain a smooth manifold by requiring then that whenever f, g are local charts, the mapping $g \circ f^{-1}$ is a diffeomorphism. This provides the additional structure required for calculus, and enables us to define tangent vectors, and so the various other geometric objects of interest. In particular, functions from one smooth manifold to another are smooth if their coordinate descriptions are smooth. In the remainder, we will usually denote coordinate mappings by $x^a, a = 1 \ldots n$.

Let x be a point in an n-dimensional manifold M: we want to attach at x a copy of

$\mathbb{R}^n$ which we can think of as tangent to at x to M . The resulting structure is called the tangent space of M at x and is denoted T_xM, and the union of all these is the tangent bundle of M, denoted TM.

We can define T_xM in the following way. If γ is a smooth curve passing through x, parameterized by t, and such that $x = \gamma(0)$, then can consider a particular coordinate patch centred on x, and think of the tangent vector to γ at x as given by $(f \circ \gamma)'(t)$, where f is the local coordinate mapping. The usual transformation law for relating this vector to the one given by a different choice of coordinate mapping then follows from the chain rule for differentiation.

However, it is cleaner to define the differential operator γ' by

$$\gamma'(f) = \frac{d}{dt}(f \circ \gamma) \tag{2.2}$$

where f is now any smooth function from M to $\mathbb{R}$. In terms of local coordinates, the curve γ is given by $\gamma^a(t)$, and

$$\gamma'^a(t)\frac{\partial}{\partial x^a}f = \frac{d}{dt}(f \circ \gamma) \tag{2.3}$$

and we take the collection of all such differential operators as the T_xM. Then the tangent space at each $x \in M$ is $\mathbb{R}^n$, where n is the dimension of M, and if U is a sufficiently small neighbourhood of x, the union of the tangent spaces to the points of U naturally has the product structure $U \times \mathbb{R}^n$. We have the natural projection $\pi : TM \to M$ which maps $(x, v) \to x$.

A detailed exposition of this material can be found in standard introductory texts on differential topology [5].

A vector field on M is a smooth function $V : M \to TM$ such that $\pi \circ V$ is the identity on M. In terms of coordinates, V is an assignment of a vector in T_xM to each

point $x \in M$, such that the components of the vector are smooth functions of the coordinates in some, and hence any coordinate system.

If $f : M \longrightarrow N$, then we define $df : TM \longrightarrow TN$ by

$$df(\gamma') = (f \circ \gamma)' \tag{2.4}$$

where γ is an arbitrary smooth curve in M.

Then given vector fields X, Y , the Lie bracket $[X, Y]$, is defined by

$$[X, Y](f) = X(Y(f)) - Y(X(f)). \tag{2.5}$$

We also define the tensor bundle $T^r_s M$ by

$$(T^r_s M)_x = (T_x M)^r \otimes (T^*_x M)^s \tag{2.6}$$

where $T^*_x M$ is the dual of $T_x M$ A tensor field in $T^r_s M$ is also called a type (r, s) tensor.

In a coordinate patch u with coordinate x^a where $a = 1 \dots n$, we use $\{\frac{\partial}{\partial x^a}\}$ as a natural basis for $T_x M$, and express tangent vectors and tensors in terms of their components in this basis. All the classical machinery of defining tensors as collections of numbers which transform according to a certain rule then follows as a consequence of the chain rule [6].

Now, let M be a real n-dimensional smooth manifold with a type $(0, 2)$ non-degenerate symmetric tensor field g, i.e. a tensor such that if U and V are smooth vector fields, then

$$g(U, V) = g(V, U) \tag{2.7}$$

and if

$$g(U, V) = 0 \tag{2.8}$$

for all V, then it follows that $U = 0$. Thus g assigns smoothly, to each point x of M, a non-degenerate symmetric bilinear form g_x on the tangent space T_xM.

Since g_x is non-degenerate on T_xM it is of constant index at all points $x \in M$ so that T_xM becomes an n-dimensional semi-Euclidean space. Then (M, g) is called a semi-Riemannian manifold with a semi-Riemannian metric g [7].

2.2 The Connection

A connection, ∇, on a manifold, M, is an assignment to each smooth vector field X of a differential operator ∇_X such that for any smooth vector fields Y, Z smooth functions f, g and constants α, β, we have [8]

$$\begin{aligned} \nabla_{fX+gY}Z &= f\nabla_X Z + g\nabla_Y Z \\ \nabla_X(\alpha Y + \beta Z) &= \alpha\nabla_X Y + \beta\nabla_X Z \\ \nabla_X(fY) &= X(f)Y + f\nabla_X Y \end{aligned} \tag{2.9}$$

If the connection is torsion free

$$\nabla_X\nabla_Y - \nabla_Y\nabla_X = [X, Y] \tag{2.10}$$

and metric- preserving

$$\nabla_X(g(Y, Z)) = g(\nabla_X Y, Z) + g(Y, \nabla_X Z) \tag{2.11}$$

(or, equivalently $\nabla_X(g) = 0$) then it is called the Levi-Civita connection associated with the metric g.

These condition allows us to express the connection in terms local coordinates,

using the Christoffel symbols,

$$\Gamma^a_{bc} = \frac{1}{2} g^{ad} \left(\frac{\partial}{\partial x^b} g_{dc} + \frac{\partial}{\partial x^c} g_{db} - \frac{\partial}{\partial x^d} g_{bc} \right) \tag{2.12}$$

so that

$$(\nabla_X Y)^b = X^a \nabla_a Y^b = X^a (\frac{\partial Y^b}{\partial x^a} + \Gamma^b_{ac} Y^c). \tag{2.13}$$

We say that a vector field X is parallel transported allong a curve γ when

$$\nabla_{\gamma'} X = 0 \tag{2.14}$$

and that γ is a geodesic if it is auto-parallel, i.e that

$$\nabla_{\gamma'} \gamma' = 0. \tag{2.15}$$

We will consider geodesics in more details in the next part of this chapter.

Finally, the Riemann (curvature) tensor is R, defined by [9]

$$R(X, Y)Z = \nabla_X \nabla_Y Z - \nabla_Y \nabla_X Z - \nabla_{[X,Y]} Z. \tag{2.16}$$

2.3 Lorentz Manifolds

We now give the required generalisation from Minkowski space to Lorentzian manifolds by requiring that the tangent space to a semi-Riemannian manifold has the same type of metric or signature of metric at each point as Minkowski space; at each point, p, we can chose coordinates so that T_pM is the same inner product space as $\mathbb{M}$.

A Lorentz metric is therefore a semi-Riemann metric with the property that the manifold locally looks like $\mathbb{M}$.

Recall that in Minkowski space, we say that the vector u is timelike if $\langle u, u\rangle < 0$ null if $\langle u, u\rangle = 0$, and spacelike if $\langle u, u\rangle > 0$ [10]. We then say that a curve in $\mathbb{M}$ is timelike if its tangent vector at each point is timelike, etc.

This generalizes immediately to curve on a Lorentz manifold. Just as in $\mathbb{M}$, a curve is timelike if its tangent vector at each point is timelike, etc. A timelike curve represents the possible history of a massive particle, and is called a worldline [11].

One particularly important example of a Lorentz manifold is that of the Schwarzschild metric, for region $r > 2m$, which describes space-time outside a spherically symmetric mass distribution, and which we will investigate in some detail later.

We have the Schwarzschild metric [12].

$$ds^2 = -\left(1 - \frac{2m}{r}\right) dt^2 + \frac{1}{\left(1 - \frac{2m}{r}\right)} dr^2 + r^2(d\theta^2 + \sin^2\theta d\phi^2). \tag{2.17}$$

This describes space-time outside a static, spherically symmetric distribution of mass, whose boundary is at some $r > 2m$; it also represents the space-time outside a black hole whose event horizon is at $r = 2m$.

We easily see that the vectors $\frac{\partial}{\partial r}, \frac{\partial}{\partial \theta}, \frac{\partial}{\partial \phi}$ are spacelike and $(\frac{\partial}{\partial t})$ is timelike, so for example any curve of the form $(t, r_0, \theta_0, \phi_0)$, which represents the worldline of an observer at rest relative to the black hole, is a timelike curve.

The causal structure of this space-time (which will be considered in more detail in Chapter 5) is determined by knowing which points can be connected by a timelike curve. Although it is easy to see that the worldline of a stationary observer is timelike, there are many other worldlines which have to be taken into account. Even in the case of Schwarzschild space-time this is difficult [13].

We will investigate the causal structure of space-time with this metric in chapter 3.

2.4 Geodesics

We now consider geodesics in more detail.

2.4.1 Definitions

Recall that we previously defined a geodesic as a curve whose tangent vector is parallel transported. In this case, the parameter is said to be an affine parameter [2] [14].

If we reparametrize a geodesic curve by arbitrary parameter t and set $\dot{x}^a = \frac{dx^a}{dt}$, then we have

$$\dot{x}^b \nabla_b \dot{x}^a = f(t) x^a \tag{2.18}$$

for some function f. In general, the right hand side of this equation does not equal zero. It only zero in the special case where t is an affine parameter, when we equivalently have

$$\ddot{x}^a + \Gamma^a_{bc} \dot{x}^b \dot{x}^c = 0 \tag{2.19}$$

If t is an affine parameter then so is $at + b$, where a, b are constant (i.e. they do not depend on position along the curve) and $a \neq 0$, and we note that affine parameters are related to one another by affine relationships [4].

We can express these ideas in index-free notation as follows.

Any curve γ that satisfies

$$\nabla_T T = f(t) T \tag{2.20}$$

where the tangent vector $T = \dot{\gamma}$ for arbitrary function f can be reparametrized to give a new tangent vector which satisfies

$$\nabla_T T = 0. \tag{2.21}$$

A useful and imortant property of geodesics is that their causal character is con-

stant.

Suppose γ is a geodesic so $\nabla_T T = 0$, where $T = \gamma'$. We need to prove that we have

$$\langle T, T \rangle = g_{ab} T^a T^b \tag{2.22}$$

constant along γ. Now,

$$\begin{aligned} \nabla_T \langle T, T \rangle &= \langle \nabla_T T, T \rangle + \langle T, \nabla_T T \rangle \\ &= \langle 0, T \rangle + \langle T, 0 \rangle \\ &= 0 \end{aligned} \tag{2.23}$$

This quantity never changes, so if we with begin the tangent vector timelike it must remain timelike; and similarly with null and spacelike tangent vectors. That is why can classify the geodesic as null or spacelike or timelike.

To summarize, geodesics on a Lorentzian manifold [10] have three classes according to the sign of the norm of their tangent vector. With a metric signature of $(-,+,+,+)$, timelike geodesics have a tangent vector whose norm is negative; null geodesics have a tangent vector whose norm is zero; and spacelike geodesics have a tangent vector whose norm is positive. (Note that we slightly abuse notation by referring to $g(U,U) =< U, U >$ as the norm of U.)

Let $\gamma(t) = x^a(t)$ be the trajectory in space-time of a particle. Then the acceleration of the particle is

$$\bigtriangledown_{\gamma'} \gamma' = \ddot{x}^a + \tilde{\Gamma}^a_{bc} \dot{x}^b \dot{x}^c, \tag{2.24}$$

and we have the geodesic equation for a freely falling particle

$$\ddot{x}^a + \tilde{\Gamma}^a_{bc} \dot{x}^b \dot{x}^c = 0 \tag{2.25}$$

when acceleration equals zero the particle is freely falling. Hence the geodesics are trajectories of particle with no forces acting on them.

2.4.2 Characterizations of Geodesics

There are several different ways of characterizing geodesics, each of which has its advantages and disadvantages when compared with the others.

First, the geodesic equations are also the Euler-Lagrange equations for an energy function.

We define

$$E(\gamma) = \frac{1}{2}\int g_\gamma(\gamma', \gamma')dt \tag{2.26}$$

or

$$E = \frac{1}{2}\int g_{ab}\dot{x}^a\dot{x}^b dt \tag{2.27}$$

Then the Euler-Lagrange equations

$$\frac{d}{dt}\left(\frac{\partial E}{\partial \dot{x}^c}\right) = \frac{\partial E}{\partial x^c} \tag{2.28}$$

are the equations of a geodesic.

Starting with

$$\frac{\partial E}{\partial x^c} = \frac{\partial}{\partial x^c}(g_{ab}\dot{x}^a\dot{x}^b) = \partial_c g_{ab}\dot{x}^a\dot{x}^b \tag{2.29}$$

we get

$$\frac{\partial E}{\partial \dot{x}^c} = g_{ab}\delta^a_c\dot{x}^b + g_{ab}\delta^b_c\dot{x}^a = 2g_{ac}\dot{x}^a \tag{2.30}$$

By the chain rule we have

$$\frac{d}{dt} = \frac{dx^c}{dt}\frac{\partial}{\partial x^c} = \dot{x}^c\partial_c \tag{2.31}$$

So

$$\frac{d}{dt}(\frac{\partial E}{\partial \dot{x}^c}) = \frac{d}{dt}(2g_{ac}\dot{x}^a) \tag{2.32}$$

Then

$$\begin{aligned}\frac{d}{dt}(\frac{\partial E}{\partial \dot{x}^c}) &= \frac{d}{dt}(2g_{ac}\dot{x}^a) \\ &= 2g_{ac}\ddot{x}^a + 2\partial_b g_{ac}\dot{x}^a\dot{x}^b\end{aligned} \tag{2.33}$$

But

$$2\partial_b g_{ac}\dot{x}^a\dot{x}^b = \partial_a g_{cb}\dot{x}^a\dot{x}^b + \partial_b g_{ac}\dot{x}^a\dot{x}^b \tag{2.34}$$

So we have

$$2g_{ac}\ddot{x}^a + (\partial_a g_{cb} + \partial_b g_{ca} - \partial_c g_{ab})\dot{x}^b\dot{x}^c = 0 \tag{2.35}$$

That is, the Euler-Lagrange equations reduce to

$$\ddot{x}^a + \Gamma^a_{bc}\dot{x}^b\dot{x}^c = 0 \tag{2.36}$$

where

$$\Gamma^a_{bc} = \frac{1}{2}g^{bd}\left(\partial_a g_{cb} + \partial_b g_{ca} - \partial_c g_{ab}\right) \tag{2.37}$$

Secondly, the geodesic equations is the Hamiltonian equations of the Hamiltonian

$$H = \frac{1}{2}g^{ab}P_aP_b \tag{2.38}$$

where $P_a = g_{ab}\dot{x}^b$.

Since the Lagrangian for a geodesic is given by

$$L = \frac{1}{2}g_{ab}\dot{x}^a\dot{x}^b \tag{2.39}$$

and the momenta P_a are given by

$$P_a = \frac{\partial L}{\partial \dot{x}^a} = g_{ab}\dot{x}^b \tag{2.40}$$

and

$$P_b = \frac{\partial L}{\partial \dot{x}^b} = g_{ab}\dot{x}^a \tag{2.41}$$

we have the Hamiltonian

$$\begin{aligned} H &= P_a\dot{x}^a + P_b\dot{x}^b - L \\ &= 2g_{ab}\dot{x}^a\dot{x}^b - L \\ &= g^{ab}P_aP_b \end{aligned} \tag{2.42}$$

The constant of the equality can be chosen ≥ 0 for a timelike geodesic or zero for a null geodesic.

2.4.3 Conformal Invariance

An important property of null geodesics is that they are conformally invariant i.e. if the metric g_{ab} (where $a;b$ take values from 1 to n) is replaced by $e^{\Omega}g_{ab}$ the null geodesics of the original metric are also null geodesics of the new metric, but not affinely parameterized: Such curves are also called pre-geodesics.

Now we define $\tilde{g}_{ab} = e^{\Omega}g_{ab}$ so that $\tilde{g}^{ab} = e^{-\Omega}g^{ab}$,and we calculate the new Christoffel symbols .

$$\begin{aligned} \tilde{\Gamma}^a_{bc} &= \frac{1}{2}\tilde{g}^{ad}\left(\partial_b\tilde{g}_{dc} + \partial_c\tilde{g}_{db} - \partial_d\tilde{g}_{bc}\right) \\ &= \frac{1}{2}(g^{ad}e^{-\Omega})\left(\partial_b(e^{\Omega}g_{dc}) + \partial_c(e^{\Omega}g_{db}) - \partial_d(e^{\Omega}g_{bc})\right) \end{aligned} \tag{2.43}$$

Then

$$\begin{aligned}\tilde{\Gamma}^a_{bc} = \frac{1}{2}(g^{ad}e^{-\Omega})(&\frac{\partial g_{dc}}{\partial x^b}e^{\Omega} + \frac{\partial \Omega}{\partial x^b}e^{\Omega}g_{dc} + \frac{\partial g_{db}}{\partial x^c}e^{\Omega} \\ &+ \frac{\partial \Omega}{\partial x^c}e^{\Omega}g_{db} - (\frac{\partial g_{bc}}{\partial x^d}e^{\Omega} + \frac{\partial \Omega}{\partial x^d}e^{\Omega}g_{bc}))\end{aligned} \tag{2.44}$$

Thus

$$\begin{aligned}\tilde{\Gamma}^a_{bc} = &\frac{1}{2}(g^{ad}e^{-\Omega})\left(\frac{\partial g_{dc}}{\partial x^b}e^{\Omega} + \frac{\partial g_{db}}{\partial x^c}e^{\Omega} - \frac{\partial g_{bc}}{\partial x^d}e^{\Omega}\right) \\ &+ \frac{1}{2}(g^{ad}e^{-\Omega})\left(\frac{\partial \Omega}{\partial x^b}e^{\Omega}g_{dc} + \frac{\partial \Omega}{\partial x^c}e^{\Omega}g_{db} - \frac{\partial \Omega}{\partial x^d}e^{\Omega}g_{bc}\right)\end{aligned} \tag{2.45}$$

So, we find that

$$\begin{aligned}\tilde{\Gamma}^a_{bc} = &\frac{1}{2}(g^{ad})\left(\frac{\partial g_{dc}}{\partial x^b} + \frac{\partial g_{db}}{\partial x^c} - \frac{\partial g_{bc}}{\partial x^d}\right) \\ &+ \frac{1}{2}(g^{ad})\left(\frac{\partial \Omega}{\partial x^b}g_{dc} + \frac{\partial \Omega}{\partial x^c}g_{db} - \frac{\partial \Omega}{\partial x^d}g_{bc}\right)\end{aligned} \tag{2.46}$$

Finally

$$\begin{aligned}\tilde{\Gamma}^a_{bc} &= \Gamma^a_{bc} + \frac{1}{2}g^{ad}\left(\frac{\partial \Omega}{\partial x^b}g_{dc} + \frac{\partial \Omega}{\partial x^c}g_{db} - \frac{\partial \Omega}{\partial x^d}g_{bc}\right) \\ &= \Gamma^a_{bc} + \frac{1}{2}\left(\frac{\partial \Omega}{\partial x^b}g^{ad}g_{dc} + \frac{\partial \Omega}{\partial x^c}g^{ad}g_{db} - \frac{\partial \Omega}{\partial x^d}g^{ad}g_{bc}\right) \\ &= \Gamma^a_{bc} + \frac{1}{2}\left(\frac{\partial \Omega}{\partial x^b}\delta^a_c + \frac{\partial \Omega}{\partial x^c}\delta^a_b - \frac{\partial \Omega}{\partial x^d}g^{ad}g_{bc}\right)\end{aligned} \tag{2.47}$$

For new Christoffel symbols the new geodesic equation is

$$\ddot{x}^a + \tilde{\Gamma}^a_{bc}\dot{x}^b\dot{x}^c = 0 \tag{2.48}$$

That leads to

$$\ddot{x}^a + \left(\Gamma^a_{bc} + \frac{1}{2} \left(\frac{\partial \Omega}{\partial x^b} \delta^a_c + \frac{\partial \Omega}{\partial x^c} \delta^a_b - \frac{\partial \Omega}{\partial x^d} g^{ad} g_{bc} \right) \right) \dot{x}^b \dot{x}^c = 0 \tag{2.49}$$

and so

$$\ddot{x}^a + \Gamma^a_{bc} \dot{x}^b \dot{x}^c + \frac{1}{2} \left(\frac{\partial \Omega}{\partial x^b} \delta^a_c \dot{x}^b \dot{x}^c + \frac{\partial \Omega}{\partial x^c} \delta^a_b \dot{x}^b \dot{x}^c - \frac{\partial \Omega}{\partial x^d} g^{ad} g_{bc} \dot{x}^b \dot{x}^c \right) = 0 \tag{2.50}$$

Then

$$\ddot{x}^a + \Gamma^a_{bc} \dot{x}^b \dot{x}^c + \frac{1}{2} \left(\dot{\Omega} \delta^a_c \dot{x}^c + \dot{\Omega} \delta^a_b \dot{x}^b - \frac{\partial \Omega}{\partial x^d} g^{ad} g_{bc} \dot{x}^b \dot{x}^c \right) = 0 \tag{2.51}$$

Finally

$$\ddot{x}^a + \Gamma^a_{bc} \dot{x}^b \dot{x}^c + \frac{1}{2} \left(2\dot{\Omega} \dot{x}^a - \Omega_d \left\| \dot{x}^a \right\|^2 g^{ad} g_{bc} \right) = 0 \tag{2.52}$$

If $\dot{x}^a$ is null then

$$\ddot{x}^a + \Gamma^a_{bc} \dot{x}^b \dot{x}^c = -\dot{x}^a \dot{\Omega} \tag{2.53}$$

i.e x^a is a pre-geodesic for $\tilde{g}_{ab}$, but is not a geodesic (i.e. is not affinely parameterised).

We can choose a different parameter in such a way that the vector in the right hand side will vanish, and we obtain the equation of a null geodesic. Then under the conformal transformation of the metric $\tilde{g} = e^{\Omega} g$ the null vectors remain null and null geodesic curves remain null geodesic curves, but the affine parameter changes.

We will use this fact to help us to study the null geodesics and hence the causal structure of certain space-times.

2.4.4 Jacobi Fields

Many properties of the geometry of a Riemannian manifold $(M; g)$ are studied using Jacobi vector fields. Jacobi fields are vector fields defined along a geodesic in a Riemannian manifold associated with a variation of geodesics, and the vanishing of Jacobi fields along null geodesics leads to some of the interesting aspects of causal

structure that we will be considering.

Let $\gamma : [a; b] \longrightarrow M$ be a geodesic, and X be a vector field along γ. X is called a Jacobi field along γ if

$$\nabla_{\gamma'}\nabla_{\gamma'}X + R(\gamma', X)\gamma' = 0. \tag{2.54}$$

A Jacobi field defines a vector in the space of geodesics and it is describes the relationship between two infinitesimally separated geodesics.

In addition, if V is a Jacobi field defined on γ and V vanishes at two points $p, q \in \gamma$ and is not vanishing at all points of γ then p and q are called conjugate points on γ . This occurs when two close geodesic meet in two points. For our purposes, the main importance of conjugate points is that a geodesic beginning at $p \in M$ is only extremal until it reaches a point conjugate to p; after that, the geodesic is no longer extremal. As a consequence, two points on a null geodesic can be connected by a timelike curve if there is a pair of conjugate points between them [15].

The set of points of M conjugate to p on geodesic are called a caustic.

2.5 Causal Structure

The causal structure of Minkowski space, $\mathbb{M}$, is particularly simple. Given two events $p, q \in \mathbb{M}$ we can consider the vector $v^a = \vec{pq}$ and a particle travelling on the corresponding trajectory. The particle travelling from p to q has velocity slower than light, equal to the speed of light or faster than light as $g_{ab}v^a v^b$ is negative, zero or positive and we say that $\vec{pq}$ is time-like, null or space-like respectively. Alternatively we consider a curve $\gamma : [0, 1] \longrightarrow M$ such that $\gamma(0) = p, \gamma(1) = q$, and consider $g_{ab}\dot{\gamma}^a\dot{\gamma}^b$ along the curve.

Then $g_{ab}v^a v^b$ is positive if and only if the curve is space-like, $g_{ab}v^a v^b$ is zero if and only if the curve is null and the $g_{ab}v^a v^b$ is negative if and only if the curve is time-like.

It then follows that $\vec{pq}$ is timelike if and only if there is a timelike curve from p to q; null if and only if there is a null curve but not timelike curve; and spacelike if there is neither a spacelike nor a timelike curve [16].

In general space-time we cannot use a connecting vector, so we must use the existence of a time-like or causal curve as our way of deciding whether a pair of points is timelike, null, or spacelike separated.

In a general spacetime, if M is a spacetime with metric g_{ab}, then there is a null cone at each point consisting tangent vectors X^a such that $g_{ab}X^aX^b = 0$. At each point, this null cone splits into two halves. Then if it is possible to choose one of these halves consistently over the whole of M, we say that M is time orientable, and arbitrarily choose one of the halves to be the future half. We can consider a curve x^a in M, and its tangent vector x'^a at each point. We define this curve to be timelike, null or spacelike at x^a depending on the sign of $g_{ab}X^aX^b$ and say that the vector is future pointing the vector points into the future half of the light cone, and past pointing otherwise [17]. In the same way we say that a curve is future pointing timelike if its tangent vector is future pointing timelike at each point, etc.

We have two particularly useful types of causal relationships between space-time points. We say that p chronologically precedes q, denoted $p \ll q$, if there exists a future directed time-like curve, $\gamma : [0,1] \longrightarrow M$ such that $\gamma(0) = p, \gamma(1) = q$.

The point p causally precedes q, denoted $p < q$, if there exists a future directed causal curve γ from p to q.

The chronological future of p, denoted $I^+(p)$, is the set of all points $q \in M$ such that p chronologically precedes q, i.e.

$$I^+(p) = \{q \in M \mid p \ll q\} \tag{2.55}$$

The chronological past of p denoted $I^-(p)$, as the set of all points $q \in M$ such that p chronologically precedes q, i.e.

$$I^-(p) = \{q \in M \mid q \ll p\} \tag{2.56}$$

The causal future of p denoted $J^+(p)$, as the set of all points $q \in M$ such that p causally precedes q, i.e.

$$J^+(p) = \{q \in M \mid p < q\} \tag{2.57}$$

The causal past of p denoted $J^-(p)$, as the set of all points $q \in M$ such that q causally precedes p, i.e.

$$J^-(p) = \{q \in M \mid q < p\} \tag{2.58}$$

The sets $I^+(p), I^-(p), J^+(p), J^-(p)$ for all $p \in M$ are collectively called the causal structure of M.

We can now use these relations to place restrictions on space-time, called causality conditions.

Causality conditions on space-time (M, g) are completely determined by the identification of space-like, time-like and null curves on M and a choice of the future direction along causal curves. Since conformally equivalent Lorentzian metric g and $\hat{g}$ distinguish the same space-like, time-like and null curves on M, any two space-time (M, g) and $(M, \hat{g})$ with $g \sim \hat{g}$ satisfy identical causality conditions, so long as their time orientations select the same future directions along causal curves.

In Minkowski space-time the boundary of $I^+(p)$ is $\partial I^+(p) = J^+(p) - I^+(p)$, and is given by the points on future directed null geodesics from p. We call this set the future light cone of p. This is not true in general space-times, i.e. the future light cone of p, may include points not on $\partial I^+(p)$ and omit points which are in $\partial I^+(p)$.

We now give a brief summary of some of the constraints that can be placed on

space-time in terms of the causal structure [18].

Chronological condition:-

A spacetime M is said to be chronological when it admits no closed timelike curves, that is, $p \in I^+(p)$ for all $p \in M$.

Causal condition :-

When M admits no closed non-spacelike curves, it is said to be causal. If $M = R$ and the metric is chosen to be $ds^2 = dtdx$, then M is chronological but not causal.

Strong causality:-

A spacetime (M, g_{ab}) is be strongly causal if for all $p \in M$ and every neighbourhood O of P, there exists a neighbourhood V of p contained in O such that no causal curve intersects V more than once [18].

These three are frequently used: in fact there is a detailed hierarchy of causal conditions, some very subtle [19]. We will omit the intermediate levels, and move to the most restrictive condition, as the space-times we will be interested in all satisfy it.

Globally hyperbolic condition:-

The condition which says that a space-time is as well-behaved as one can ask is that of global hyperbolicity. Proofs of the following statements can be found in Penrose and Hawking and Ellis [15] [11]. The most convenient formal definition of global hyperbolicity is the following. In a spacetime (M, g) , a subset S of M is called a Cauchy surface if every inextendible causal (i.e., timelike or lightlike) curve intersects S exactly once. A spacetime is globally hyperbolic if and only if it admits a Cauchy surface. The name globally hyperbolic refers to the fact that for hyperbolic differential equations, like the wave equation, existence and uniqueness of a global solution is guaranteed for initial data given on a Cauchy surface.

In more detail, we say that a set $S \subseteq M$ is achronal if no two points of S are time-like related (i.e. if $p, q \in S$ then we never have $p \ll q$). Let $S \subset M$ be closed and a

chronal. We define the future domain of dependence of S denoted $D^+(S)$ by

$$D^+(S) = p \in S| \text{ every past causal curve through } p \text{ intersects } S. \tag{2.59}$$

A closed achronal set Σ for which $D(\Sigma) = M$ is called Cauchy surface. A space-time (M, g_{ab}) which has Cauchy surface Σ is said to be globally hyperbolic.

A space-time which is globally hyperbolic is particularly well-behaved. In particular in globally hyperbolic space-time the boundary of $I^+(p)$ is a subset of the future light cone of p points connected to p by a future pointint null geodesic, but some null geodesics may enter $I^+(p)$ so not every point on such a null geodesic is on the boundary of $I^+(p)$.

It can be shown that a globally hyperbolic spacetime admits a continuous function $t : M \longrightarrow R$ such that $t^{-1}(t_0)$ is a Cauchy surface for every $t_0 \in R$. It follows that a Lorentzian manifold is globally hyperbolic if it contains a Cauchy surface or a foliation by Cauchy surfaces. Hence if a spacetime is globally hyperbolic then it is of the form $S \times \mathbb{R}$, with coordinate (x, t), such the $\frac{\partial}{\partial t}$ is timelike and $S \times t$ is a Cauchy surface for all t [20] [16] [21].

In the following chapters, we will develop an approach to visualizing the light cones of points in some particular globally hyperbolic space-times, and so of understanding their causal structure.

Chapter 3

Static Space-Times

3.1 Introduction

Because general spacetimes are too complicated too deal with, we restrict our attention to those with extra structure that makes them more tractable, in particular to those with a high degree of symmetry [11] [22] [23]. In this chapter we review the notions of stationary and static space-time, and use the conformal invariance of null geodesics to provide a basis for the numerical approach to visualizing light cones which we will use in the remainder of this thesis. We will pay particular attention to Schwarzschild space, and also see how to generalize to more general (but not fully general) space-times.

3.2 Definitions

First, we recall some basic material on symmetry in the differential geometric setting.

Let (M, g) be a semi-Riemannian manifold, $f : M \longrightarrow M$, be a diffeomorphism,

and let p be an arbitrary element of M. Then we say that f is an isometry if

$$g_{f(p)}(df(v), df(u)) = g_p(v, u) \tag{3.1}$$

for all $u, v \in T_pM$.

Then if φ_t is a diffeomorphism for $t \in \mathbb{R}$, we say that φ_t is a one-parameter r group of isometries of M if φ_t is an isometry for all $t \in \mathbb{R}$, and

$$\begin{aligned} \varphi_t \circ \varphi_s &= \varphi_{t+s} \\ \varphi_t^{-1} &= \varphi_{-t} \end{aligned} \tag{3.2}$$

for all $s, t \in \mathbb{R}$.

Now pick $p \in M$ and consider

$$\gamma(t) = \varphi_t(p) \tag{3.3}$$

The map $t \longrightarrow \phi_t(p)$ defines a curve through p for each p in M. Define a vector field V by defining $V(p)$ to be tangent to this curve at p. Then V is called a Killing vector field, and ϕ_t is called the flow of v.

It can be shown [24] that V is locally a Killing vector field if and only if

$$\nabla_a V_b + \nabla_b V_a = 0 \tag{3.4}$$

A stationary gravitational field is described by a spacetime on which a timelike Killing vector field V exists. If we choose local coordinates (t, x^a) where $a, b = 1 \ldots n-1$ such that $V = \frac{\partial}{\partial t}$, then g_{ab} is independent of time (t).

If, moreover, the Killing field is irrotational, i.e.

$$V_{[a}\nabla_b V_{c]} = 0 \tag{3.5}$$

where the square brackets denote the completely skew symmetric part of the tensor, it follows that V is hypersurface orthogonal. [12] As a consequence, the metric can be put in the from

$$-f(x^a)dt^2 + g_{ab}dx^a dx^b \tag{3.6}$$

where by a slight abuse of notation, x^a now denotes only the spatial coordinates.

Here $f(x^a)$ is strictly positive, the g_{ab} do not depend on t, and g_{ab} is a Riemannian metric. Note that in addition to the metric coefficients all being independent of time, all the $dx^\alpha dt$ terms are now zero.

Intuitively speaking, a stationary metric means that the space-time is locally independent of time, while a static metric means that in addition the notion of time is global.

For example, the static spherically symmetric Schwarzschild metric will describe the exterior of non-rotating stars or black holes, while axisymmetric rotating systems which keep rotating in the same way at all times will be described by stationary metrics such as the Kerr metric [25].

3.3 Null Geodesics

We now consider the null geodesics of a static space-time, and see how they are determined by the geodesics in the induced Riemannian metric of a surface of constant time. We will eventually apply this to the problem of visualising light cones in a static space-time.

To summarize, a space-time is static if it has coordinates (t, x^a) (where $a = 1 \ldots n -$

1) such that the metric is

$$d\tilde{s}^2 = -f(x^a)dt^2 + \tilde{g}_{ab}dx^a dx^b \tag{3.7}$$

where f is a strictly positive function of x^a and $\tilde{g}_{ab}$ is Riemannian.

We can now consider the conformally related metric

$$ds^2 = -dt^2 + g_{ab}dx^a dx^b \tag{3.8}$$

where

$$g_{ab} = \frac{1}{f(x^a)}\tilde{g}_{ab} \tag{3.9}$$

is again a Riemannian metric.

We will use the conformal invariance of null geodesics (as curves) to find a particularly useful description of the light cones of the original space-time in terms of the arc-length parameterized geodesics of the Riemannian metric g_{ab}.

So let $c(p) = (t(p), x^a(p))$ be a curve parameterized by p, where $\frac{dx^a}{dp} = \dot{x^a}$.

Then we can consider the Lagrangian

$$L = -\dot{t}^2 + g_{ab}\dot{x}^a\dot{x}^b \tag{3.10}$$

and the Euler-Lagrange equation for this Lagrangian are the general equations for the geodesics of the metric ds^2.

Now, we have

$$\frac{\partial L}{\partial t} = 0 \tag{3.11}$$

and

$$\frac{\partial L}{\partial \dot{t}} = -2\dot{t} \tag{3.12}$$

We differentiate the last equation with respect to parameter p, and we find that

$$\frac{d}{dp}(\frac{\partial L}{\partial \dot{t}}) = -2\ddot{t} \tag{3.13}$$

From the Euler-Lagrange equation we have

$$\frac{d}{dp}\left(\frac{\partial L}{\partial \dot{t}}\right) = \frac{\partial L}{\partial t} \tag{3.14}$$

Then

$$-2\ddot{t} = 0 \tag{3.15}$$

This gives

$$t = ap + b \tag{3.16}$$

and without loss of generality we can assume that $t = p$.

We chose the conformal factor so that $\ddot{t} = 0$, i.e is as simple as possible. As a consequence, it is easy to find null geodesics of the space-time once we have the (Riemannian) arc-length parametrised geodesics of the spatial part of the metric [4].

We now consider the remaining geodesic equations for ds^2, making use of the fact the g_{ab} is independent of time , and relate the null geodesics of ds^2 to the arc-length parameterised geodesics of g_{ab}. So we must now find the remaining Euler-Lagrange equation for

$$L = -\dot{t}^2 + g_{ab}\dot{x}^a\dot{x}^b \tag{3.17}$$

We differentiate with respect to parameter x^c, and we find that

$$\frac{\partial L}{\partial x^c} = \frac{\partial g_{ab}}{\partial x^c}\dot{x}^a\dot{x}^b = \partial_c g_{ab}\dot{x}^a\dot{x}^b \tag{3.18}$$

and

$$\begin{aligned}\frac{\partial L}{\partial \dot{x}^c} &= g_{cb}\delta^c_a \dot{x}^b + g_{ca}\delta^c_b \dot{x}^c \\ &= g_{cb}\dot{x}^b + g_{ca}\dot{x}^a \\ &= 2g_{ac}\dot{x}^a\end{aligned} \tag{3.19}$$

Then differentiating with respect to p we find that

$$\frac{d}{dp}(\frac{\partial L}{\partial \dot{x}^c}) = 2\frac{dg_{ac}}{dp}\dot{x}^a + 2g_{ac}\ddot{x}^a \tag{3.20}$$

From the Euler-Lagrange equation we have

$$\frac{d}{dp}\left(\frac{\partial L}{\partial \dot{x}^c}\right) = \frac{\partial L}{\partial x^c} \tag{3.21}$$

Then

$$\frac{d}{dp}(\frac{\partial L}{\partial \dot{x}^c}) = 2(\partial_b g_{ac} + \partial_a g_{bc})\dot{x}^a\dot{x}^b + 2g_{ac}\ddot{x}^a \tag{3.22}$$

where

$$\frac{dg_{ac}}{dp} = \partial_b g_{ac}\dot{x}^b \tag{3.23}$$

So, we find that

$$\begin{aligned}2g_{ac}\ddot{x}^a + 2(\partial_b g_{ac} + \partial_a g_{bc})\dot{x}^a\dot{x}^b &= \partial_c g_{ab}\dot{x}^a\dot{x}^b \\ 2g_{ac}\ddot{x}^a + (2\partial_b g_{ac} + 2\partial_a g_{bc} - \partial_c g_{ab})\dot{x}^a\dot{x}^b &= 0\end{aligned} \tag{3.24}$$

Finally

$$\ddot{x}^a + g^{ac}\frac{1}{2}(2\partial_b g_{ac} + 2\partial_a g_{bc} - \partial_c g_{ab})\dot{x}^a\dot{x}^b = 0 \tag{3.25}$$

The Euler Lagrange equation for $x^a(p)$ are just the geodesic equations for g_{ab}. We make the important note that t is naturally an affine parameter for these geodesics.

We therefore consider curves of the form $c(p) = (t(p), x^a(p))$ where

$$\begin{aligned} t &= p \\ \ddot{x}^a + \Gamma^a_{bc}\dot{x}^b\dot{x}^c &= 0 \end{aligned} \tag{3.26}$$

Then we note that $c(p) = (p, x^a(p))$ is specified by the tangent when $p = 0$, and

$$\|\dot{c}(p)\|^2 = -1 + g_{ab}\dot{x}^a\dot{x}^b \tag{3.27}$$

for all p.

If $x^a(p)$ is determined by an initial tangent vector $\dot{x}^a(0)$ such that

$$g_{ab}\dot{x}^a(0)\dot{x}^b(0) = 1 \tag{3.28}$$

then $x^a(p)$ is an arc-length parameterised geodesic of g_{ab} . It follows that $(p, x^a(p))$ is a null geodesic of ds^2, since it satisfies the Euler-Lagrange equations for the metric ds^2, with the useful property that the arc-length coincides with coordinate time. Because of the conformal invariance of null geodesics, this curve is also a null pre-geodesic of the original metric, $d\tilde{s}^2$, but parameterized by t rather than by an affine parameter.

In fact, this is a better parameter for our purposes, because it makes it easy to find the light cone of a point between two values of t, which is what we want to do in order to visualize the causal structure.

It is important to note that if $g_{ab}\dot{x}^a(0)\dot{x}^b(0) < 1$, then we have a timelike geodesic of ds^2, which is a timelike curve of $d\tilde{s}^2$, but not in general a geodesic. Similarly, if $g_{ab}\dot{x}^a(0)\dot{x}^b(0) > 1$, we have a spacelike geodesic of ds^2 which is a spacelike curve of $d\tilde{s}^2$, but not in general a geodesic.

So, although we cannot find the general geodesics of $d\tilde{s}^2$ by this approach, we can find the null ones, and these suffice for visualising the light cones, and hence the

causal structure of $d\tilde{s}^2$.

3.4 Schwarzschild Space-time

We now consider the example of exterior Schwarzschild space-time. In standard Schwarzschild coordinates the metric is given by

$$-(1-2m/r)dt^2 + (1-2m/r)^{-1}dr^2 + r^2 d\Omega^2 \tag{3.29}$$

where $d\Omega^2 = d\theta^2 + \sin^2\theta d\phi^2$ and is clearly static.

We set $z = (1 - \frac{2m}{r})$ for convenience, so we can write this as

$$-zdt^2 + z^{-1}dr^2 + r^2\left(d\theta^2 + \sin^2\theta d\phi^2\right) \tag{3.30}$$

we divide this equation by z to get

$$-dt^2 + (1-2m/r)^{-2}dr^2 + (1-2m/r)^{-1}r^2 d\Omega^2 \tag{3.31}$$

and we now have the Lagrangian

$$L = -\dot{t}^2 + z^{-2}\dot{r}^2 + z^{-1}r^2(\dot{\theta}^2 + \sin^2\theta\dot{\phi}^2) \tag{3.32}$$

where the dot represents differentiation with respect to the parameter p.

Now, we differentiate L with respect to t so that

$$\frac{\partial L}{\partial t} = 0 \tag{3.33}$$

Differentiating L with respect to $\dot{t}$ we get

$$\frac{\partial L}{\partial \dot{t}} = -2\dot{t} \tag{3.34}$$

We find that

$$\frac{d}{dp}\left(\frac{\partial L}{\partial \dot{t}}\right) = -2\ddot{t} \tag{3.35}$$

From the Euler-Lagrange equations we have eq. 3.33 equal to eq. 3.35 Then

$$-2\ddot{t} = 0 \tag{3.36}$$

which essentially tells us that t is an affine parameter.

Generally, therefore

$$t = ap + b \tag{3.37}$$

where a, b are constant and we take t=p, as in the general discussion.

Next, we differentiate L with respect to r and $\dot{r}$.

From Euler-Lagrange equation we have

$$\frac{d}{dp}\left(\frac{\partial L}{\partial \dot{r}}\right) = \frac{\partial L}{\partial r} \tag{3.38}$$

and we find that

$$\frac{\partial L}{\partial r} = \frac{-4mr}{(r-2m)^3}\dot{r}^2 + \frac{2r^2(r-3m)}{(r-2m)^2}(\dot{\theta}^2 + \sin^2\theta\dot{\phi}^2) \tag{3.39}$$

We also have

$$\frac{\partial L}{\partial \dot{r}} = 2(1-\frac{2m}{r})^{-2}\dot{r} \tag{3.40}$$

So, we differentiate last equation with respect to parameter p, giving

$$\begin{aligned}\frac{d}{dp}\left(\frac{\partial L}{\partial \dot{r}}\right) &= \frac{d}{dp}(2(1-\frac{2m}{r})^{-2}\dot{r}) \\ &= \frac{-4mr}{(r-2m)^3}\dot{r} + \frac{2r^2}{(r-2m)^2}\ddot{r}\end{aligned} \tag{3.41}$$

From the Euler-Lagrange equation we have eq. 3.39 equal to eq. 3.41

$$\frac{-4mr}{(r-2m)^3}\dot{r} + \frac{2r^2}{(r-2m)^2}\ddot{r} = \frac{-4mr}{(r-2m)^3}\dot{r}^2 + \frac{2r^2(r-3m)}{(r-2m)^2}(\dot{\theta}^2 + \sin^2\theta\dot{\phi}^2) \tag{3.42}$$

giving

$$\ddot{r} + 2mr^{-2}(1-\frac{2m}{r})^{-1}\dot{r}^2 = (m + r(1-\frac{2m}{r}))(\dot{\theta}^2 + \sin^2\theta\dot{\phi}^2) \tag{3.43}$$

and so

$$\ddot{r} = \frac{2m}{r(r-2m)}\dot{r}^2 + (r-3m)(\dot{\theta}^2 + \sin^2\theta\dot{\phi}^2) \tag{3.44}$$

The case for ϕ is similar. Now, we differentiate L with respect to ϕ that find that

$$\frac{\partial L}{\partial \phi} = 0 \tag{3.45}$$

Differentiating L with respect to $\dot{\phi}$ we get

$$\frac{\partial L}{\partial \dot{\phi}} = 2r^2\dot{\phi}z^{-1}\sin^2\theta \tag{3.46}$$

We find that

$$\begin{aligned}\frac{d}{dp}\left(\frac{\partial L}{\partial \dot{\phi}}\right) &= z^{-1}2r^2\ddot{\phi} + z^{-1}4r\dot{r}\dot{\phi} + 2r^2\dot{\phi}(-1)z^{-2}2mr^{-2}\dot{r} + 2r^2z^{-1}2\sin\theta\cos\theta\dot{\theta}\dot{\phi} \\ &= z^{-1}2r^2\ddot{\phi} + z^{-1}2r\dot{r}\dot{\phi}(2 + z^{-1}2mr^{-1}) + 2r^2z^{-1}2\sin\theta\cos\theta\dot{\theta}\dot{\phi}\end{aligned} \tag{3.47}$$

From the Euler-Lagrange equation we have the right hand side of eq. 3.45 equal to eq. 3.47. Therefore

$$z^{-1}2r^2\ddot{\phi} + z^{-1}2r\dot{r}\dot{\phi}(2 - z^{-1}2mr^{-1}) - 2r^2z^{-1}2\sin\theta\cos\theta\dot{\theta}\dot{\phi} = 0 \tag{3.48}$$

Therefore

$$\ddot{\phi} + \frac{1}{r}\dot{r}\dot{\phi}(2 + z^{-1}2mr^{-1}) - 2\sin\theta\cos\theta\dot{\theta}\dot{\phi} = 0 \tag{3.49}$$

and so finally

$$\ddot{\phi} = \frac{2(3m - r)}{r(r - 2m)}\dot{r}\dot{\phi} + 2\sin\theta\cos\theta\dot{\theta}\dot{\phi} \tag{3.50}$$

Finally, we differentiate L with respect to θ and $\dot{\theta}$. From the Euler-Lagrange equations we have

$$\frac{d}{dp}\left(\frac{\partial L}{\partial\dot{\theta}}\right) = \frac{\partial L}{\partial\theta} \tag{3.51}$$

Now, we differentiate L with respect to θ that find that

$$\frac{\partial L}{\partial\theta} = -2\sin\theta\cos\theta(r^2z^{-1})\dot{\phi}^2\dot{\theta} \tag{3.52}$$

and we get

$$\frac{\partial L}{\partial\dot{\theta}} = 2r^2z^{-1}\dot{\theta} \tag{3.53}$$

So, we differentiate this last equation with respect to the parameter p, giving

$$\begin{aligned}\frac{d}{dp}\left(\frac{\partial L}{\partial\dot{\theta}}\right) &= \frac{d}{dp}(2r^2z^{-1}\dot{\theta}) \\ &= \frac{2r^3}{(r - 2m)}\ddot{\theta} + \frac{(r - 2m)6r^2 - 2r^3}{(r - 2m)^2}\dot{\theta}\dot{r} \\ &= \frac{2r^3}{(r - 2m)}\ddot{\theta} + \frac{4r^2(r - 3m)}{(r - 2m)^2}\dot{\theta}\dot{r}\end{aligned} \tag{3.54}$$

From the Euler-Lagrange equation we have eq. 3.52=3.54

$$\frac{2r^3}{(r-2m)}\ddot{\theta} + \frac{4r^2(r-3m)}{(r-2m)^2}\dot{\theta}\dot{r} = -\sin\theta\cos\theta\frac{2r^3}{(r-2m)}\dot{\phi}^2\dot{\theta} \tag{3.55}$$

and so

$$\ddot{\theta} = -\sin\theta\cos\theta\dot{\phi}^2\dot{\theta} - \frac{2(r-3m)}{r(r-2m)}\dot{\theta}\dot{r} \tag{3.56}$$

which is the final equation for an affinely parameterized in the metric obtained from the Schwarzschild metric by a conformal transformation.

Gathering these together, we have the equations for an affinely parameterized geodesic in our new metric,

$$\begin{aligned}
\ddot{r} &= \frac{2m}{r(r-2m)}\dot{r}^2 + (r-3m)(\dot{\theta}^2 + \sin^2\theta\dot{\phi}^2) \\
\ddot{\theta} &= -\sin\theta\cos\theta\dot{\phi}^2\dot{\theta} - \frac{2(r-3m)}{r(r-2m)}\dot{\theta}\dot{r} \\
\ddot{\phi} &= \frac{2(3m-r)}{r(r-2m)}\dot{r}\dot{\phi} + 2\sin\theta\cos\theta\dot{\theta}\dot{\phi}
\end{aligned} \tag{3.57}$$

If we take initial conditions $\theta = \pi/2$, $\dot{\theta} = 0$, we find that $\theta = \pi/2$ is a solution. Since any geodesic can be put in this form by a rotation we can reduce the equations by taking $\theta = \pi/2$ resulting in

$$\begin{aligned}
\ddot{r} &= \frac{2m}{r(r-2m)}\dot{r}^2 + (r-3m)\dot{\phi}^2 \\
\ddot{\phi} &= \frac{2(3m-r)}{r(r-2m)}\dot{r}\dot{\phi}
\end{aligned} \tag{3.58}$$

This is similar to the situation for Schwarzschild space, in which also all geodesics can be considered to lie in the equatorial plane by an appropriate choice of coordinates [17]. Clearly, the same argument will apply in any spherically symmetric static space-time.

In the next chapter we will see how we can solve these equations in Matlab and hence visualise the light cones in Schwarzschild space.

3.5 The general (2+1) metric

In the Schwarzchild case, we saw how we can use the symmetries to reduce the problem of finding the light cone of a point that of finding the geodesics in a 2-dimensional Riemannian manifold. This can also be done in the case of other metrics of sufficiently high symmetry.

We will therefore consider the visualization of light cones in (2+1)-dimensional static space-time as an approach to providing insight into the causal structure of space-time of sufficiently high symmetry.

In the next chapter we will consider the particular case of Schwarzschild space-time, with a specific Matlab code tailored to that purpose. However, we will also consider the problem of visualising the light cones in a metric which can be chosen by the user. For this purpose, it is useful to find the geodesic equations for a general two dimensional Riemannian manifold, with Lagrangian given by

$$L = E\dot{x}^2 + 2F\dot{x}\dot{y} + G\dot{y}^2 \tag{3.59}$$

and so we derive these equations here, for use in chapter 5.

We have

$$\frac{\partial L}{\partial \dot{x}} = 2E\dot{x} + 2F\dot{y} \tag{3.60}$$

and

$$\begin{aligned} \frac{d}{dt}\frac{\partial L}{\partial \dot{x}} &= 2\left[E\ddot{x} + F\ddot{y} + E_x\dot{x}^2 + E_y\dot{x}\dot{y} + F_x\dot{x}\dot{y} + F_y\dot{y}^2\right] \\ &= 2\left[E\ddot{x} + F\ddot{y} + E_x\dot{x}^2 + (E_y + F_x)\dot{x}\dot{y} + F_y\dot{y}^2\right] \end{aligned} \tag{3.61}$$

Finally

$$\frac{\partial L}{\partial x} = E_x\dot{x}^2 + 2F_x\dot{x}\dot{y} + G_x\dot{y}^2 \tag{3.62}$$

From the Lagrange equation we have

$$\frac{d}{dt}\left(\frac{\partial L}{\partial \dot{x}}\right) = \frac{\partial L}{\partial x} \tag{3.63}$$

which in this case gives

$$2\left[E\ddot{x} + F\ddot{y} + E_x\dot{x}^2 + (E_y + F_x)\dot{x}\dot{y} + F_y\dot{y}^2\right] = E_x\dot{x}^2 + 2F_x\dot{x}\dot{y} + G_x\dot{y}^2 \tag{3.64}$$

and so

$$2E\ddot{x} + 2F\ddot{y} = (-E_x)\dot{x}^2 + (-2E_y - 2F_x + 2F_x)\dot{x}\dot{y} + (-2F_y + G_x)\dot{y}^2 \tag{3.65}$$

Thus we finally have

$$E\ddot{x} + F\ddot{y} = \frac{1}{2}\left((-E_x)\dot{x}^2 + (-2E_y)\dot{x}\dot{y} + (-2F_y + G_x)\dot{y}^2\right). \tag{3.66}$$

Similarly

$$\frac{\partial L}{\partial \dot{y}} = 2F\dot{x} + 2G\dot{y} \tag{3.67}$$

$$\begin{aligned}\frac{d}{dt}\left(\frac{\partial L}{\partial \dot{y}}\right) &= 2\left(\dot{y}\frac{\partial G}{\partial t} + G\ddot{y} + \frac{\partial F}{\partial t}\dot{x} + F\ddot{x}\right) \\ &= 2\left[G\ddot{y} + F\ddot{x} + \dot{y}\left(G_x\dot{x} + G_y\dot{y}\right) + \left(F_x\dot{x} + F_y\dot{y}\right)\dot{x}\right] \\ &= 2\left[F\ddot{x} + G\ddot{y} + (F_y + G_x)\dot{x}\dot{y} + F_x\dot{x}^2 + G_y\dot{y}^2\right]\end{aligned} \tag{3.68}$$

and

$$\frac{\partial L}{\partial y} = E_y\dot{x}^2 + 2F_y\dot{x}\dot{y} + G_y\dot{y}^2 \tag{3.69}$$

From the Euler-Lagrange equation we have

$$\frac{d}{dt}\left(\frac{\partial L}{\partial \dot{y}}\right) = \frac{\partial L}{\partial y}. \tag{3.70}$$

Then similarly to the previous case,

$$F\ddot{x} + G\ddot{y} = \frac{1}{2}\left((E_y - 2F_x)\dot{x}^2 + (-2G_x)\dot{x}\dot{y} - (G_y)\dot{y}^2\right) \tag{3.71}$$

From 3.66 and 3.71 we get

$$\begin{bmatrix} E & F \\ F & G \end{bmatrix}\begin{bmatrix} \ddot{x} \\ \ddot{y} \end{bmatrix} = \frac{1}{2}\begin{bmatrix} (-E_x)\dot{x}^2 + (-2E_y)\dot{x}\dot{y} + (-2F_y + G_x)\dot{y}^2 \\ (E_y - 2F_x)\dot{x}^2 + (-2G_x)\dot{x}\dot{y} - (G_y)\dot{y}^2 \end{bmatrix} \tag{3.72}$$

so premultiplying by the inverse matrix

$$\begin{bmatrix} \ddot{x} \\ \ddot{y} \end{bmatrix} = \frac{1}{2}\begin{bmatrix} E & F \\ F & G \end{bmatrix}^{-1}\begin{bmatrix} (-E_x)\dot{x}^2 + (-2E_y)\dot{x}\dot{y} + (-2F_y + G_x)\dot{y}^2 \\ (E_y - 2F_x)\dot{x}^2 + (-2G_x)\dot{x}\dot{y} - (G_y)\dot{y}^2 \end{bmatrix} \tag{3.73}$$

which gives us the explicit differential coupled system of equations

$$\begin{bmatrix} \ddot{x} \\ \ddot{y} \end{bmatrix} = \frac{1}{2(EG - F^2)}\begin{bmatrix} G & -F \\ -F & E \end{bmatrix}\begin{bmatrix} (-E_x)\dot{x}^2 + (-2E_y)\dot{x}\dot{y} + (-2F_y + G_x)\dot{y}^2 \\ (E_y - 2F_x)\dot{x}^2 + (-2G_x)\dot{x}\dot{y} - (G_y)\dot{y}^2 \end{bmatrix} \tag{3.74}$$

Separating out the components of these two gives

$$\begin{aligned} \ddot{x} = \frac{1}{2(EG - F^2)}&[(-GE_x)\dot{x}^2 + (-2GE_y)\dot{x}\dot{y} - G(-2F_y + G_x)\dot{y}^2 \\ &+ (-F)(E_y - 2F_x)\dot{x}^2 + (-F)(-2G_x)\dot{x}\dot{y} + (FG_y)\dot{y}^2] \end{aligned} \tag{3.75}$$

and

$$\begin{aligned}\ddot{y} = \frac{1}{2(EG-F^2)}[&(FE_x)\dot{x}^2 + (2FE_y)\dot{x}\dot{y} + (2FF_y - FG_x)\dot{y}^2 \\ &+ (EE_y - 2EF_x)\dot{x}^2 + (-2EG_x)\dot{x}\dot{y} - EG_y\dot{y}^2]\end{aligned} \tag{3.76}$$

which we can simplify slightly to

$$\begin{aligned}\ddot{x} = \frac{1}{2(EG-F^2)}[&(-GE_x - FE_y + 2FF_x)\dot{x}^2 \\ &+ (-2GE_y + 2FG_x)\dot{x}\dot{y} + (-GG_x + 2GF_y + FG_y)\dot{y}^2]\end{aligned} \tag{3.77}$$

and

$$\begin{aligned}\ddot{y} = \frac{1}{2(EG-F^2)}[&(FE_x + EE_y - 2EF_x)\dot{x}^2 \\ &+ (-2EG_x + 2FE_y)\dot{x}\dot{y} - (EG_y + 2FF_y - FG_x)\dot{y}^2]\end{aligned} \tag{3.78}$$

Later, we will exploit this in Matlab to find null geodesics and hence visualise light cones in a space-time chosen by the user.

3.6 Schwarzschild again

As a consistency check, we now reconsider the example of exterior Schwarzschild space-time, where we restrict the metric to the equatorial plane. In standard Schwarzchild coordinates the metric is given by

$$-(1 - \frac{2m}{r})dt^2 + (1 - \frac{2m}{r})^{-1}dr^2 + r^2(d\theta^2 + \sin^2\theta d\phi^2) \tag{3.79}$$

If we set $\theta = \frac{\pi}{2}$, then we have

$$-(1 - \frac{2m}{r})dt^2 + (1 - \frac{2m}{r})^{-1}dr^2 + r^2 d\phi^2 \tag{3.80}$$

We now divide this equation by $(1-\frac{2m}{r})$, and we find that

$$L = -\dot{t}^2 + (1-\frac{2m}{r})^{-2}\dot{r}^2 + (1-\frac{2m}{r})^{-1}r^2\dot{\phi}^2 \tag{3.81}$$

Restricting out attention to the spatial part, we identify

$$(1-\frac{2m}{r})^{-2}\dot{r}^2 + (1-\frac{2m}{r})^{-1}r^2\dot{\phi}^2 \tag{3.82}$$

with

$$L = E\dot{x}^2 + 2F\dot{x}\dot{y} + G\dot{y}^2 \tag{3.83}$$

so here $x = r, y = \phi$.

To simplify the calculations we again suppose $z = (1-\frac{2m}{r})$.

Then

$$\begin{aligned} E &= (1-\frac{2m}{r})^{-2} = \frac{r^2}{(r-2m)^2} = z^{-2}, \\ F &= 0, \\ G &= (1-\frac{2m}{r})^{-1}r^2 = \frac{r^3}{(r-2m)} = z^{-1}r^2, \end{aligned} \tag{3.84}$$

From this we find that

$$\begin{aligned} E_\phi &= 0, \\ E_r &= \frac{-4z^{-3}}{r^2}, \\ F_\phi &= F_r = 0, \\ G_\phi &= 0, \\ G_r &= 2rz^{-1} - 2z^{-2} \end{aligned} \tag{3.85}$$

Now, we substitute these in the general case to obtain

$$\begin{aligned}\ddot{r} = \frac{1}{2(EG-F^2)}[&(-GE_r - FE_\phi + 2FF_r)\dot{r}^2 \\ &+ (-2GE_\phi + 2FG_r)\dot{r}\dot{\phi} + (-GG_r + 2GF_\phi + FG_\phi)\dot{\phi}^2]\end{aligned} \tag{3.86}$$

so that

$$\begin{aligned}\ddot{r} = \frac{1}{2(z^{-2}z^{-1}r^2 - 0)}[&(-z^{-1}r^2(z^{-3}r^{-2}) - 0)\dot{r}^2 \\ &+ (0+0)\dot{r}\dot{\phi} + (-z^{-1}r^2(2rz^{-1} - 2z^{-2}) + 0 + 0)\dot{\phi}^2]\end{aligned} \tag{3.87}$$

We therefore find

$$\ddot{r} = \frac{2}{r^2(1-\frac{2m}{r})}\dot{r}^2 + (-(1-\frac{2m}{r})r + 1)\dot{\phi}^2 \tag{3.88}$$

and finally

$$\ddot{r} = \frac{2m}{r(r-2m)}\dot{r}^2 + (r-3m)\dot{\phi}^2 \tag{3.89}$$

Similarly,

$$\begin{aligned}\ddot{\phi} = \frac{1}{2(EG-F^2)}[&(FE_r + EE_\phi - 2EF_r)\dot{r}^2 \\ &+ (2FE_\phi - 2EG_r)\dot{r}\dot{\phi} + (2FF_\phi - FG_r - EG_\phi)\dot{\phi}^2]\end{aligned} \tag{3.90}$$

so that

$$\begin{aligned}\ddot{\phi} = \frac{1}{2(z^{-2}z^{-1}r^2 - 0)}[&(0+0-0)\dot{r}^2 \\ &+ (0 - 2z^{-2}2rz^{-1} - 2z^{-2})\dot{r}\dot{\phi} + (0-0-0)\dot{\phi}^2]\end{aligned} \tag{3.91}$$

finally giving

$$\ddot{\phi} = \frac{-2}{r^2}(r - (1-\frac{2m}{r})^{-1})\dot{r}\dot{\phi} \tag{3.92}$$

This simplifies to

$$\ddot{\phi} = \frac{2(3m - r)}{r(r - 2m)} \dot{r}\dot{\phi} \tag{3.93}$$

Gathering the two equations together then, we have

$$\begin{aligned} \ddot{r} &= \frac{2m}{r(r - 2m)} \dot{r}^2 + (r - 3m)\dot{\phi}^2 \\ \ddot{\phi} &= \frac{2(3m - r)}{r(r - 2m)} \dot{r}\dot{\phi} \end{aligned} \tag{3.94}$$

which are same as were obtained previously.

In the next chapter we will use Matlab to solve these equations numerically, and hence to visualise the light cones in Schwarzschild space.

Chapter 4

Light Cones and Causal Structure for Schwarzschild Space-Time

This chapter will be about the visualisation of the causal structure of space in the vicinity of a Schwarzschild black hole.

4.1 A first look at causality in Schwarzchild space-time

As stated earlier, the metric of Schwarzschild space-time is

$$ds^2 = -(1 - \frac{2m}{r})dt^2 + (1 - \frac{2m}{r})^{-1}dr^2 + r^2(d\theta^2 + \sin^2\theta d\phi^2) \tag{4.1}$$

We will restrict our attention to $r > 2m$, the region outside the event horizon of the black hole.

Note that if we choose $r >> 2m$ then in the limit we find

$$ds^2 = -dt^2 + dr^2 + r^2(d\theta^2 + \sin^2\theta d\phi^2) \tag{4.2}$$

and if we set $(m = 0)$ we find the same metric, so when $r >> 2m$ the metric will be

very close to that of Minkoswki space time, and so will the causal structure.

If we choose another coordinate system such as the Eddington-Finkelstein or Kruskal coordinates [26], we can extend space-time inside the event horizon but we can not use our approach to study this region.

As stated earlier, in Minkowski space, given any two points P and Q, the vector $\overrightarrow{PQ}$ tells us the type of causal separation between P and Q. For example if we have P, Q two points the coordinate vector $\overrightarrow{PQ}$ satisfies $\langle \overrightarrow{PQ}, \overrightarrow{PQ} \rangle < 0, \langle \overrightarrow{PQ}, \overrightarrow{PQ} \rangle = 0, \langle \overrightarrow{PQ}, \overrightarrow{PQ} \rangle > 0$ depending on the separation are time-like, null, or space- like.

However, the situation is more complicated in Schwarzschild space-time. To see this, we consider the null geodesics in the (r, t) plane, which are given by

$$-(1 - \frac{2m}{r})dt^2 + (1 - \frac{2m}{r})^{-1}dr^2 = 0 \tag{4.3}$$

We rearrange to obtain

$$\left(\frac{dt}{dr}\right)^2 = (1 - \frac{2m}{r})^{-2} \tag{4.4}$$

and thus

$$\frac{dt}{dr} = \pm(1 - \frac{2m}{r})^{-1} \tag{4.5}$$

Now, when $r >> 2m$ we find

$$\frac{dt}{dr} = \pm 1 \tag{4.6}$$

so, $dt = -dr$ or $dt = dr$ giving us the Minkowski space situation very far from $r = 2m$. But we also need to consider the case when r is not much greater than $2m$.

For general $r > 2m$, selecting the $(+)$ sign, $\frac{dr}{dt} > 0$ and we integrate to have an outgoing radial null geodesic

$$t = r + 2m \ln |r - 2m| + constant \tag{4.7}$$

Alternatively, by selecting the $(-)$ sign then $\frac{dr}{dt} < 0$ and we integrate to have an ingoing radial null geodesic

$$t = -(r + 2m \ln |r - 2m| + constant) \tag{4.8}$$

This measures the slope of the light cones on spacetime diagram of the (t, r) plane. For large r the slope is (± 1), as it would be in flat space, and at $(r \to 2m)$ we get ,$(\frac{dt}{dr} \to \pm\infty)$, the light cone will close up, which we can interpret as light slowing down when it approaches the event horizon, or as red shift.

In (r, t) plane we can see no causal curve crosses event horizon. The situation is therefore much less straightforward than in the case of Minkowski space, even if we restrict to the (r, t) plane. But in order to understand the causal structure of Schwarzschild space-time, we need to know the other null geodesics, which are not radial. Even though we can compute the radial geodesics, the others cannot be found analytically in terms of standard elementary functions, so we have no easy way of describing the chronological future of a point.

However, building on what we have done before we will be able to use the numerical methods to visualise the light cone of P (with $t = 0$) for some range of values of t.

We will use Matlab to find light cones in equatorial plane when $(\theta = \pi/2)$. Furthermore, we will then use this to construct animations of growth of three dimensional wave front.

4.2 Matlab Code for Light Cones in Schwarzschild

As the purpose of this project was to produce code that would be made generally available for others to carry out their own investigations, we give a detailed explana-

tion of how it works to help a user either use it as it stands, or to adapt it to his or her own needs.

First, we now discuss the specialized Matlab code `wave_front_s.m`, which can be seen in Appendix A, and which gives visualizations of light cones in the equatorial plane in Schwarzschild space-time.

First, we will assume $m = 1$, so that the event horizon is at $r = 2$. Then the region $r < 2$ is inside the black hole where our approach does not work, so the region of interest is $r > 2$. We set $\theta = \pi/2$, then we have

$$ds^2 = -(1 - \frac{2}{r})dt^2 + (1 - \frac{2}{r})^{-1}dr^2 + r^2 d\phi^2 \tag{4.9}$$

and make the conformal transformation dividing by $1 - \frac{2}{r}$ to give the Riemannian metric

$$\left(1 - \frac{2}{r}\right)^{-2} dr^2 + \left(1 - \frac{2}{r}\right)^{-1} r^2 d\phi^2 = \frac{r^2}{(r-2)^2}dr^2 + \frac{r^3}{(r-2)^2}d\phi^2 \tag{4.10}$$

From this we obtain the equations for an arc-length parameterised geodesic:

$$\begin{aligned} \ddot{r} &= \frac{2}{r(r-2)}\dot{r}^2 + (r-3)\dot{\phi}^2 \\ \ddot{\phi} &= \frac{2(3-r)}{r(r-2)}\dot{r}\dot{\phi} \end{aligned} \tag{4.11}$$

Now, we will explain in some detail what the Matlab code does.

```
clf;
hold on;
axis equal;
```

These commands above will clear graphical screen, and set aspect ratio using axis

equal command to make data units the the same in every direction: thus in regions where the metric is nearly Minkowskian, the light rays will be at 45° to the horizontal, as in a standard space-time diagram.

This ensures that the diagram is appropriate for the interpretation of r and t as distance and time coordinates.

The next section of the code enables the user to specify just what he or she wants to examine.

```
T=input('Enter the evolution time period: ');
r=input('Enter the initial radial coordinate: ');
phi=0;
```

Here the user inputs time for which light cone develops, and the initial distance from origin. We can assume $\phi = 0$ without any loss of generality because of the radial symmetry, which permits us to use a rotation about the origin to give any initial point a ϕ coordinate of 0.

This allows the user to investigate how the development of the light cone light cone depends on distance from the event horizon, to focus on ranges of particular interest.

Next we calculate the conformal Schwarzschild metric at initial point

```
M=r^2/(r-2)*[1/(r-2) 0;0 r];
```

This sets up the Riemannian metric at the initial point, which must be used to construct unit vectors for initial conditions.

```
fprintf('Enter the range of tangent directions\n')
infin=input('you want to investigate in the form [start end]: ');
ndirs=input('Enter the number of directions: ');
circle=linspace(infin(1),infin(2),ndirs);
```

With these command the user is able to choose the range of initial directions and number of null geodesics to draw. The range $[0, 2\pi]$ gives full light cone, other choices allow detailed investigation of smaller sections. Choice of the number of directions, which are given equal angular separations, allows more detailed investigation when the geodesics have spread far apart. We will show examples later.

```
for theta=circle
```

The loop started here draws the null geodesic for each initial condition specified. Note that here we will need to express the initial vector in terms of polar coordinates rather than Cartesian.

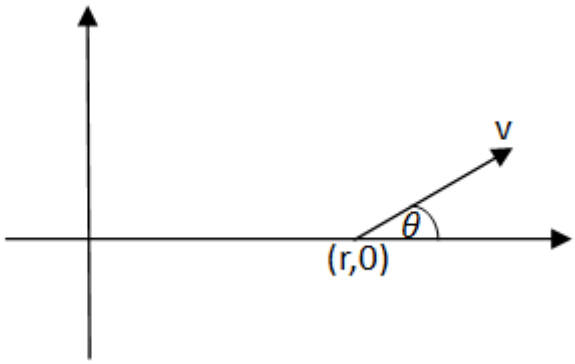

In terms of Cartesian coordinates, we have the tangent vector pointing in the direction θ at the point P with coordinates x, y [33].

$$\cos(\theta)e_x + \sin(\theta)e_y = [\cos(\theta), \sin(\theta)] \tag{4.12}$$

But we need to express this in terms of e_r, e_ϕ given by the polar coordinates r, ϕ. We have

$$x = r\cos(\phi), y = r\sin(\phi) \tag{4.13}$$

so we have

$$e_r = \frac{\partial}{\partial r} = \frac{\partial x}{\partial r}\frac{\partial}{\partial x} + \frac{\partial y}{\partial r}\frac{\partial}{\partial y} = \cos(\phi)e_x + \sin(\phi)e_y \tag{4.14}$$

and

$$e_\phi = \frac{\partial}{\partial \phi} = \frac{\partial x}{\partial \phi}\frac{\partial}{\partial x} + \frac{\partial y}{\partial \phi}\frac{\partial}{\partial y} = -r\sin(\phi)e_x + r\cos(\phi)e_y \tag{4.15}$$

which can we solve to give

$$\begin{aligned} e_x &= \cos(\phi)e_r - \frac{\sin(\phi)}{r}e_\phi \\ e_y &= \sin(\phi)e_r + \frac{\cos(\phi)}{r}e_\phi \end{aligned} \tag{4.16}$$

Therefore the vector

$$\cos(\theta)e_x + \sin(\theta)e_y \tag{4.17}$$

is, in terms of e_x, e_y,

$$\cos(\theta)\left(\cos(\phi)e_r - \frac{\sin(\phi)}{r}e_\phi\right) + \sin(\theta)\left(\sin(\phi)e_r + \frac{\cos(\phi)}{r}e_\phi\right) \tag{4.18}$$

i.e

$$(\cos(\theta)\cos(\phi) - \sin(\theta)\sin(\phi))e_r + ((\sin(\theta)\cos(\phi) - \cos(\theta)\sin(\phi))e_\phi)/r \tag{4.19}$$

which we can write as

$$[(\cos(\theta)\cos(\phi) - \sin(\theta)\sin(\phi)), ((\sin(\theta)\cos(\phi) - \cos(\theta)\sin(\phi)))/r] \tag{4.20}$$

In the case of our Schwarzschild code, we assumed $\phi = 0$, so this reduces to

$$[\cos(\theta), -\sin(\theta)/r] \tag{4.21}$$

for the initial vector, which is set up by the code

```
v= [cos(theta)  -sin(theta)/r]
```

But we also require our geodesics to be parametrised by arclength, which means that the initial tangent vector must be a unit vector.

For our case we will use this command

```
m=sqrt(v*M*v');
v=v/m;
```

it will make the initial vector of unit norm.

We now solve the geodesic starting at $(r, 0)$ in the direction θ using a built-in differential equation solver in Matlab by this command

```
[t,rphi]=ode45(@covdiff,[0,T],[r;phi;v(1);v(2)]);
```

where `covdiff` is the function to calculate covariant derivatives, given below.

Next, for each of these Riemannian geodesics, we can plot the corresponding null geodesic curve of Schwarzschild space, using

```
plot3(rphi(:,1).*cos(rphi(:,2)),rphi(:,1).*sin(rphi(:,2)),t);
```

Note that since we have computed the geodesics in terms of the polar coordinate (r, ϕ), we convert to Cartesian to plot them.

The previous commands draw the cone of null geodesics coming out from P at time 0. We finish the cone off by finding the wave front at the final time, obtained by joining together the end-points of the null geodesics.

```
TP=rphi(length(t),:);
TP=[TP(1),TP(2)];
ep=[ep;[TP(1)*cos(TP(2)),TP(1)*sin(TP(2))]];
```

These commands above find the end point of each geodesic and convert to Cartesian form for plotting, by picking off the end point to plot the front at time T.

To plot the curve joining the end points of each null geodesic to give the wave front at time t, we will use this command.

```
plot3(ep(:,1),ep(:,2),T*ones(size(ep(:,1))),'Color','black');
```

Since we know that the event horizon of Schwarzshild space (with $m = 1$) is at $r = 2$, we can also plot the event horizon:

```
colormap([1,0,0]);
[evX,evY,evZ]=cylinder(2,30); evZ=evZ*T; mesh(evX,evY,evZ);
```

The first command makes the event horizon red, since it is the surface of infinite red shift, and the second plots a cylinder of radius 2 and height the time the light cone grows for.

Included at the end of the m-file is the function which calculates the required covariant derivative of the tangent vector along the geodesic:

```
function dy = covdiff(t,y)
  dy = zeros(4,1);
  dy(1)=y(3);
  dy(2)=y(4);
  dy(3)=(2*y(3)^2/(y(1)*(y(1)-2)))+((y(1)-3)*y(4)^2);
  dy(4)=(-2*(y(1)-3)*y(3)*y(4)/(y(1)*(y(1)-2)));
end
```

In the function code above we use $y(1) = r, y(2) = \phi, y(3) = \dot{r}$, and $y(4) = \dot{\phi}$. Substituting these terms into the Matlab code recovers the original equations

$$\begin{aligned} \ddot{r} &= \frac{2}{r(r-2)}\dot{r}^2 + (r-3)\dot{\phi}^2 \\ \ddot{\phi} &= \frac{2(3-r)}{r(r-2)}\dot{r}\dot{\phi} \end{aligned} \tag{4.22}$$

4.3 Investigating the Light Cones of Schwarzschild Space-Time

In this section we will see how the Matlab code works to help us investigate the light cone and null geodesics in Schwarzchild space. We will examine how the light cone growth starting at a particular value of r is affected by the value of r.

Furthermore we will change the evolution time period to see how the growth progresses, and, when necessary, the number of geodesics to improve the quality.

In each figure the event horizon is shown as a red cylinder, ruled by vertical straight lines which are null geodesics.

4.3.1 Case Stude 1: Initial $r >> 2$

First we investigate the growth of the light cone for $r >> 2$, i. e. far from the event horizon. The dialogue

```
>>wave_front_s
Enter the evolution time period:   5
Enter the initial radial coordinate:   30
Enter the range of tangent directions
 you want to investigate:   [-pi  pi]
Enter the number of directions:   150
```

is to produce a light cone developed for a time of 5, with initial radial coordinate 30, the initial directions covering the entire circle, and 150 geodesics.

The dialogue for an evolution time of 10 is similar. This results in Fig (4.1)(4.2) As we expect, this looks very similar to the Minkowski case.

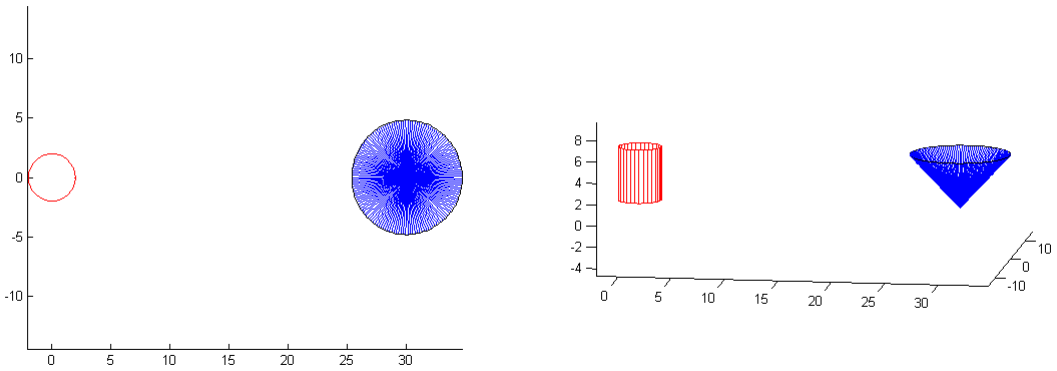

Figure 4.1: $t = 5, r = 30, n = 150$

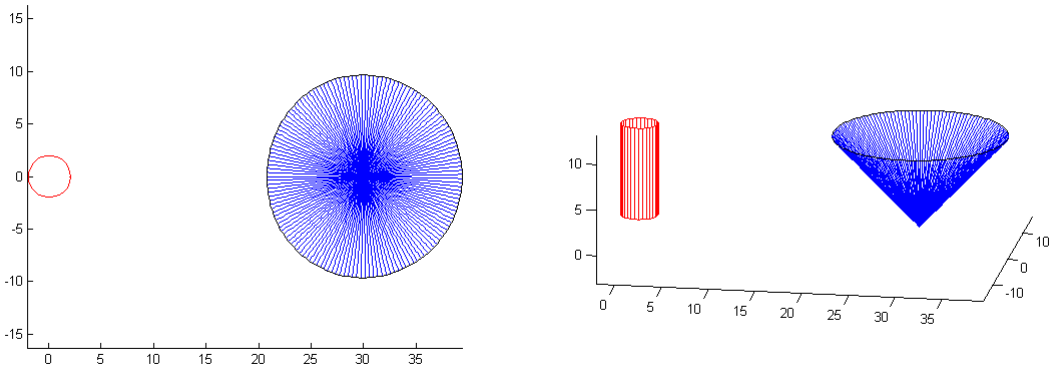

Figure 4.2: $t = 10, r = 30, n = 150$

4.3.2 Investigation (2)

Next , in the Fig(4.5) to (4.9) we consider light cones evolved for the same time, $t = 10, 15, 20$ but starting at different initial distances for $r = 4, 3, 2.5$.

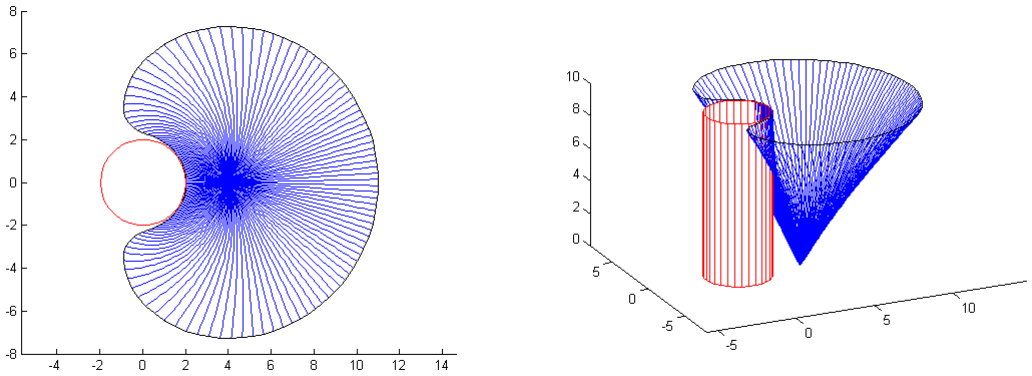

Figure 4.3: $r = 4, t = 10, n = 150$

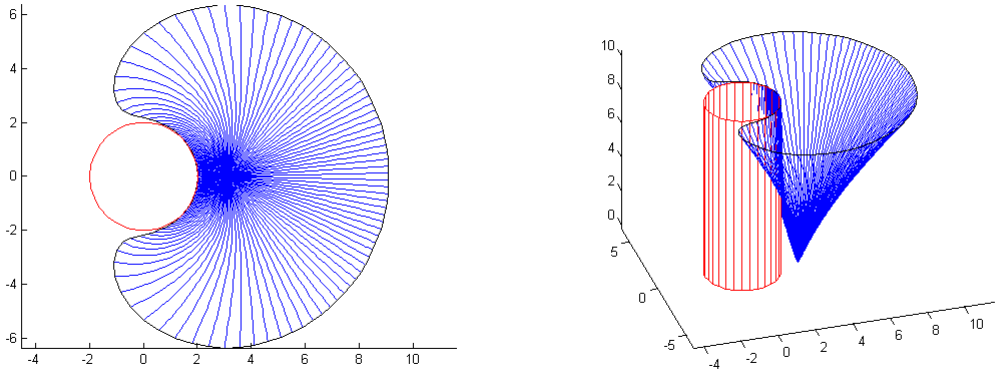

Figure 4.4: $r = 3, t = 10, n = 150$

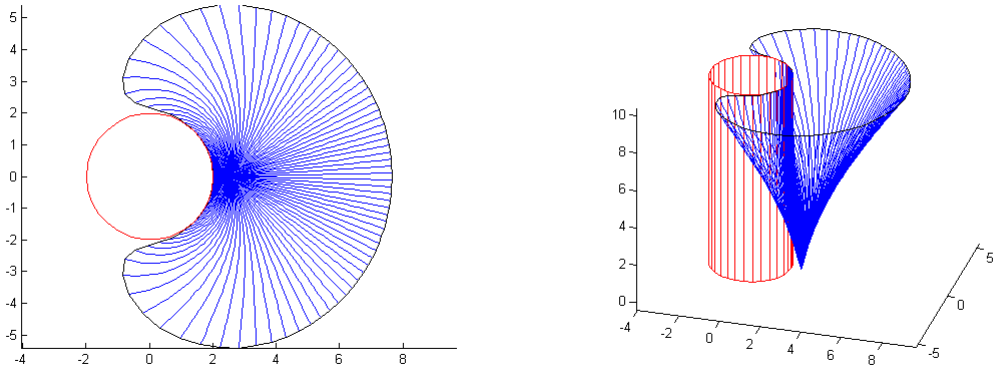

Figure 4.5: $r = 2.5, t = 10, n = 150$

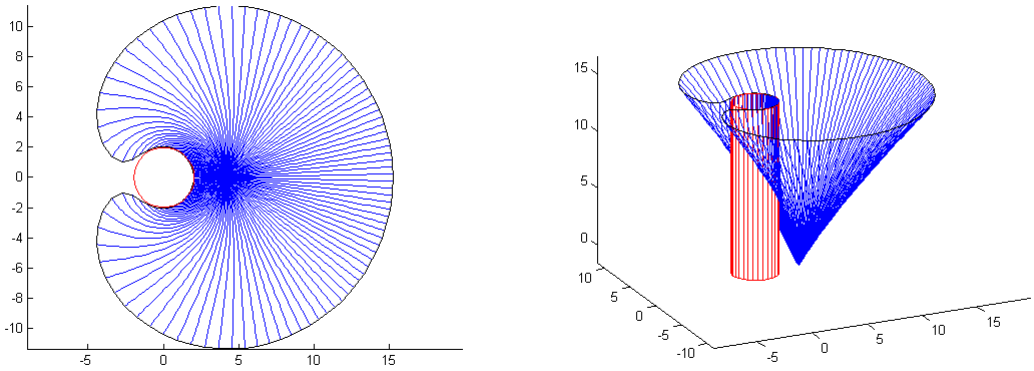

Figure 4.6: $r = 4, t = 15, n = 150$

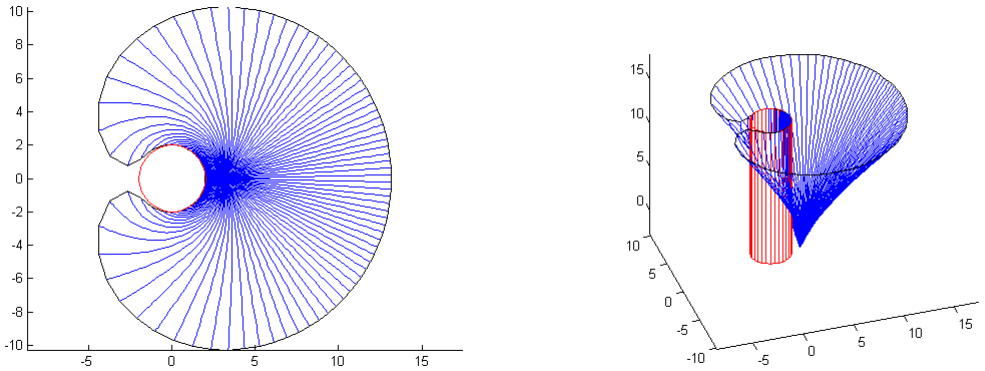

Figure 4.7: $r = 3, t = 15, n = 150$

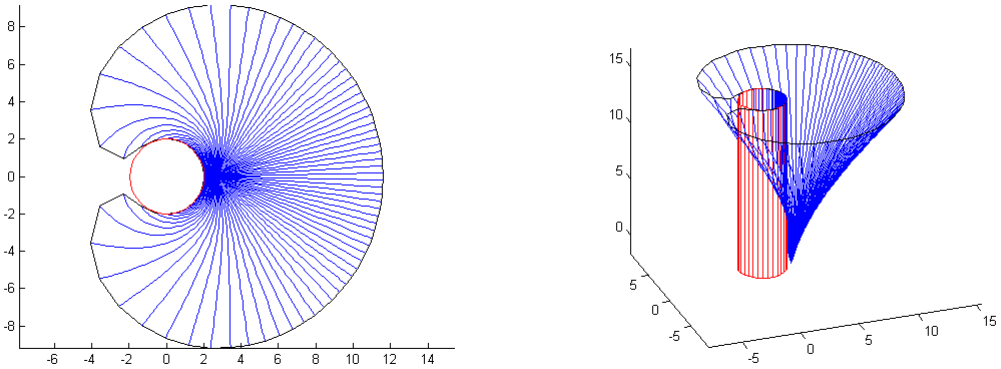

Figure 4.8: $r = 2.5, t = 15, n = 150$

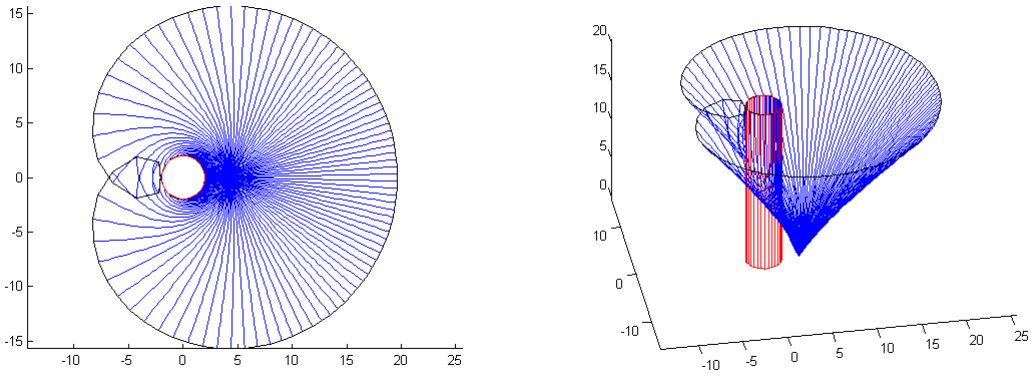

Figure 4.9: $r = 4, t = 20, n = 150$

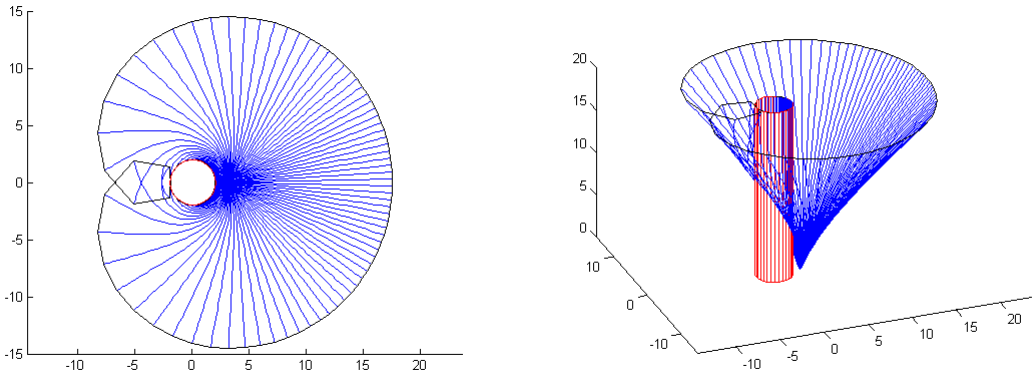

Figure 4.10: $r = 3, t = 20, n = 150$

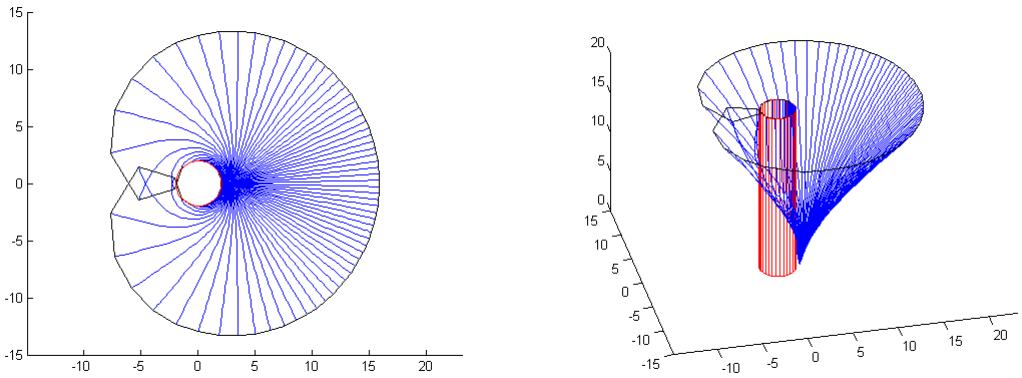

Figure 4.11: $r = 2.5, t = 20, n = 150$

At this point, because the null geodesics have spread out, we can see the pictures are not smooth. So, we redraw with $n = 300$ to obtain a better picture.

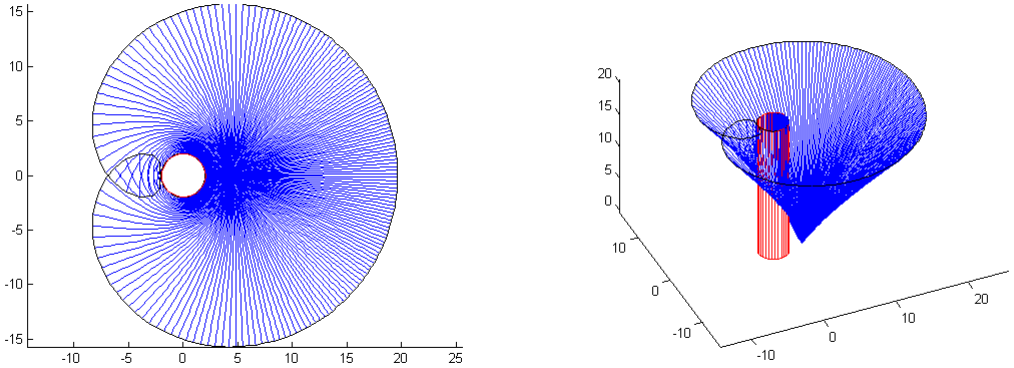

Figure 4.12: $r = 4, t = 20, n = 300$

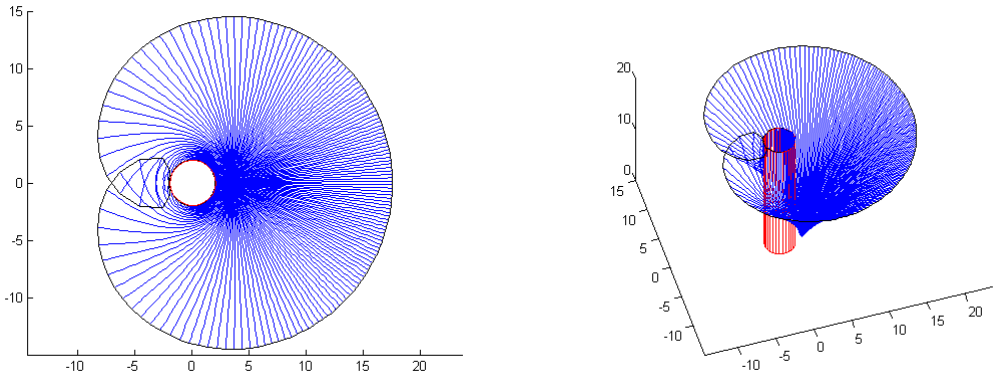

Figure 4.13: $r = 3, t = 20, n = 300$

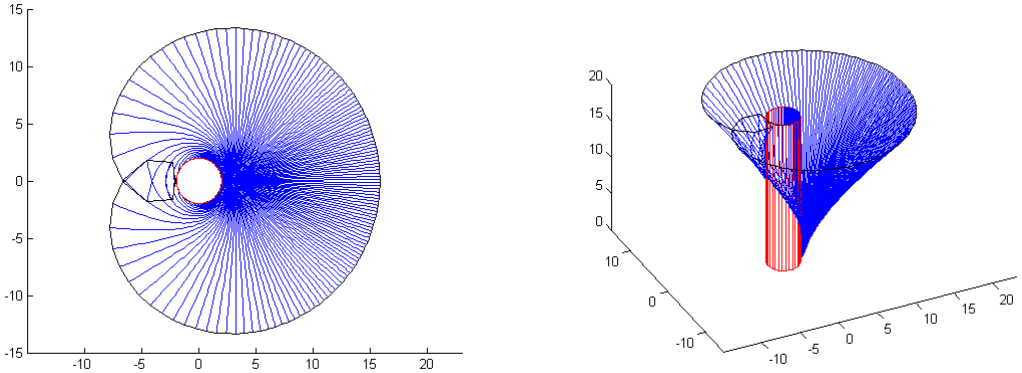

Figure 4.14: $r = 2.5, t = 20, n = 300$

We can interact with these figures panning, zooming and rotating to produce other images which shows how the null geodesics (at least initially) form the boundary of $I^+(P)$. We can also see more clearly how the light cone of P develops, in particular how it wraps around the event horizon at $r = 2$ without crossing it.

In these figures the lines emanating from the point P with coordinates $r = 4, 3, 2.5$, $\phi = 0$ are the null geodesics, and we can see how they are deflected and spread out by the black hole. Allowing the development to continue for a long enough lets a pairs null geodesics meet. Then an observer at the point at which they meet would see the point of origin at each side of the black hole. Recalling that the full situation is obtained by rotating about an axis connecting the origin of the plane P, we see that this produces the famous Einstein ring. Then, allowing the light cone to develop still further, we enter the situation where some of the null geodesics no longer lie on the boundary of $I^+(P)$, but enter $I^+(P)$[11].

By $t = 20$ we can see how the light cone has wrapped around the event horizon at $r = 2$

In a first course on general relativity we usually study and explain the gravitational lens effect, but not causal structure, except in the simple case of Minkowski space. Here we can clearly see from the diagrams how the gravitational lens is related with this idea of causal structure.

Furthermore, the figures show which points lie inside the light cone, i.e. those to the future of the initial point, and help us to understand how the causal structure of Schwarzchild space different from that of Minkowski space.

4.3.3 Case Study 2: Spreading of Null Geodesics

Now, instead of looking at the entire light cone, we consider a small portion of it in the neighbourhood of one particular geodesic to examine how the null geodesics spread out or focus.

We want to examine how the null geodesics in Schwarzchild space spread out. This spreading is determined by the Jacobi equation, which we cannot solve explicitly; however, the illustrations give extra insight into the behaviour we can obtain from the Jacobi equation [27].

In general, the way in which the geodesics leaving a single point spread out is determined by the Jacobi equation, which in two dimensions reduces to

$$\ddot{p} + Kp = 0, \tag{4.23}$$

where $p(0) = 0, \dot{p}(0) = 1$.

Here, p is the distance between points at the same affine parameter value a pair of neighbouring null geodesics and, K is the curvature operator (Gaussian Curvature), in the 2-d Riemannian space [28].

Note: in Minkowski space, $K = 0$, so geodesics spread out linearly.

We can find this equation explicitly: though we cannot solve it explicitly in terms of elementary functions, we can still obtain information from its form.

Now, we have an orthogonal coordinate system ($F = 0$), so the Gaussian curvature K is given by [29]

$$K = (\frac{-1}{2})(EG)^{-1/2}[(E_r(EG)^{(-1/2)}))_r + (G_\theta(EG)^{(-1/2)})_\theta] \tag{4.24}$$

and, we have

$$\begin{aligned} E &= ((1-2/r)^{-2}), \\ F &= 0, \\ G &= r^2(1-2/r)^{-1} \end{aligned} \tag{4.25}$$

and furthermore these functions depend only on r; we find

$$\begin{aligned} E_r &= -4r/(r-2)^3, \\ E_{rr} &= 8(r+1)/(r-2)^4 \\ G_r &= r^2(3r-6-r)/(r-2)^2 \\ G_\theta &= 0 \end{aligned} \tag{4.26}$$

We substitute E, F, G and find the Gaussian curvature, we find

$$\begin{aligned} K = (\frac{-1}{2})(((1-2/r)^{-2})(r^2(1-2/r)^{-1}))^{(\frac{-1}{2})}[(E_r(((1-2/r)^{-2})(r^2(1-2/r)^{-1}))^{(\frac{-1}{2})})_r \\ + (G_\theta(((1-2/r)^{-2})(r^2(1-2/r)^{-1}))^{(\frac{-1}{2})})_\theta] \end{aligned} \tag{4.27}$$

which simplifies to

$$\begin{aligned} K = (\frac{-1}{2})(((1-2/r)^{-2})(r^2(1-2/r)^{-1}))^{(\frac{-1}{2})}[(((-4r/(r-2)^3) \\ (((1-2/r)^{-2})(r^2(1-2/r)^{-1}))^{(\frac{-1}{2})}))_r + 0] \end{aligned} \tag{4.28}$$

and finally

$$K = -\frac{6(r-1)}{r^5(r-2)} \tag{4.29}$$

For $r > 2$, this is always negative, and so p has no zeros except at 0. This tells us that there are no conjugate points on any null geodesics in Schwarzschild space.

In general it is very difficult to solve the Jacobi equation, since we have to solve for the geodesic first, but we can consider the special case of null geodesics on the photosphere, $r = 3$ [30].

We can calculate Gaussian curvature when $r = 3$ then

$$k = -\frac{6(r-1)}{r^5(r-2)} \tag{4.30}$$

$$k = -\frac{6(3-1)}{3^5(3-2)} \tag{4.31}$$

$$k = \frac{-4}{81} \tag{4.32}$$

Then, the Jacobi equation is

$$p'' + \frac{-4}{81}p = 0, \tag{4.33}$$

we which can easily solve and we get exponential growth: the following diagrams show how they spread out.

The following dialogue plots the development of a fan of null geodesics centred on one lying on the photosphere, $r = 3$.

```
>>wave_front_s
Enter the evolution time period:  30
Enter the initial radial coordinate:   3
Enter the range of tangent directions
 you want to investigate:   [pi/2 +.01    pi/2 -.01]
Enter the number of directions:   15
```

Figure(4.15) shows the surface produced by a choice of 30 for the development times, an initial radial coordinate of 3, so that the initial point lies on the photon sphere, and the range $[\pi/2 + .01, \pi/2 - .01]$ for tangent direction, so that a geodesic

of constant r is included. Only a small part of the full circle is produced and 15 geodesics are plotted. We clearly see in this diagram how the geodesics spread out

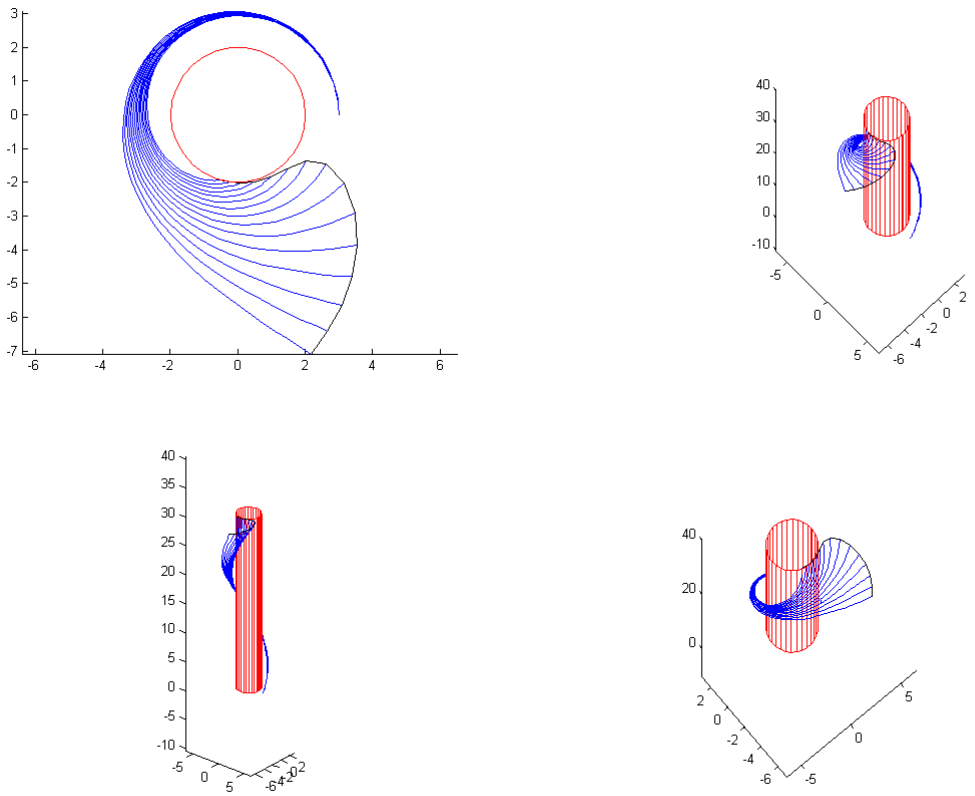

Figure 4.15: $r = 3, t = 30$, $n = 15, \theta = [pi/2 + .01, pi/2 - .01]$

very rapidly.

We can also consider a fan of geodesics leaving p centred on other directions and the approach slowing down near the event horizon, as shown in Fig (4.16), which displays geodesics starting at $r = 3$, but now in a small interval around $\theta = \pi$, so these null geodesics heading approximately directly towards the event horizon. Note that in the diagrams it seems as if some geodesics stop separating as they approach $r = 2$. This is an illusion caused by our choice of coordinates, as the spatial part of the metric in fact diverges at $r = 2$, and so these points are in fact very far apart.

In fig (4.17), on the other hand the null geodesics travel away from the event hori-

zon leaving p in directions centred on $\theta = 0$; the light rays behaviour in this case is like the Minkowski case.

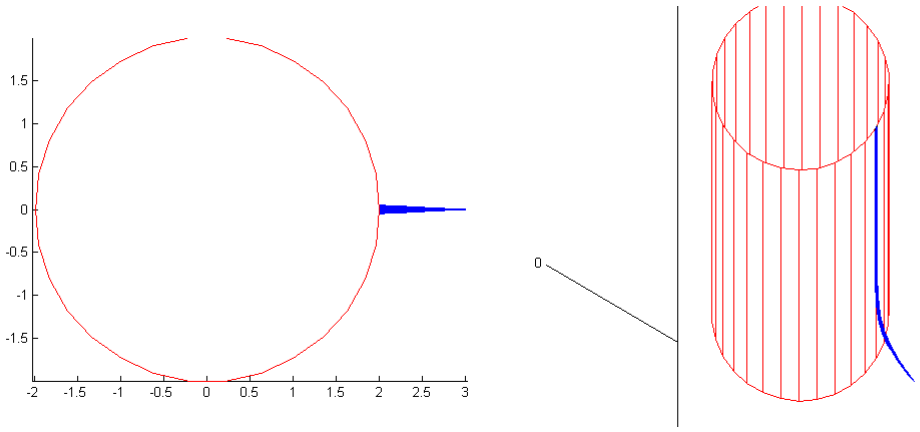

Figure 4.16: $r = 3, t = 30$, $n = 15, \theta = [pi + .05, pi - .05]$

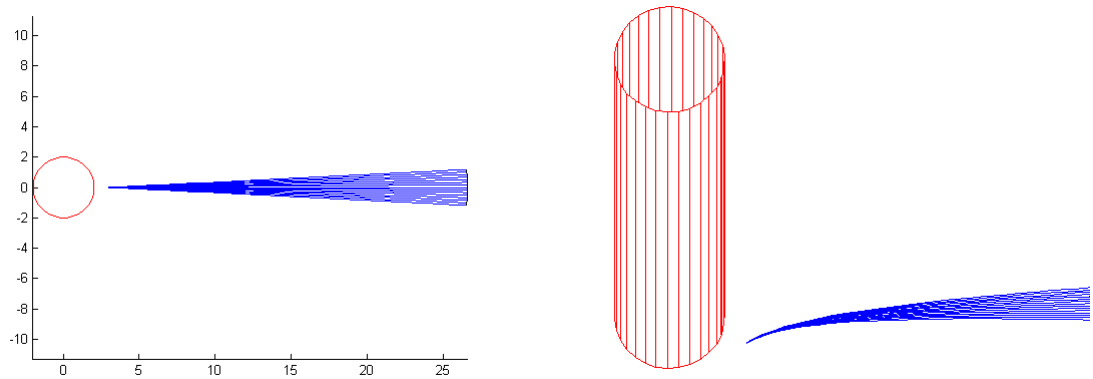

Figure 4.17: $r = 3, t = 30$, $n = 15, \theta = [0 + .05, 0 - .05]$

4.3.4 Case Study 4: Single Null Geodesics

Finally we can look at individual null geodesics and connect this approach with the standard one of drawing a diagram in the (r, ϕ) plane to illustrate the gravitational bending of light.

The dialogue

```
>> wave_front_s
Enter the evolution time period:   30
Enter the initial radial coordinate:   3
Enter the range of tangent directions
 you want to investigate:   [pi/2   pi/2 ]
Enter the number of directions:   1
```

produces a single null geodesic with initially $r = 0$, and $\theta = \pi$, so the geodesic is a closed circle in the (r, ϕ) plane. Figure(4.18) shows this,

and we can see explicitly here how the trajectory is a closed circle in the (r, ϕ) plane,

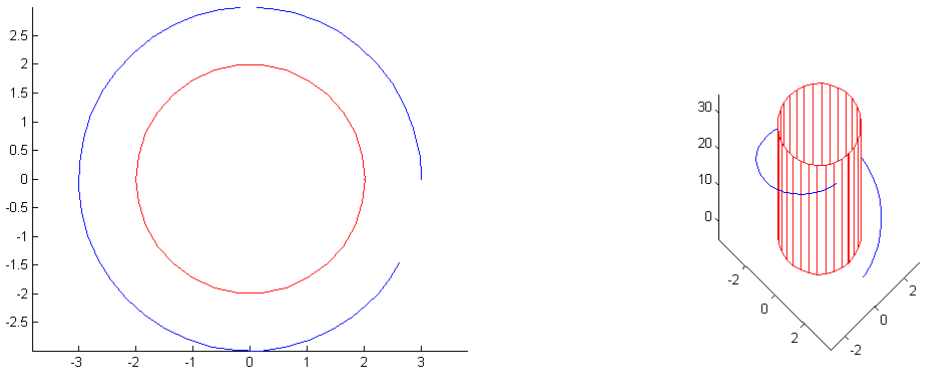

Figure 4.18: $r = 3, t = 30$, $n = 1, \theta = [\pi/2, \pi/2]$

and a spiral wrapping around the event horizon in the space-time picture.

We can also see how a light ray which does not pass too close to the event horizon is deflected, in the next figures.

We see that if the light ray does not pass too closely, then it starts off as a nearly straight line for $r >> 1$, then is deflected, and finally approaches a new straight line at $r >> 1$, but after being turned through some possibly large angle.

Figures 4.19 to 4.21 show some illustrative examples of a light ray bending around the event horizon, as we vary r, t, θ.

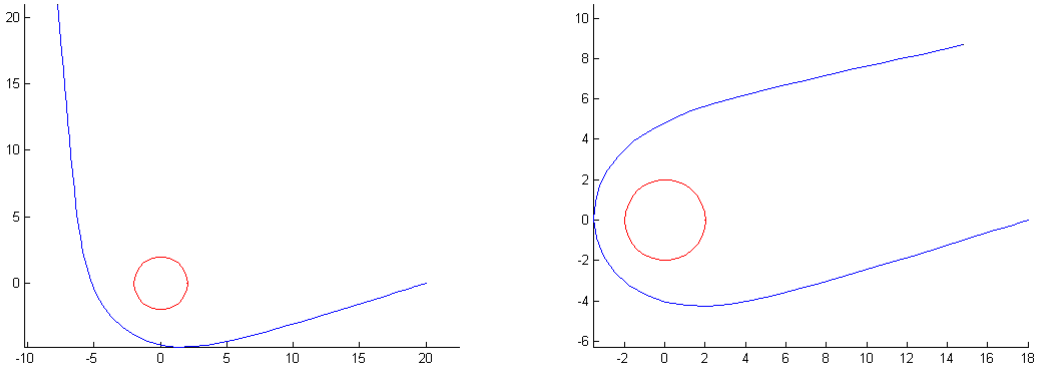

Figure 4.19: $r = 20, 18, t = 60$, $n = 1$, $\theta = [pi + 0.3, pi + 0.3]$

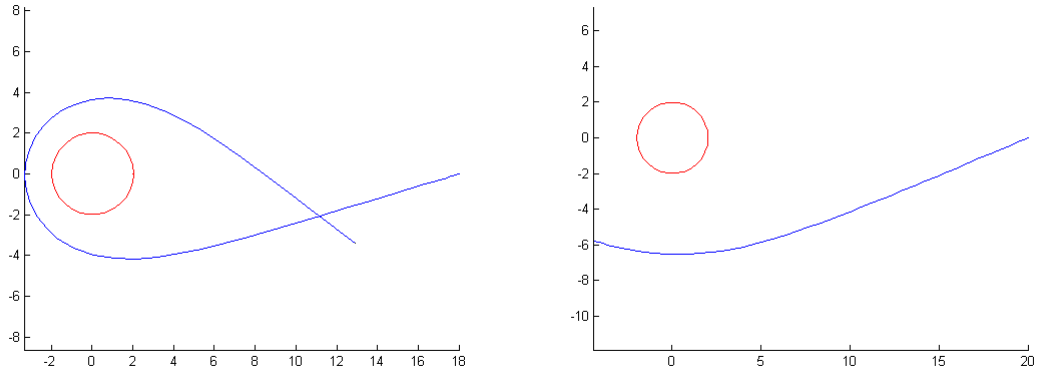

Figure 4.20: $r = 18, 20, t = 60, 30$, $n = 1$, $\theta = [pi + 0.295 pi + 0.295]$,and $\theta = [pi + 0.4, pi + 0.4]$

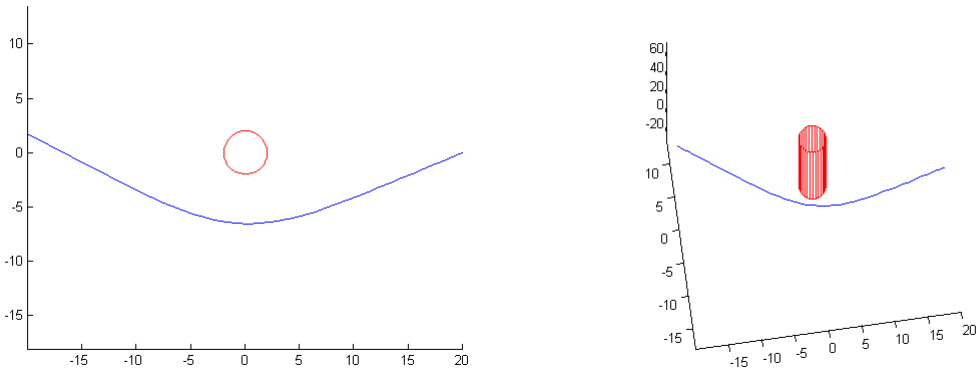

Figure 4.21: $r = 20, t = 50, n = 1, \theta = pi + 04$

Finally, in fig 4.22 to fig 4.24 we see how that a light ray which passes too close to event horizon becomes trapped and cannot escape. This shows how the general relativistic picture is qualitatively different from an attempt to treat light deflection as the orbit of a particle in Newtonian mechanics, since in Newtonian mechanics, all orbits of this form would be either elliptical or hyperbolic, and would eventually escape to infinity.

In fig (4.22), we can also see how the null geodesic travels around and approaches close to event horizon. By rotating the figure, we can inspect how the null geodesic develops in space-time, and in particular here we can see how as time passes the null geodesic asymptotically approaches one of the generating null geodesics of the event horizon.

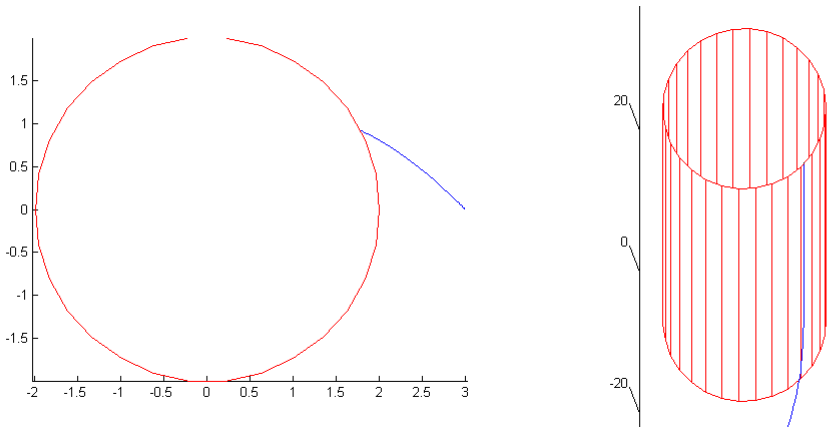

Figure 4.22: $r = 3, t = 30$, $n = 15, \theta = [3pi/4 + .01, 3pi/4 - .01]$

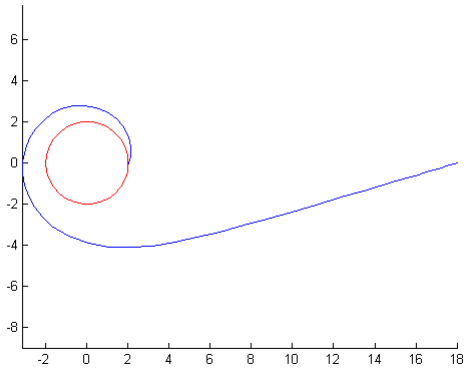

Figure 4.23: $r = 18, t = 60, n = 1, \theta = [pi + 0.29pi + 0.29]$

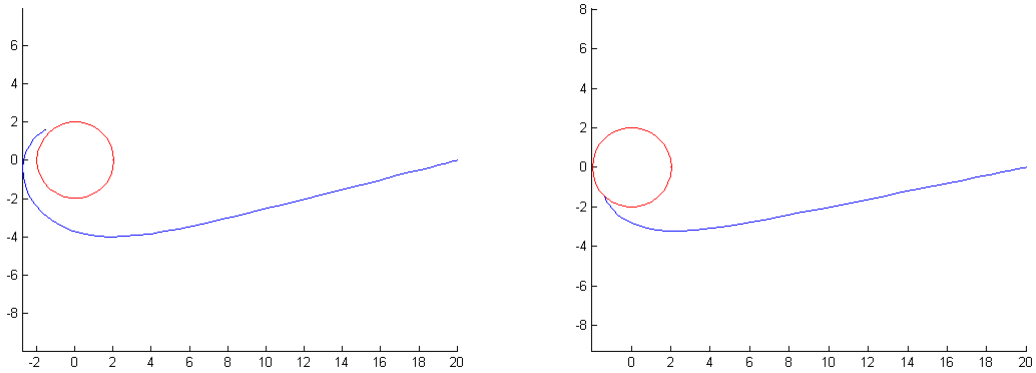

Figure 4.24: $r = 20, t =, 40, 50$, $n = 1$, $\theta = pi + .25$, and $\theta = pi + 0.2$

4.4 3-dimensional Wave-Fronts

A second program, `wave_front_3d_s.m` which is heavily based on `wave_front__s.m`, produces an animation of the growth of the full light cone in three spatial dimensions.

We can get a section of the full light cone at a given time by rotation of the equatorial section around an axis of symmetry passing through $r = 0$ and the initial point.

In this program the user can select the initial event, the time of development, the number of geodesics to compute in the equatorial plane, and the number of frames to build for the animation. The interaction dialogue is of the following form:

```
>> wave_front_3d_s
Enter the evolution time period: 15
Enter the initial radial coordinate: 3
Enter the number of geodesics to compute: 150
How many frames? 20
```

and the associated code initializes `Ts`, the amount of time the light cone develops form, `r`, the initial radial coordinate, `ndirs` the number of different geodesics which will be used to construct the surface, and k, the number of frames in the animation from $t = 0$ to $t = Ts$.

The Matlab code is based on the previous one but extended to compute snapshots of the development of the light cone, not just the final version, and also to produce the full light cone at each t, not just the equatorial section.

This loop

```
for k = 1:frames
  T=k*Ts/frames;
```

is to calculate each frame of the animation depended on evolution time and number of frames, with an equal time internal between the frames.

The geodesics are then calculated in just the same way as previously, but now for all the intermediate values of t, not just the final one. At each intermediate time, to build the 3-dimensional surface of revolution, with a number of angular steps determined by the value of the variable `rots` steps we used this code

```
x=ep(:,1);
y=ep(:,2);
rots=40;
theta=linspace(0,pi,rots);
X=kron(x,ones(size(theta)));
Y=kron(y,cos(theta));
Z=kron(y,sin(theta));
```

which rotates the wave front at each time about the line joining the origin to P.

Next,

```
surf(X,Y,Z);
axis([r-Ts,r+Ts,-Ts,Ts,-Ts,Ts]);
axis square;
```

plots the surface inside a square box of appropriate size, centred on the initial point and with a side length large enough to contain the final wave front.

The code

```
alpha(0.5);
```

sets the degree of transparency of the surface, and finally

```
W(k)=getframe;
```

constructs the animation of the light cone's development, and stores it in `W`, the value returned by the m-file.

It is not possible to show the animation in this document, but we can show some snapshots of the development: If desired, rather than constructing and running the

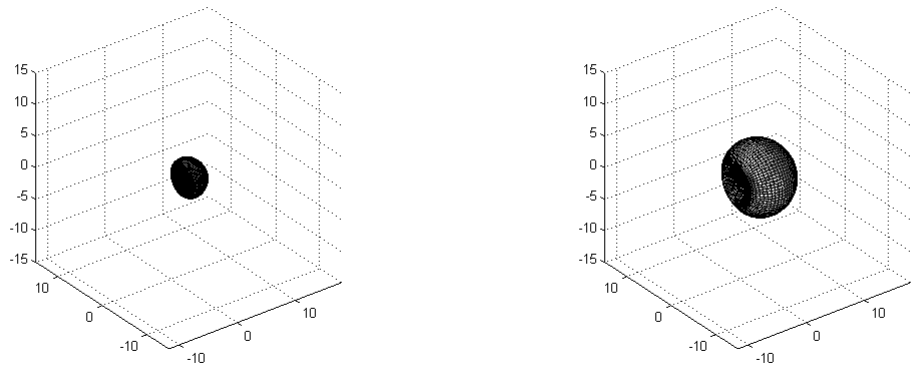

Figure 4.25: $t = 5, 10, r = 3, n = 150, frames = 20$

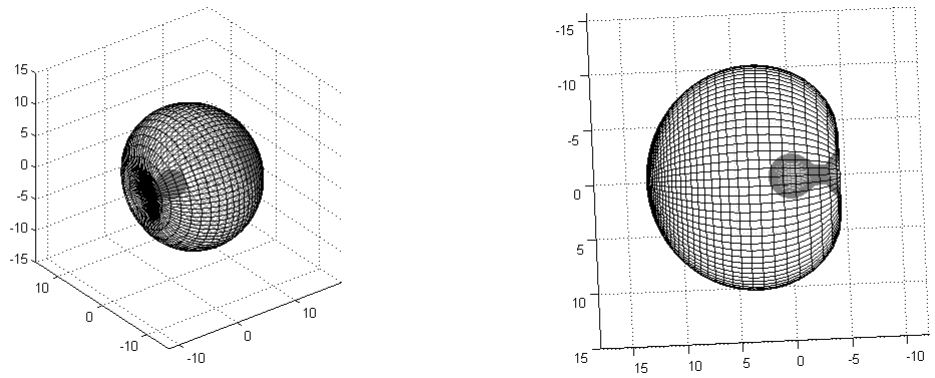

Figure 4.26: $t = 15, r = 3, n = 150, frames = 20$

animation interactively, we can use the command

```
>> w= wave_front_3d_s.m
```

to save the animation, and

```
>> w= movie(w)
```

to play it, or

```
>> movie2avi(w,'file name', )
```

to construct an avi file that can be viewed using any appropriate media player.

In addition, by editing the file so that we do not rotate the equatorial section completely in figure 4.27, we can see a part of the rotation inside the wave front, or a part of section by changing the code as follows:

```
theta=linspace(0,pi/2,rots);
```

or

```
theta=linspace(0,pi/6,rots);
```

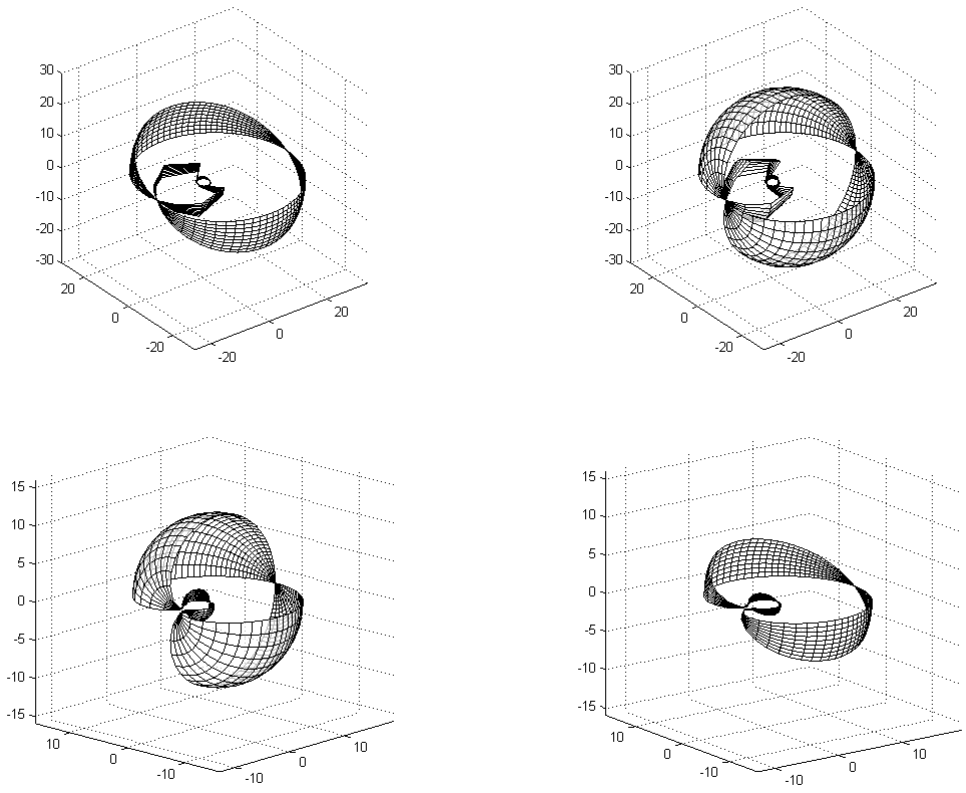

Figure 4.27: Theta= linspace $(0, pi/2, rots)$, linspace$(0, pi/6, rots)$, with different time development.

4.5 Conclusion

We have seen how we can use Matlab functions to investigate the light rays, and light cones of Schwarzchild space in a user-friendly and interactive way.

In the next chapter we will see how to extend this to allow the user to specify the metric in either polar or Cartesian coordinates, and explore a variety of metrics.

Chapter 5

Matlab for General Metrics

5.1 Introduction

In Chapter 5 we considered Matlab code which enables us to explore the null geodesics and light cones of Schwarzschild space, using polar coordinates. This code was specific to Schwarzchild space, used only basic Matlab commands, and can easily be converted to work in free versions of Matlab such as Octave.

In this chapter we will generalise this to an arbitrary static (2+1) dimensional space-time, using the more specialized symbolic manipulation facilities of Matlab to compute the geodesic differential equations for a user specified metric. For this we have use the Matlab symbolic manipulation toolbox; Octave also has a symbolic manipulation toolbox, but the syntax is different, and the code can not be so easily converted to work in Octave.

In this section we will assume that the space-time is asymptotically flat [12], so that it makes sense to use background polar or Cartesian coordinates, and we allow the user to choose between these two.

This general code will then be used to explore some interesting metrics, including Schwarzschild and some other black hole metrics. In the cases where spherical sym-

metry holds, it is also possible to constrict the full (3+1) development of the light cone by the same method as on Chapter 5.

The procedure that a user follows will be first to run the program `choose_metric.m` this allows the user to specify the riemannian two-metric and produces mfiles containing the functions required to solve the null geodesics equation numerically. Once this program has been used, the user can run `wave_front_general` to carry out investigations of this metric in just the same way as was done in the previous section for the Schwarzschild metric.

In the remainder of this chapter we will give an explanation of the Matlab code, and describe a couple of simple tests which check that it agrees with earlier results.

5.2 Matlab code

The first m-file allows the user to specify a metric, and computes the coefficients of the geodesic equations using the symbolic toolbox.

The user inputs the metric components in terms of coordinates x, y, which may be Cartesian or polar, and the code produces the function which specifies the geodesic equations for this metric.

The first section,

```
disp('Please select the metric coefficients E,F,G as functions of x,y so');
disp(' that the metric is Edx^2+2Fdxdy+Gdy^2 ');
E=input('E =' );
F=input('F =' );
G=input('G =' );
```

allows the user to input the functions E, F and G as strings in standard matlab notation.

Next,

```
I=[E F;F G];
If=matlabFunction(I);
Ex=diff(E,x);
Ey=diff(E,y);
Fx=diff(F,x);
Fy=diff(F,y);
Gx=diff(G,x);
Gy=diff(G,y);
```

computes all the required derivatives of E, F and G.

Next,

```
p= (1/(2*(E*G-F^2)))*((-G*Ex-F*Ey+2*F*Fx)*xd^2+
(- 2*G*Ey+2*F*Gx)*xd*yd+(G*Gx-2*G*Fy+F*Gy)*yd^2);
q= (1/(2*(E*G-F^2)))*((F*Ex+E*Ey-2*E*Fx)*xd^2+
(2*F*Ey-2*E*Gx)*xd*yd+(2*F*Fy-F*Gx-E*Gy)*yd^2);
xdd=matlabFunction(p);
ydd=matlabFunction(q);
```

defines the functions p and q such that $\ddot{x} = p(x, y, \dot{x}, \dot{y})$ and $\ddot{y} = q(x, y, dotx, \dot{y})$, and finally

```
Mf=matlabFunction(I,'vars',[x,y],'file','M');
xdd=matlabFunction(xdd,'vars', [x,y,xd,yd],'file', 'p');
ydd=matlabFunction(ydd,'vars', [x,y,xd,yd],'file', 'q');
```

creates m-files which calculate p and q, for use by the differential equation solving routine.

We also have an m-file `pdode.m` which uses the functions p and q to calculate the covariant derivative along a curve and combine these into a single function . This is the function called by the ordinary differential equations solver in `wave_front_general`.

```
function dy = pqode(t,y)
dy = zeros(4,1);
dy(1)=y(3);
dy(2)=y(4);
dy(3)=p(y(1),y(2),y(3),y(4));
dy(4)=q(y(1),y(2),y(3),y(4));
end
```

Once this has been done, and the geodesic equations set up, we use the general Matlab code `wave_front_general` to calculate and display the development of the light cone for this metric for a user-specified choice of Cartesian or polar coordinates, time of evolution, initial point, range of directions and number of null geodesics.

This work is carried out by a separate mfile to the one which sets up the differential equations, since we may wish to carry out many investigations of light cones for the metric, and it would be inefficient to have to carry out the same work before each investigation.

First, the user selects the background coordinate system.

```
test=-1;
while test~= 1 && test~=2
test= input('For cartesian coordinates enter 1
and for polar coordinates enter 2:  ');
end
```

We use the logical variable cartesian and polar to make the code more intelligible.

```
cartesian=test==1;polar=test==2;
```

Next, we obtain the parameters of the initial point and light cone, using the logical variables to make the appropriate prompt to the user.

```
T=input('Enter the evolution time period: ');
if cartesian
    x0=input('Enter the initial value of x: ');
    y0=input('Enter the initial value of y: ');
end
if polar
    x0=input('Enter the initial value of r: ');
    y0=input('Enter the initial value of phi: ');
end
```

In this section, since we do not assume that the metric is radially symmetric, we must allow a free choice of the initial value of ϕ.

We next input the directions which will be used to construct the light cone and the endpoints for the light cone as a vector, which is much the same as the Schwarzschild code.

```
fprintf('Enter the range of tangent directions\n')
infin=input('you want to investigate in the form [start end]: ');
ndirs=input('Enter the number of directions: ');
circle=linspace(infin(1),infin(2),ndirs);
```

The program now calculates the null geodesics emanating from $(x0, y0)$ and their endpoints. `ep` will be the locus of geodesic endpoints after time T and we must now express the initial vector in terms of the appropriate coordinates

```
ep=[];
 for theta=circle
   if cartesian v=[cos(theta),sin(theta)]; end
   if polar v=[cos(theta)*cos(y0)+sin(theta)*sin(y0),
   (sin(theta)*cos(y0)-cos(theta)*sin(y0))/x0]; end
```

Note that in the case of polar coordinates we must now use the general form for the initial tangent vector, since we no longer assume that $\phi = 0$.

Next, we normalise to obtain a unit vector

```
m=sqrt(v*M(x0,y0)*v');
v=v/m;
```

Finally, we solve the geodesic starting at $(x0, y0)$ in direction θ and convert from polar to Cartesian if necessary for plotting:

```
[t,xy]=ode45(@pqode,[0,T],[x0;y0;v(1);v(2)]);
if polar
    xtemp=xy(:,1).*cos(xy(:,2)); ytemp=xy(:,1).*sin(xy(:,2));
     xy(:,1)=xtemp; xy(:,2)=ytemp;
end;
```

Next, we plot the geodesic from $(x0, y0)$ with initial direction θ, and collect the end points which will be drawn to show the final wave front at $t = T$.

```
plot3(xy(:,1),xy(:,2),t)
TP=xy(length(t),:);
ep=[ep;TP];
```

```
end
```

And finally, plot the locus of the endpoints of the geodesics.

```
plot3(ep(:,1),ep(:,2),T*ones(size(ep(:,1))),'Color','black');
```

5.3 Test

It is sensible to check the code against known results. Here, we check that it gives the cones we expect in Minkoski space, and that it produces the same results as the specialist Schwarzschild code when we choose the Schwarzschild metric.

5.3.1 Minkowski Space in Cartesian Coordinates

Here, we will apply the general program to Minkowski space in Cartesian coordinates: we have $E = 1, F = 0, G = 1$, and choose $(x_0, y_0) = (10, 10)$ and $t = 5$. Because Matlab needs to see some dependence on a symbolic variable for the metric to work as a function, we cannot simply set E and G to be 1, but must use an expression involving at least one symbolic variable which reduces to 1.

```
Please select the metric coefficients E,F,G as functions of x,y
 so that the metric is Edx^2+2Fdxdy+Gdy^2
E =x/x
F =0
G =x/x
```

After choosing the metric and setting up the geodesic equations, we run `wave_front_general`

```
For cartesian coordinates enter 1 and for polar coordinates enter 2:  1
Enter the evolution time period: 5
```

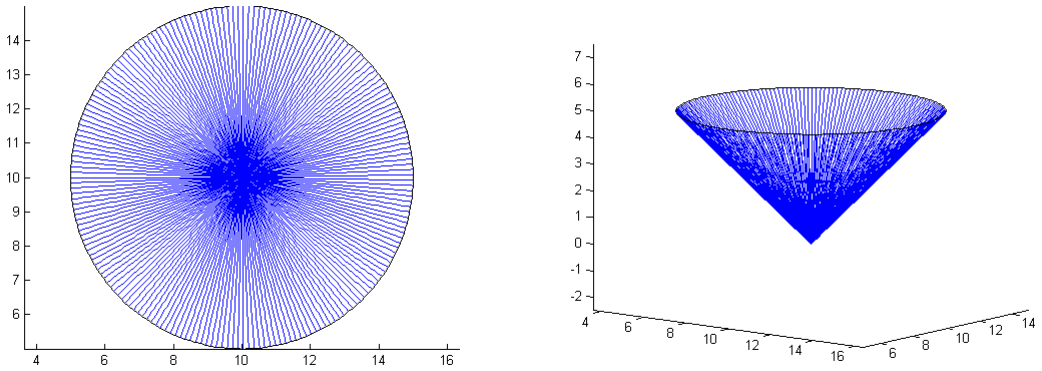

Figure 5.1: Minkowski Space in Cartesian Coordinates

```
Enter the initial value of x: 10
Enter the initial value of y: 10
Enter the range of tangent directions
you want to investigate in the form [start end]: [-pi pi]
Enter the number of directions: 200
>>
```

we find these figures 5.1 So when we choose the flat metric in Cartesian coordinates, we obtain the cones which we expect.

5.3.2 Minkowski Space in Polar Coordinates

Now, we will apply the general program with Minkowski Space Polar Coordinates, when $E = 1, F = 0, G = r^2$, $(r_0, \phi_0) = (10, \pi/4)$ and $t = 5$. In this case the metric is

$$dr^2 + r^2 d\phi^2 \tag{5.1}$$

An we have the dialogue dialogue

```
Please select the metric coefficients E,F,G as functions of x,y
```

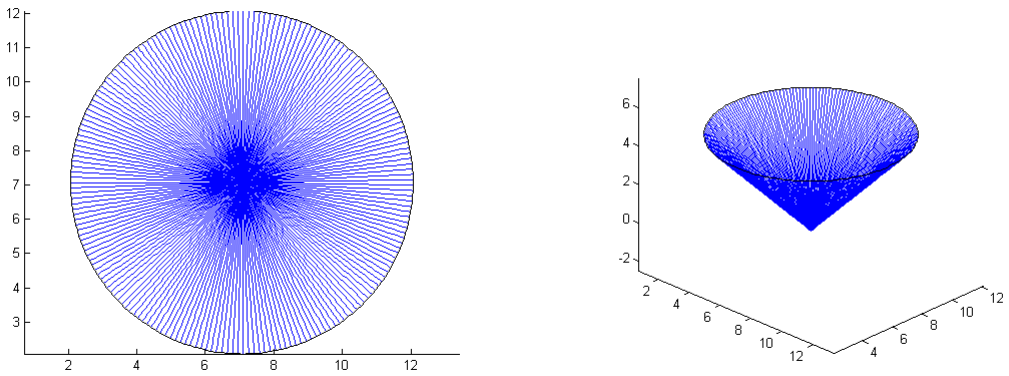

Figure 5.2: Minkowski Space Cartesian Coordinates

```
 so that the metric is Edx^2+2Fdxdy+Gdy^2
E =1
F =0
G =x^2
```

After choosing the metric and setting up the geodesic equations, we run `wave_front_general`

```
For Cartesian coordinates enter 1 and for polar coordinates enter 2:  2
Enter the evolution time period: 5
Enter the initial value of r: 10
Enter the initial value of phi: pi/4
Enter the range of tangent directions
you want to investigate in the form [start end]: [-pi pi]
Enter the number of directions: 200
```

we find these figures 5.2. These figures agree with the previous ones, and, of course with the known correct result.

5.3.3 Schwarzschild

We now apply the general program to Schwarzschild space, where the Riemannian metric is

$$\frac{r^2}{(r-2)^2}dr^2 + \frac{r^3}{(r-2)}d\phi^2 \tag{5.2}$$

so that $E = r^2/(r-2)^2, F = 0, G = r^3/(r-2)$. We choose $(r_0, \phi_0) = (4, 0)$ and $t = 13$.

Then we select the metric by running `choose_metric.m` with the following dialogue:

```
Please select the metric coefficients E,F,G as functions of x,y so
 that the metric is Edx^2+2Fdxdy+Gdy^2
E =x^2/(x-2)^2
F =0
G =x^3/(x-2)
```

After choosing the metric and setting up the geodesic equations, we run `wave_front_general`

```
For Cartesian coordinates enter 1 and for polar coordinates enter 2:  2
Enter the evolution time period: 13
Enter the initial value of r: 4
Enter the initial value of phi: 0
Enter the range of tangent directions
you want to investigate in the form [start end]: [-pi pi]
Enter the number of directions: 200
>>
```

and we find the figures 5.3 which match those obtained earlier.

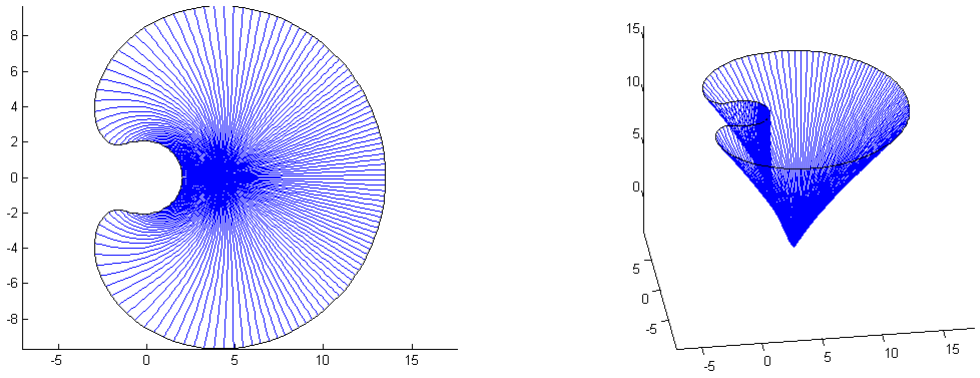

Figure 5.3: Schwarzschild when t= 13, r= 4, phi=0, the number of directions: 200

Because of spherical symmetry, we know that a different initial value of ϕ should just rotate the light cone around. Running `wavefront+general+` again, changing the initial value of ϕ to $\pi/2$ produces.

We reproduce a couple of Schwarzschild diagrams to test correctness, one with $\phi = 0$, and $\phi = \pi/2$. as we expect.

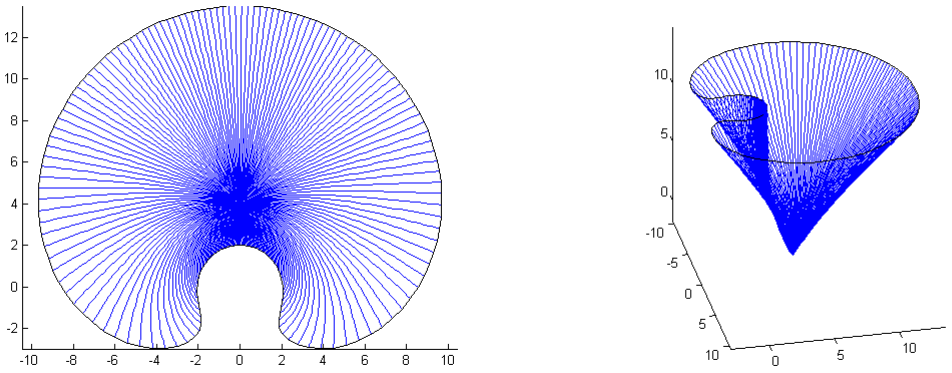

Figure 5.4: At $\phi = \pi/2$

Note that since we know this is Schwarzschild space, we can simply execute the commands

```
colormap([1,0,0]);
```

```
[evX,evY,evZ]=cylinder(2,30); evZ=evZ*T; mesh(evX,evY,evZ);
```

in the Matlab command window to add in the event horizon.

5.4 Conclusion

We now have a code which will construct light cones for an arbitrary metric, where the user decides whether the coordinates should be treated as Cartesian or polar, and the various parameters for the light cone. We have tested the code on the cases of flat and Schwarzschild space-times, and have obtained the results we expect, and so have some confidence that it is correct.

In the next chapter we will apply it to a selection of metrics, investigating the light cones of several metrics with interesting geometric or physical properties.

Chapter 6

Applications

6.1 Introduction

In this chapter we will use the Matlab code described in the previous chapter as a starting point to investigate some metrics. In turn, we will look at a metric which has a region of positive curvature near the origin, which acts as a gravitational lens. Then we will consider the Reissner-Nordström metric, the charged generalization of the Schwarzschild metric. The third example will be a different description of a charged black hole in which space-time is not coupled to standard electromagnetic theory, but to an alternative model in which a point charge does not give rise to a singularity. We will see how the code allows us to investigate aspects of the space-time which in a way which answers some questions, and raises others.

6.2 Case Study 1: A Gravitational Lens Space

In this example we explain a model of space-time which is asymptotically flat, but has a region of positive curvature near the origin which acts as a gravitational lens. We will use Cartesian coordinates to describe this static space-time, which is given by

$\mathbb{R}^3$ with the metric:

$$-dt^2 + (1 + e^{-x^2-y^2})dx^2 + (1 + e^{-x^2-y^2})dy^2 \tag{6.1}$$

When $x^2 + y^2$ is large (so we consider a region far from the origin) it is easy to see that the metic is approximately

$$-dt^2 + dx^2 + dy^2 \tag{6.2}$$

i.e. the metric of Minkowski space-time, which is flat.

Then we have $E = 1 + e^{-x^2-y^2}$, $F = 0$ and $G = 1 + e^{-x^2-y^2}$ we substitute it in the Matlab code with this dialogue

```
>> choose_metric
Please select the metric coefficients E,F,G as functions
 of x,y so  that the metric is Edx^2+2fdxdy+Gdy^2
E =exp(-x^2-y^2)+1
F =0
G =exp(-x^2-y^2)+1
```

This automatically sets up the geodesic equations

$$\begin{aligned}\ddot{x} = \frac{1}{2(EG - F^2)}[&(-GE_x - FE_y + 2FF_x)\dot{x}^2 \\ &+ (-2GE_y + 2FG_x)\dot{x}\dot{y} + (-GG_x + 2GF_y + FG_y)\dot{y}^2]\end{aligned} \tag{6.3}$$

and

$$\begin{aligned}\ddot{y} = \frac{1}{2(EG - F^2)}[&(FE_x + EE_y - 2EF_x)\dot{x}^2 \\ &+ (2FE_y - 2EG_x)\dot{x}\dot{y} + (2FF_y - FG_x - EG_y)\dot{y}^2]\end{aligned} \tag{6.4}$$

Because $E = G$ and $F = 0$, then we have

$$\ddot{x} = \frac{1}{2E^2}\left(-EE_x\dot{x}^2 - 2EE_y\dot{x}\dot{y} - EE_x\dot{y}^2\right) \tag{6.5}$$

$$\ddot{x} = \frac{1}{2E}\left(-E_x(\dot{x}^2 + \dot{y}^2) - 2E_y\dot{x}\dot{y}\right) \tag{6.6}$$

and

$$\ddot{y} = \frac{1}{2E}\left(G_y(\dot{x}^2 - \dot{y}^2) - 2G_x\dot{x}\dot{y}\right) \tag{6.7}$$

By substituting $E = G = e^{(-x^2-y^2)} + 1$ we find

$$\ddot{x} = \frac{1}{2(e^{(x^2+y^2)}+1)}\left(2x(\dot{x}^2 + \dot{y}^2) + 2y\dot{x}\dot{y}\right) \tag{6.8}$$

and

$$\ddot{y} = \frac{1}{2(e^{(x^2+y^2)}+1)}\left(-2y(\dot{x}^2 - \dot{y}^2) + 2x\dot{x}\dot{y}\right) \tag{6.9}$$

6.2.1 Light Cones

After choosing the metric and setting up the geodesic equations, we run `wave_front_general`

```
>> wave_front_general
For cartesian coordinates enter 1 and for polar coordinates enter 2:  1
Enter the evolution time period: 15
Enter the initial value of x: 5
Enter the initial value of y: 5
Enter the range of tangent directions
you want to investigate in the form [start end]: [-pi pi]
Enter the number of directions: 200
```

We get the figures 6.1 which show that the light cone develops much as in Minkowski space as it travels away from the origin, and also show the development of conjugate points and a caustic on the far side of the origin from the point of origin of the light cone.

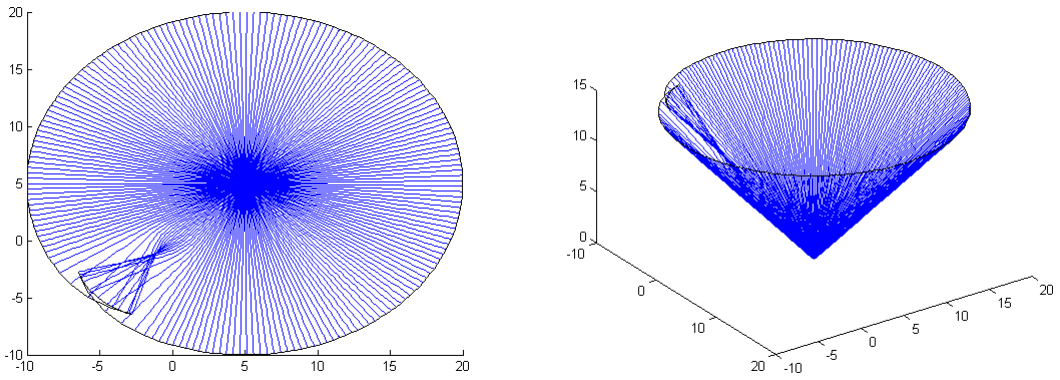

Figure 6.1: Example

From this we see that a the boundary of the future of a point is determined by the light cone, but the two are not identical. After passing through a conjugate point, a

null geodesic enters the future set. This shows a different way in which the future light cone can develop from the Schwarzschild case.

6.2.2 Curvature and Conjugate Points

We examine the Gaussian curvature again. As before, we have an orthogonal coordinate system (F = 0), so the Gaussian curvature K is given by

$$K = (\frac{-1}{2})(EG)^{(\frac{-1}{2})}[(E_x(EG)^{(\frac{-1}{2})}))_x + (G_y(EG)^{(\frac{-1}{2})})_y] \tag{6.10}$$

we have

$$\begin{aligned} E &= e^{(-x^2-y^2)} + 1, \\ F &= 0, \\ G &= e^{(-x^2-y^2)} + 1, \\ E_x &= G_x = -2xe^{(-x^2-y^2)}, \\ E_y &= G_y = -2ye^{(-x^2-y^2)} \end{aligned} \tag{6.11}$$

where E_x the derivative of E with respect to x, etc.

We substitute E, F, G to find the Gaussian curvature, so that

$$\begin{aligned} K = \frac{-1}{2}((e^{-x^2-y^2}+1)(e^{-x^2-y^2}+1))^{\frac{-1}{2}}[-2xe^{-x^2-y^2}(e^{-x^2-y^2}+1) \\ ((e^{-x^2-y^2}+1)^{\frac{-1}{2}})_x + (-2ye^{-x^2-y^2}((e^{-x^2-y^2}+1)(e^{-x^2-y^2}+1))^{\frac{-1}{2}})_y] \end{aligned} \tag{6.12}$$

and simplifying, we find

$$K = -2e^{x^2+y^2}\frac{(-e^{x^2+y^2}-1+(x^2+y^2)e^{x^2+y^2})}{(e^{x^2+y^2}+1)^3} \tag{6.13}$$

We see that K depends only on r, the distance from the origin. Setting $r^2 = x^2 + y^2$,

we obtain

$$K = -2e^{r^2} \frac{(-e^{r^2} - 1 + r^2 e^{r^2})}{(e^{r^2} + 1)^3} \tag{6.14}$$

Now, plotting K as a function of r using Maple gives the following diagram.

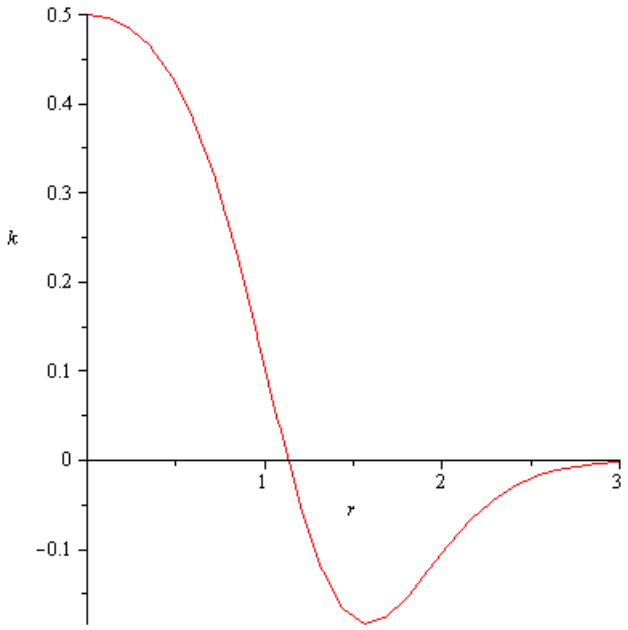

Figure 6.2: Relation between the curvature and Radius

and so we see that K is negative for r greater than approximately 1.2, and positive for r less than 2. This tells us that the effect of the curvature is to focus nearby geodesics if r is less than 2, and to spread them out if r is greater than 2, showing that conjugate points are indeed possible. We can look at this in more detail by investigating the spread of a fan of geodesics starting at $(4, 0)$ and another starting at $(1, 0)$ and this confirms that the geodesics far from the origin spread out, while those within the region of positive curvatures show focussing.

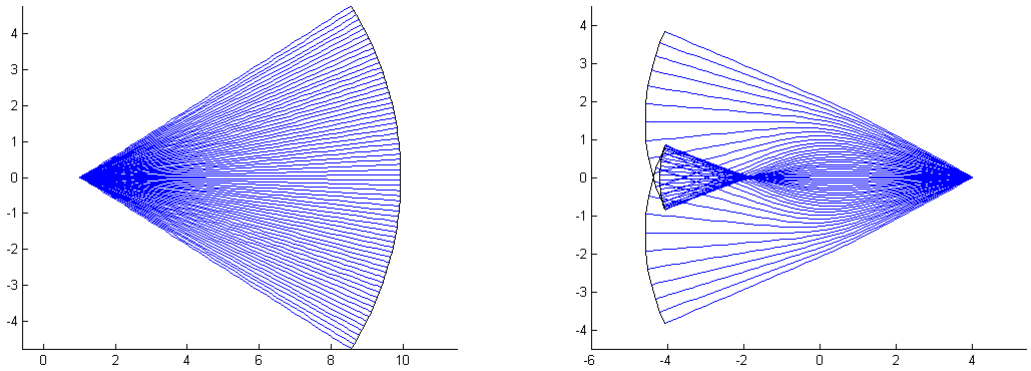

Figure 6.3: At (1,0) (4,0), t=9, n=70, with $\theta = [-0.5, 0.5]$ and $\theta = [\pi - 0.5, \pi 0.5]$

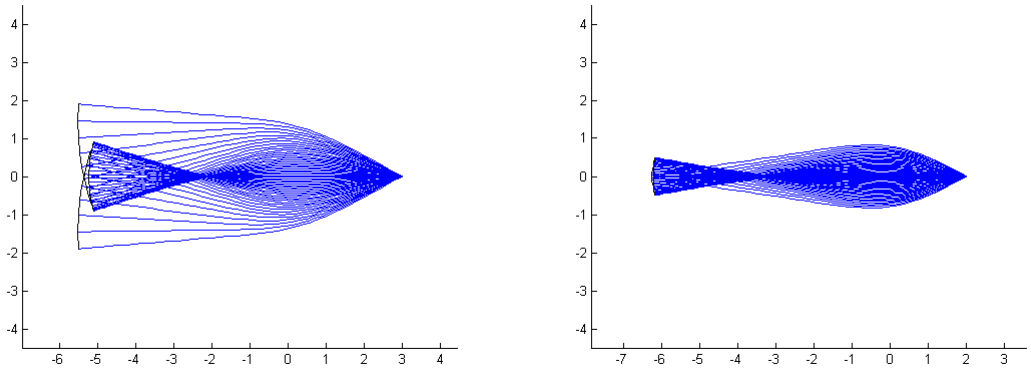

Figure 6.4: At (3,0) and (2,0), t=9, n=70, with $\theta = [\pi + 0.5\ ,\ \pi - 0.5]$

6.3 Case Study 2: The Reissner-Nordström metric

The Reissner-Nordström metric is a solution to the Einstein field equation coupled to the Maxwell equations for empty space around a spherically symmetric mass distribution in the presence of charge. This metric gives a representation of a universe consisting of a charged black hole [31].

The line element of this metric is given by

$$ds^2 = -(1 - \frac{2m}{r} + \frac{Q^2}{r^2})dt^2 + (1 - \frac{2m}{r} + \frac{Q^2}{r^2})^{-1}dr^2 + r^2(d\theta^2 + \sin^2\theta d\phi^2) \qquad (6.15)$$

where m is the mass of the hole, Q is the charge and we have used units with the speed of light c and the gravitational constant G equal to one. We can easily see that for any m and Q, if r is very large, then the metric tends to the Minkowski metric, so the space-time is asymptotically flat, and we expect the light cones to look like those of Minkowski space far from the origin.

This metric has a coordinate singularity when

$$1 - \frac{2m}{r} + \frac{Q^2}{r^2} = 0 \qquad (6.16)$$

and a curvature singularity when $r = 0$. For $Q < m$, there are two values at which this is zero, which we can denote $r_\pm$. The larger value, r_+, is the radius of the event horizon; the smaller value is the radius of the Cauchy horizon. The space-time outside r_+ is, like Schwarzchilds space-time, globally hyperbolic, and the surfaces of constant t are Cauchy surfaces.

If $Q > m$, there is no event horizon, and the space-time is not globally hyperbolic, because the singularity at $r = 0$ is not behind an event horizon. See [11] for a discussion of this aspect of the structure of Reisner-Nordström space-time.

As before, we will make a conformal transformation to a new metric. In this new

metric, there is a curvature singularity at $r = r_{\pm}$, as we will see when we calculate the curvature.

We suppose $m = 1$, restrict our attention to the equatorial plane $\theta = \pi/2$ as before and we study this metric. By conformal transformation we have, by dividing by z,

$$-dt^2 + z^{-2}dr^2 + r^2 z^{-1} d\phi^2 \tag{6.17}$$

where $z = 1 - \frac{2}{r} + \frac{Q^2}{r^2}$.

Then we have

$$\begin{aligned} E &= z^{-2}, \\ F &= 0, \text{ and} \\ G &= r^2 z^{-1} \end{aligned} \tag{6.18}$$

By substituting these in the general equations for a geodesic as before, we get

$$\begin{aligned} \ddot{r} = \frac{1}{2(EG - F^2)}[&(-GE_r - FE_\phi + 2FF_r)\dot{r}^2 \\ &+ (-2GE_\phi + 2FG_r)\dot{r}\dot{\phi} + (-GG_r + 2GF_\phi + FG_\phi)\dot{\phi}^2] \end{aligned} \tag{6.19}$$

and

$$\begin{aligned} \ddot{\phi} = \frac{1}{2(EG - F^2)}[&(FE_r + EE_\phi - 2EF_r)\dot{r}^2 \\ &+ (2FE_\phi - 2EG_r)\dot{r}\dot{\phi} + (2FF_\phi - FG_r - EG_\phi)\dot{\phi}^2] \end{aligned} \tag{6.20}$$

We find

$$\ddot{r} = z^{-1}\dot{r}^2 - \left(\frac{r^2\dot{z}}{2} + rz\right)\dot{\phi}^2 \tag{6.21}$$

and

$$\ddot{\phi} = \left(-\dot{z}z^{-1} + 2r^{-1}\right)\dot{r}\dot{\phi} \tag{6.22}$$

Where $\dot{z} = 2r^{-2} - 2Q^2r^{-3}$.

First, to understand this metric we have to see how the event horizon radius r is determined by the charge Q when $m = 1$. This is given by the values of r which make $z = 0$, where

$$z = 1 - \frac{2}{r} + \frac{Q^2}{r^2} \tag{6.23}$$

At $z = 0$, we have

$$1 - \frac{2}{r} + \frac{Q^2}{r^2} = 0 \tag{6.24}$$

The figure (6.5) shows the relationship between Q and $r_\pm$ as Q increases from 0 through 1. We can consider how the metric behaves for different values of Q.

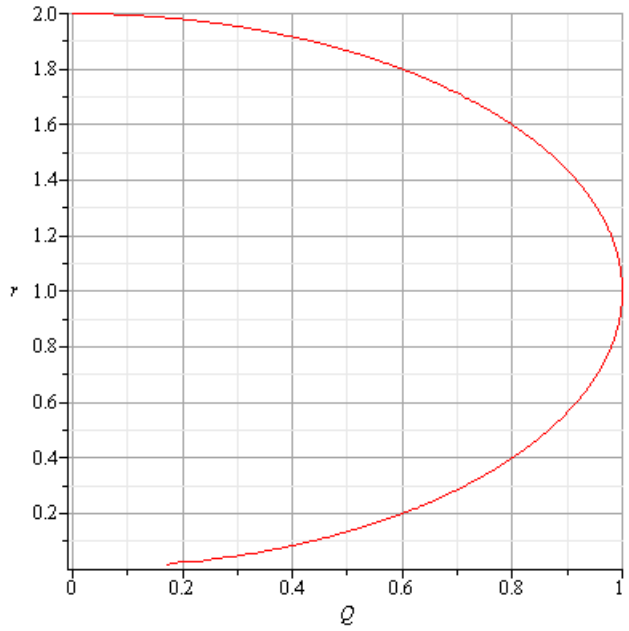

Figure 6.5: The Reissner-Nordstrom radius r and charge Q relation

We can see when $Q = 0$ the metric is just the Schwarzchild metric, and when Q is very small theis very small the metric is similar to Schwarzschild metric, except for a small region near $r = 0$.

We also see that for $Q < 1$ there is an inner Cauchy horizon and an outer event horizon. In the region between the two, z is positive, so r is the time coordinate and t

is a space coordinate, like inside the event horizon of Schwarzschild space-time.

As Q increases through 1, the two horizons meet and vanish, leaving a regular space-time with no event horizon, but a naked singularity at $r = 0$.

6.3.1 Light Cones

We can now use `choose_metric.m` to construct the metric and geodesic equations for varying values of Q, and see how the behaviour of the light cones is affected as Q increases.

As we expect, a light cone with an initial point far from the horizon grows in nearly the same way as in Minkowski space , Figures(6.6), (6.7).

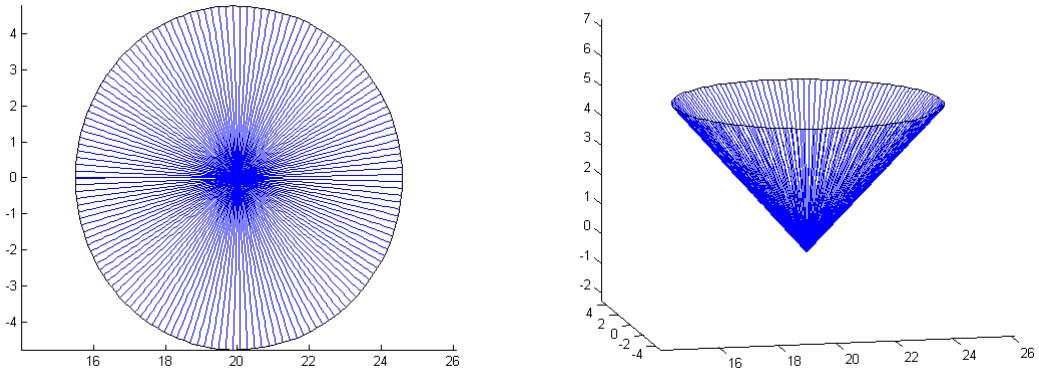

Figure 6.6: When r=20, t=5, Q=2

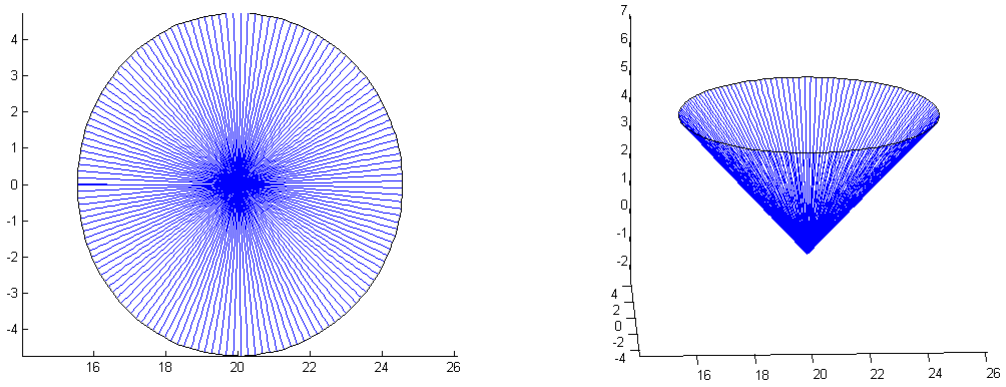

Figure 6.7: When r=20, t=5, Q=0.5

Next, we see that as Q increases up to 1, the general behaviour of the light cones is the same as for Schwarzschild space: the light cones wrap around the event horizon, and eventually cross themselves, but we do not see the caustics or conjugate points.

But the situation is very different for $Q > 1$. The light cones still do not seem to develop conjugate points see Fig from 6.8 , However, when a null geodesic gets to close to $r = 0$ the numerical approach is destroyed by the infinities at $r = 0$, as we see in the final figure from 6.15.

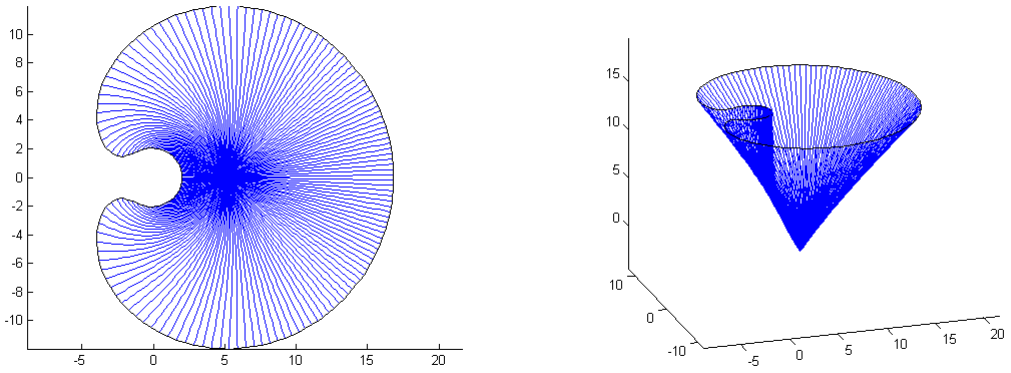

Figure 6.8: When r=5, t=15, Q=0

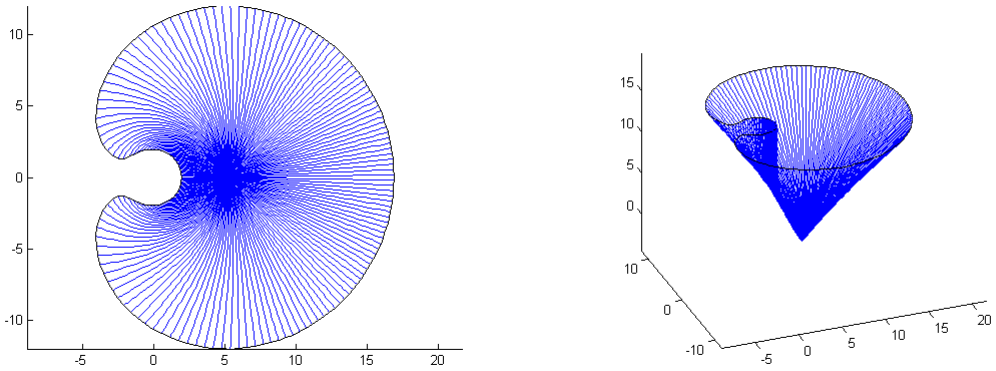

Figure 6.9: When r=5, t=15, Q=0.4

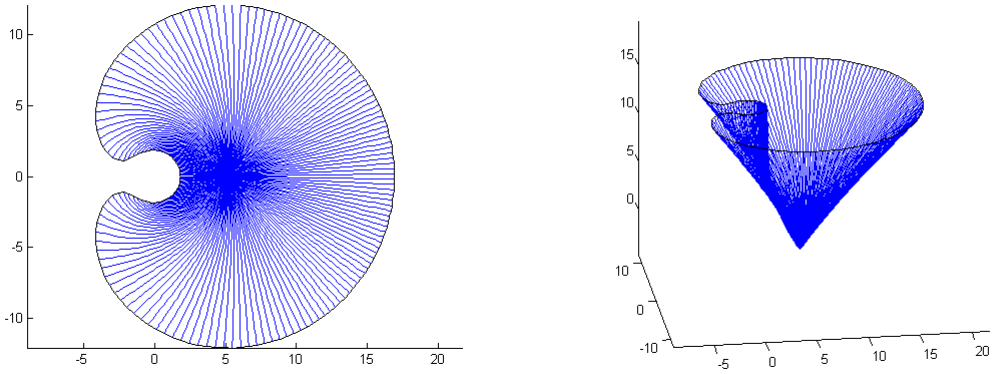

Figure 6.10: When r=5, t=15, Q= 0.6

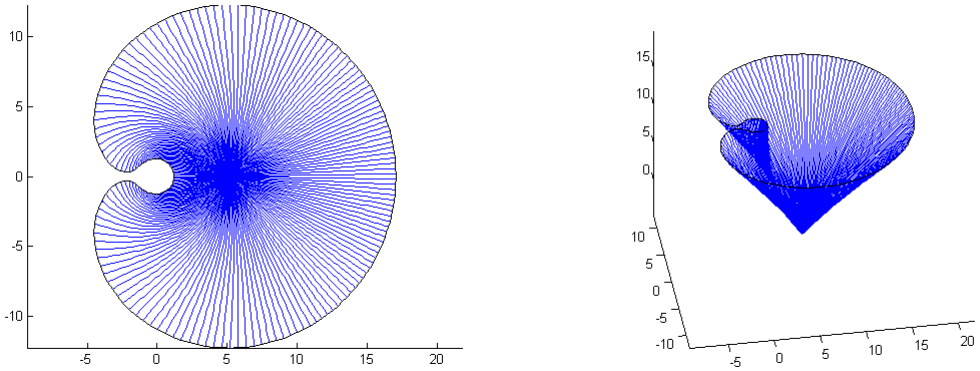

Figure 6.11: When r=5, t=15, Q= 1

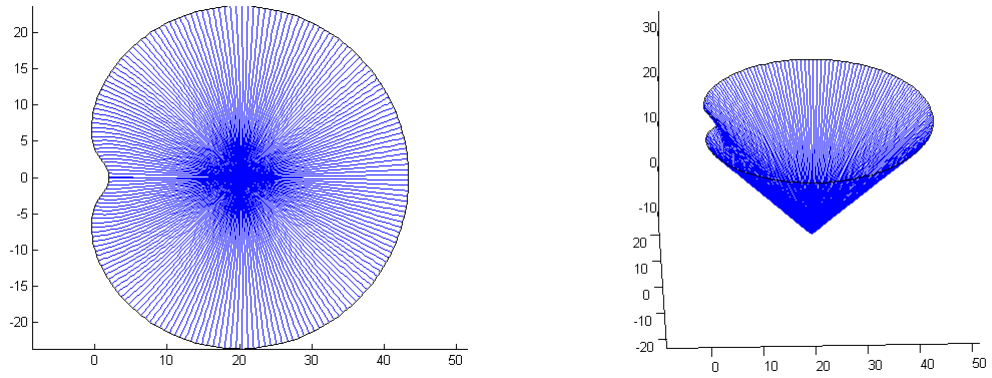

Figure 6.12: When r=20, t=25, Q= 1

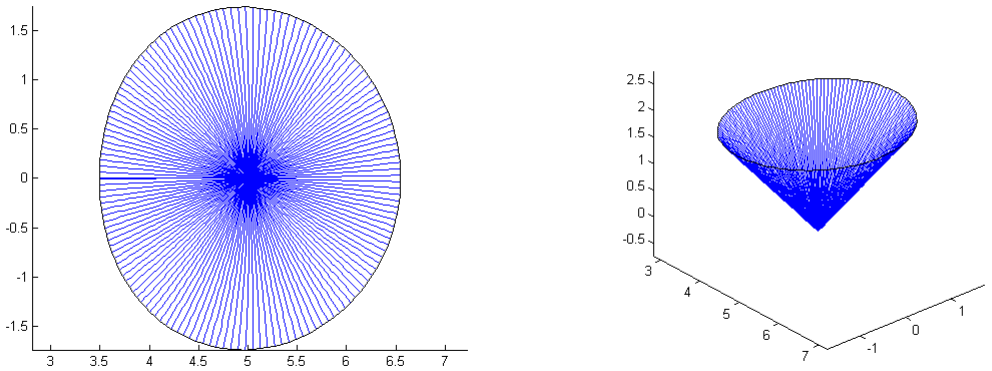

Figure 6.13: When r=5, t=2, Q=2

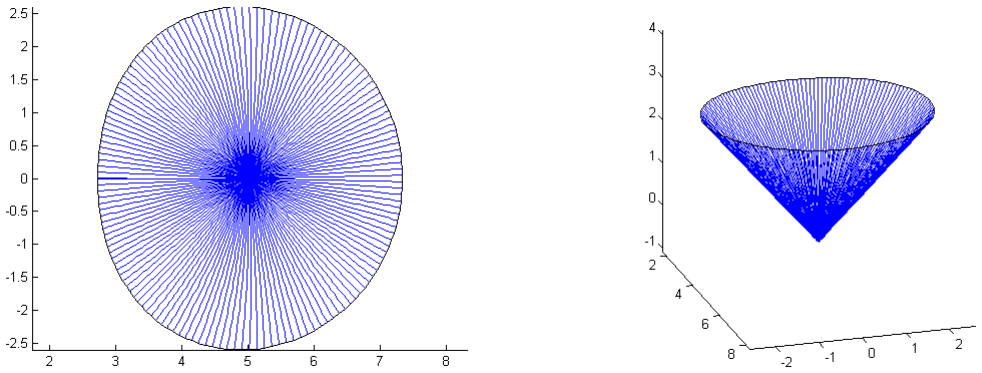

Figure 6.14: When r=5, t=3, Q=2

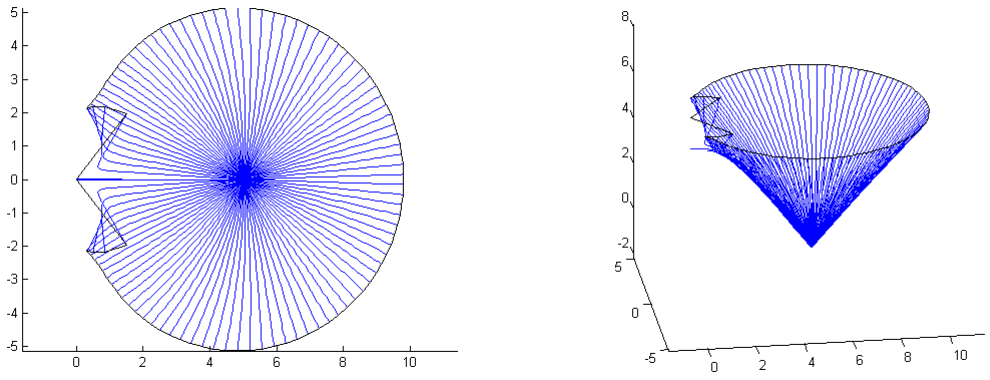

Figure 6.15: When r=5, t=6, Q= 2

In the last figure, we see what goes wrong as the radial null geodesic reaches $r = 0$ in a finite time.

It suggests taking a closer look to see what happens to the light cone near the singularity, and we can do this if we are careful.

Now we see what happens for Q=2 with t=0.03, and 0.035 r=0.7: this shows that the radial geodesic is attracted towards $r = 0$ strongly, while the other null geodesics are repelled by it

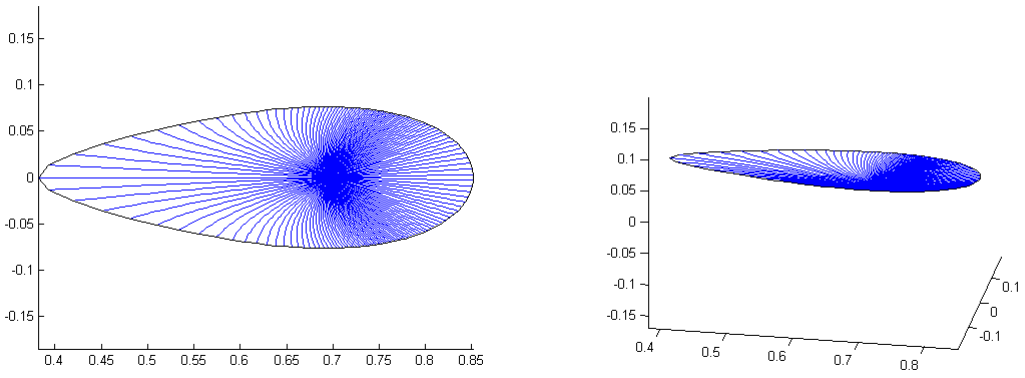

Figure 6.16: When r=0.7, t=0.03, Q=2

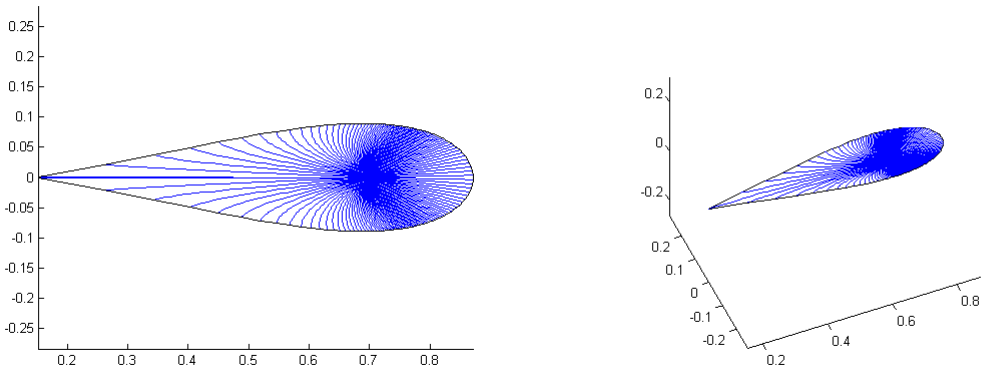

Figure 6.17: When r=0.7, t=0.035, Q= 2

6.3.2 Curvature

As before, since we have radial symmetry, we can examine the curvature scalar as a function of r, but now we have to consider the different possible values of Q.

Since the coordinates are still orthogonal, we still have

$$K = (\frac{-1}{2})(EG)^{-1/2}[(E_r(EG)^{-1/2})_r + (G_\phi(EG)^{-1/2})_\phi] \tag{6.25}$$

where

$$\begin{aligned} E &= \left(1 - \frac{2}{r} + \frac{Q^2}{r^2}\right)^{-2}, \\ G &= r^2\left(1 - \frac{2}{r} + \frac{Q^2}{r^2}\right)^{-1} \end{aligned} \tag{6.26}$$

so that

$$\begin{aligned} (EG)^{-1/2} &= \frac{1}{\sqrt{r^2\left(1 - \frac{2}{r} + \frac{Q^2}{r^2}\right)^{-3}}} \text{ and} \\ E_r &= -2\left(2r^{-2} - 2\frac{Q^2}{r^3}\right)\left(1 - 2r^{-1} + \frac{Q^2}{r^2}\right)^{-3} \end{aligned} \tag{6.27}$$

while $G_\phi = 0$.

By substituting these in to the formula for the curvature K we find

$$K = 2\,\frac{3\,r^2 - 5\,rQ^2 + Q^4 - 3\,r^3 + 4\,r^2Q^2}{(r^2 - 2\,r + Q^2)\,r^6}. \tag{6.28}$$

As a simple check, we see that at $Q = 0$ we have got

$$K = = \frac{-6(r-1)}{r^5\,(r-2)} \tag{6.29}$$

which gives us the result from Schwarzshild space-time.

We can now plot K as a function of $r > r_+$ for values of Q increasing up through 1.

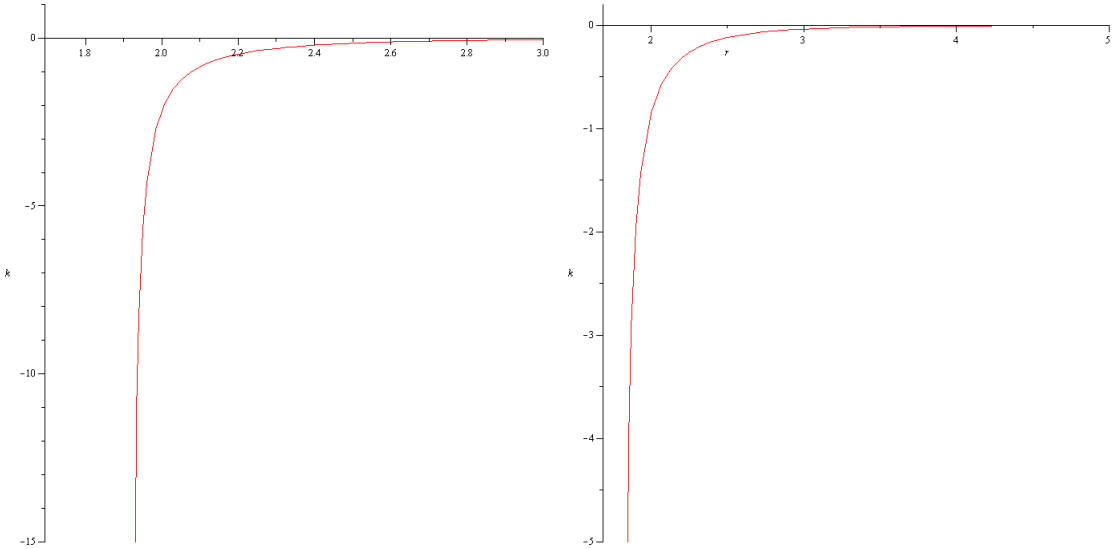

Figure 6.18: Curvature K and Radius r in Reissner-Nordstrom when charge $Q = 0.4, 0.6$

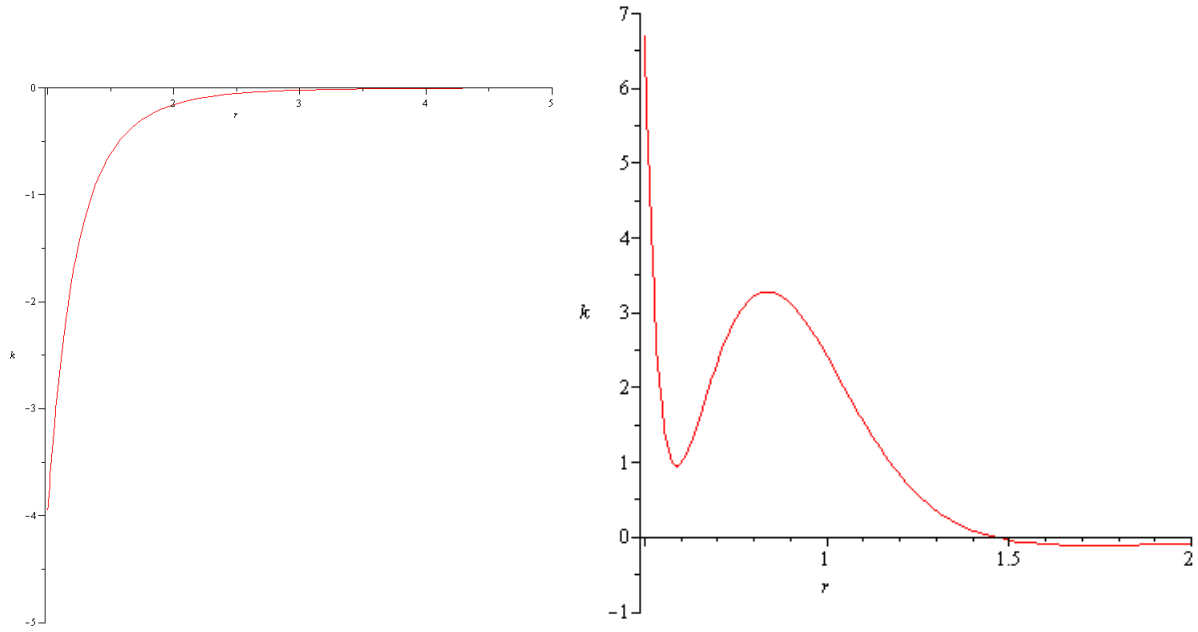

Figure 6.19: Curvature K and Radius r in Reissner-Nordstrom when charge $Q = 1, 1.1$

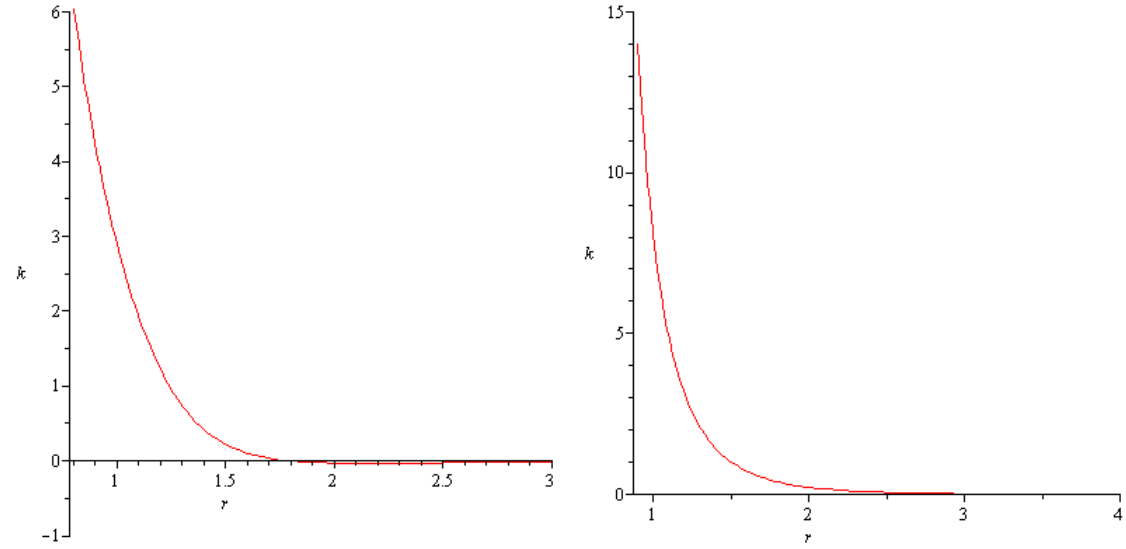

Figure 6.20: Curvature K and Radius r in Reissner-Nordstrom when charge $Q = 1.2, 2$

For $Q < 1$, we see that the curvature in the exterior region is always negative, again just as in Schwarzschild space, and so there cannot be any conjugate points.

However, when $Q > 1$ we see that there is a region of positive curvature near the origin, and then it is negative sufficiently far away. This suggests the possibility

that caustics might develop on a light cone starting near enough $r = 0$; however, investigation using the Matlab code does not reveal any. This suggests that a more detailed look at the curvature of the Reissner-Nordström space-time and the Jacobi equation would be of interest.

In the next section we look at a metric which has mass and charge, but uses a different theory of electromagnetism, and so is better behaved.

6.4 Case Study 3: Ayon-Beato-Garcia space time

As we saw above, the Reissner-Nordström space-time behaves badly when the charge grows larger than 1, because it has a naked singularity. We can still look at light cones starting an any point, but we cannot allow them to grow for too long, or they hit the singularity.

An alternative approach to studying a charged black hole is to make use of an alternative model of electromagnetism. One approach leads to the Ayon-Beato-Garcia metric [32]

$$ds^2 = -g_{tt}dt^2 + g_{rr}dr^2 + r^2(d\theta^2 + \sin^2\theta d\phi^2) \tag{6.30}$$

where

$$g_{tt} = \frac{1}{g_{rr}} = 1 - \frac{2mr^2}{(r^2+Q^2)^{3/2}} + \frac{r^2Q^2}{(r^2+Q^2)^2} \tag{6.31}$$

Here Q is charge, and without loss of generality we will suppose $m = 1$, and restrict attention to the equatorial plane $\theta = \pi/2$ when we study this metric.

Note that as before, for large r both g_{tt} and g_{rr} tend to 1, so this metric is asymptotically flat.

It is also easy to see that if Q is zero, we recover the Schwarzschild metric, and that if Q is very large, both g_{tt} and g_{rr} tend to 1, so the metric approaches the metric of Minkowski space.

We thus have a spherically symmetric static metric which couples gravity to a non-standard electromagnetic theory, while avoiding infinities at $r = 0$.

By out standard conformal transformation we have the new metric

$$-dt^2 + \frac{g_{rr}dr^2}{g_{tt}} + \frac{r^2d\phi^2}{g_{tt}} \tag{6.32}$$

giving

$$\begin{aligned} E &= \frac{g_{rr}}{g_{tt}} = (g_{tt})^{-2}, \\ F &= 0, \text{ and} \\ G &= \frac{r^2}{g_{tt}} = r^2(g_{tt})^{-1}. \end{aligned} \tag{6.33}$$

By substituting these in these equations

$$\begin{aligned} \ddot{r} = \frac{1}{2(EG-F^2)}[&(-GE_r - FE_\phi + 2FF_r)\dot{r}^2 \\ &+ (-2GE_\phi + 2FG_r)\dot{r}\dot{\phi} + (-GG_r + 2GF_\phi + FG_\phi)\dot{\phi}^2] \end{aligned} \tag{6.34}$$

and

$$\begin{aligned} \ddot{\phi} = \frac{1}{2(EG-F^2)}[&(FE_r + EE_\phi - 2EF_r)\dot{r}^2 \\ &+ (2FE_\phi - 2EG_r)\dot{r}\dot{\phi} + (2FF_\phi - FG_r - EG_\phi)\dot{\phi}^2] \end{aligned} \tag{6.35}$$

we find

$$\ddot{r} = \frac{1}{2(g^{-2})}\left(2g^{-3}g_r\dot{r}^2 + (-r^2g^{-1})_r\dot{\phi}^2\right) \tag{6.36}$$

and

$$\ddot{\phi} = \left(g^{-3}g_r - 2r^{-1}\right)\dot{r}\dot{\phi} \tag{6.37}$$

Where $g = g_{tt}$.

As a first step to understand this metric we have to see how the event horizon radius r is determined by the charge Q when $m = 1$.

Now,

$$g_{tt} = 1 - \frac{2r^2}{(r^2+Q^2)^{3/2}} + \frac{r^2Q^2}{(r^2+Q^2)^2} \tag{6.38}$$

so at $g_{tt} = 0$,

$$\frac{2r^2}{(r^2+Q^2)^{3/2}} - \frac{r^2Q^2}{(r^2+Q^2)^2} = 1 \tag{6.39}$$

From figure (6.21) we see that the situation is similar to that of the Reissner-Nordström space-time. As Q increases, we have a pair of horizons, and exterior and an interior one which meet and vanish when Q reaches a critical value, Q_c, which here is about 0.63417.

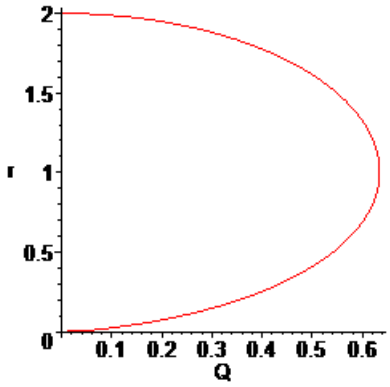

Figure 6.21: radius r and charge Q relation

We see from this that for $Q < Q_c$ there is an inner event horizon and an outer event horizon. In the region between the two, g_{tt} is positive , so r is the time coordinate and t is a space coordinate, and as before we consider only the exterior region. As Q increases through Q_c, the two event horizons meet and vanish, leaving a regular space-time with no event horizon. This is different from the Reissner-Nordström case in which there was no event horizon, but there was a naked singularity at $r = 0$.

We first note that when $Q = 0$ we can see the event horizon is the same as in the Schwarzschild metric, with a curvature singularity in the conformally transformed space-time, but not in the original space-time at $r = 2$.

We can now consider how the space-time changes as the value of Q varies. We can see when the Q is very small the metric is close to the Schwarzschild metric and at very large Q it is like Minkowski space time. We expect that the exterior space-time

will be very like Schwarzschild for Q less than the Q_c, and like Minkowski space-time for Q much greater than Q_c. We will use our general purpose code to investigate how the behaviour of light cones changes as Q varies.

6.4.1 Light Cones

We go through the same procedure as previously, using `choose_metric.m` to set up the metric and the geodesic equations obtained above Next, using `wave_front_general.m` we can investigate the light cones of this space-time.

As we expect, if r is large and t is small, the light cones look just like the Minkowski space-time ones.

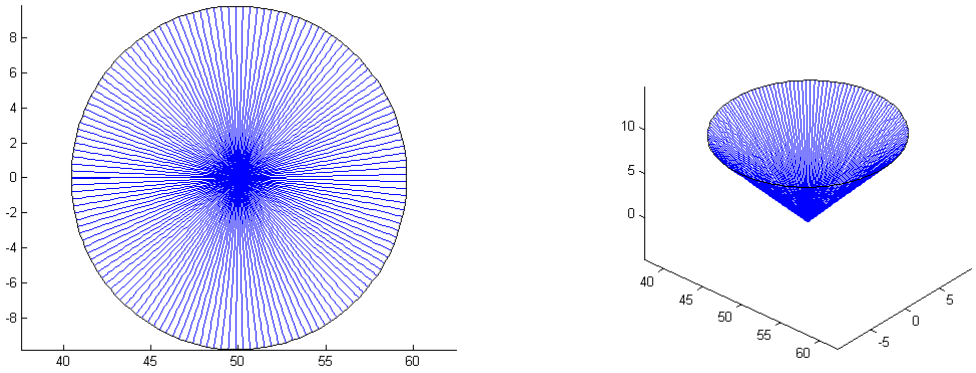

Figure 6.22: When r=50, t=10, Q=0.5

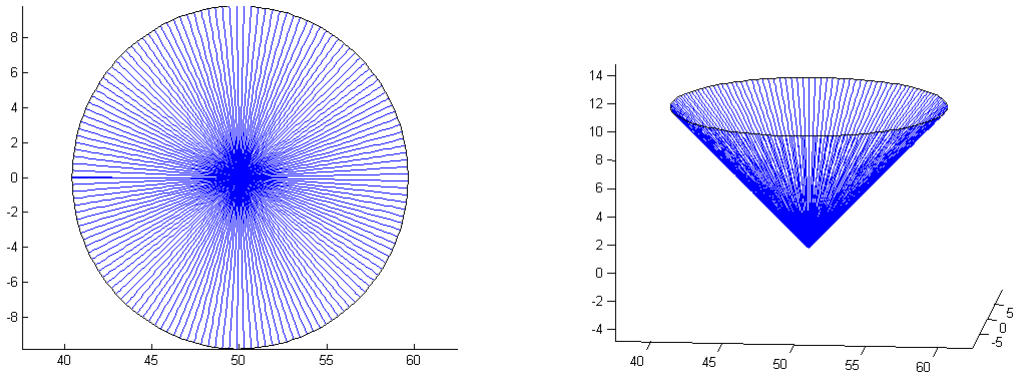

Figure 6.23: When r=50, t=10, Q=2

Next, we can examine light cones which approach the event horizon, for $Q < Q_c$. As Q grows from 0 to Q_c, the light cones are all of the same general form as in Schwarzschild space-time. They wrap around the event horizon, without developing caustics.

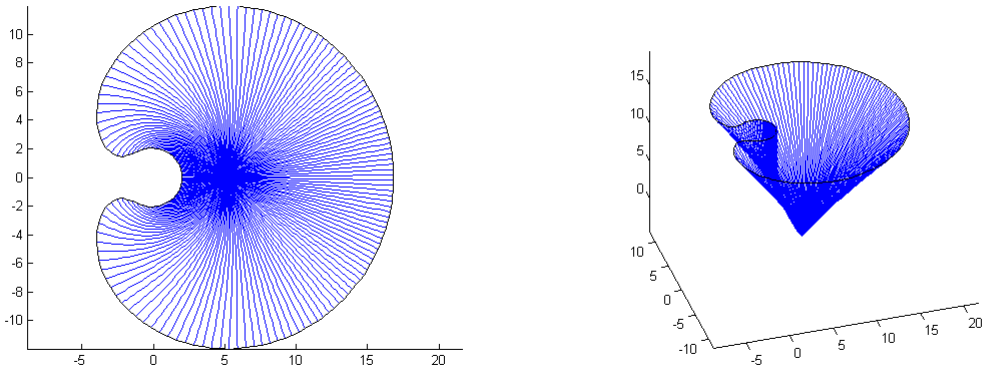

Figure 6.24: When r=5, t=15, Q=0

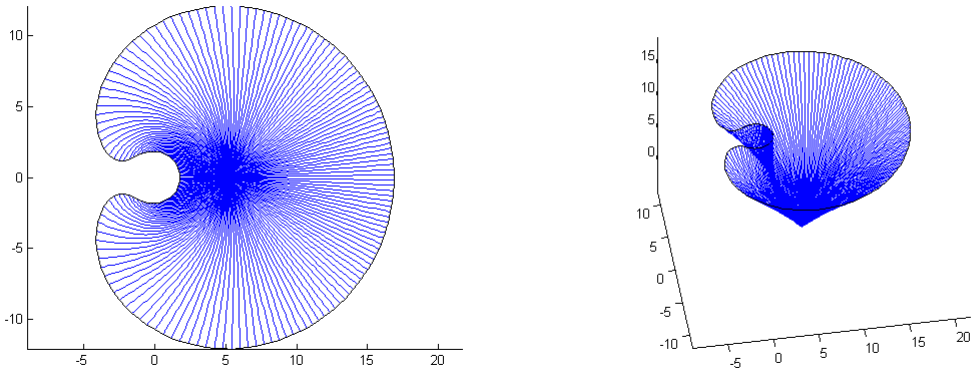

Figure 6.25: When r=5, t=15, Q=0.4

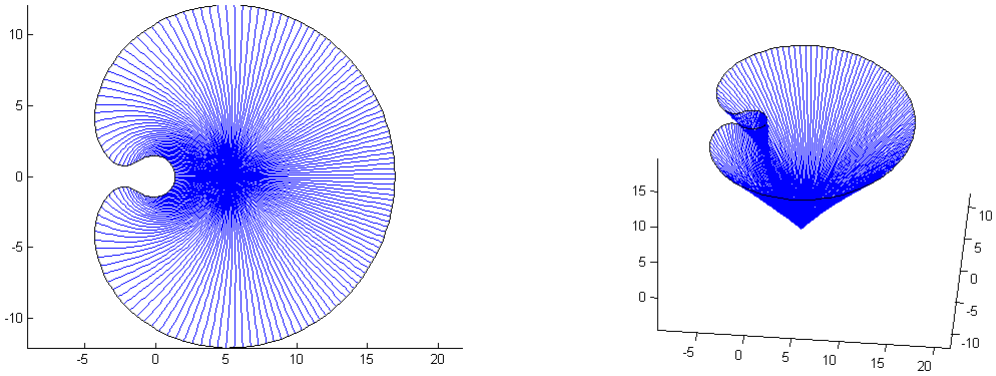

Figure 6.26: When r=5, t=15, Q= 0.6

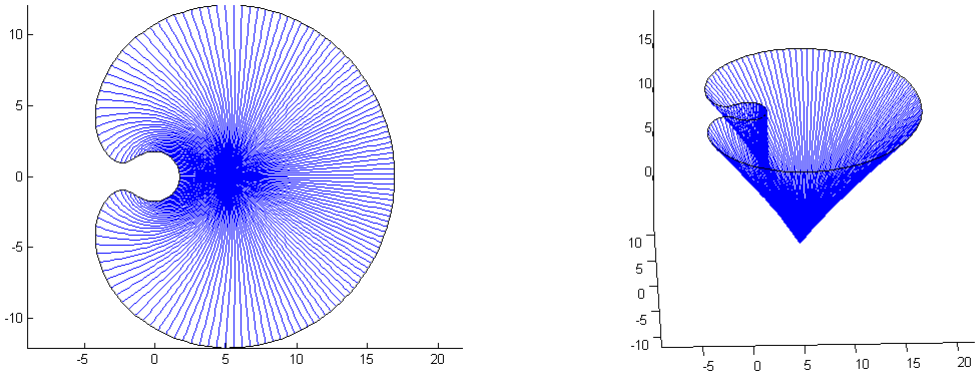

Figure 6.27: When r=5, t=15, Q= 0.7

But when Q becomes larger, for example $Q = 1$, we see a different type of behaviour. There is now no event horizon, and the null cones keep on growing through $r = 0$. But now we see that there are conjugate points and caustics developing on the light cone.

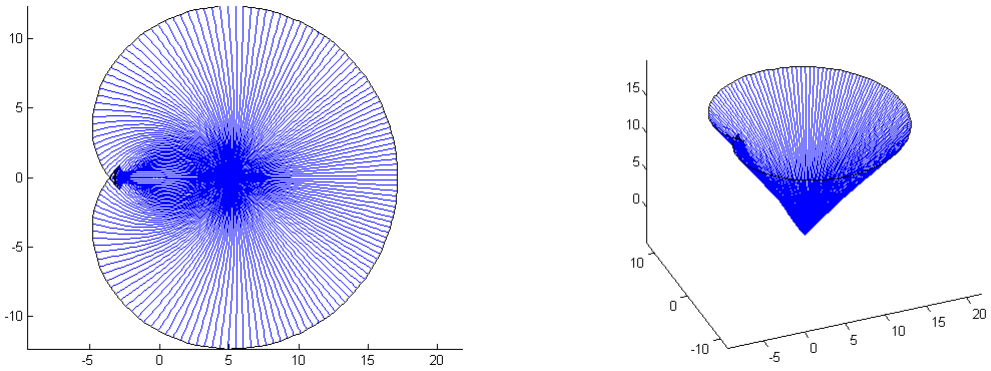

Figure 6.28: When r=5, t=15, Q= 1

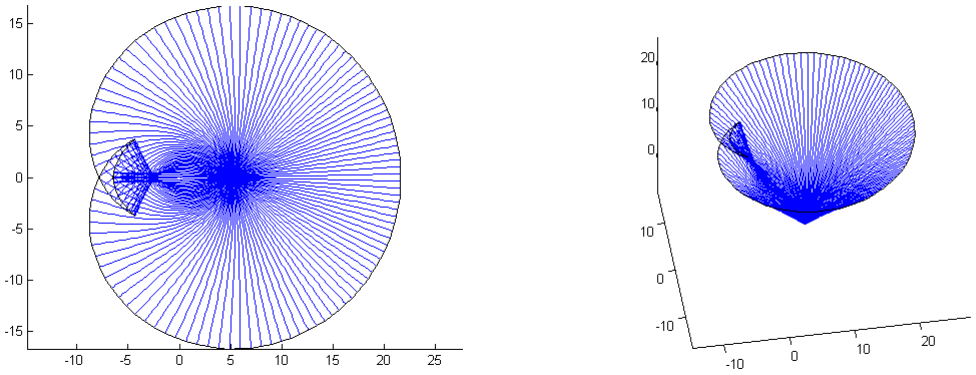

Figure 6.29: When r=5, t=20, Q= 1

Finally, we can consider what happens for large Q. For example, with $Q = 10$, we obtain light cones which now look very similar to those in Minkowski space, even though the pass through $r = 0$.

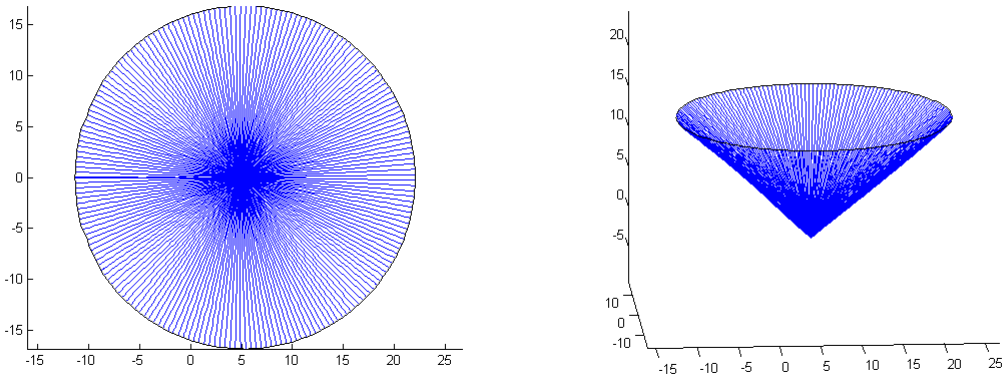

Figure 6.30: When r=5, t=15, Q= 10

We can understand this last figure by noting that if Q is large compared to 1, g_{tt} and g_{rr} are approximately 1, so the metric is nearly Minkowskian again.

6.4.2 Curvature

We can also investigate the curvature in this case, but the situation is again rather complicated.

As in the other cases, since the coordinate system in the Riemannian metric we are using is orthogonal, we have

$$K = (\frac{-1}{2})(EG)^{-1/2}[(E_r(EG)^{-1/2})_r + (G_\phi(EG)^{-1/2})_\phi] \tag{6.40}$$

In this case,

$$\begin{aligned} E &= \left(1 - \frac{2r^2}{(r^2+Q^2)^{3/2}} + \frac{r^2Q^2}{(r^2+Q^2)^2}\right)^{-2} \\ G &= r^2\left(1 - 2\frac{r^2}{(r^2+Q^2)^{3/2}} + \frac{r^2Q^2}{(r^2+Q^2)^2}\right)^{-1} \end{aligned} \tag{6.41}$$

so that

$$(EG)^{-1/2} = \frac{1}{\sqrt{r^2\left(1 - 2\frac{r^2}{(r^2+Q^2)^{3/2}} + \frac{r^2Q^2}{(r^2+Q^2)^2}\right)^{-3}}}. \tag{6.42}$$

From this we finally obtain

$$\begin{aligned} E_r = [&-4 * (r^2+Q^2)^2 r(r^8 + r^6Q^2 - 3r^4 * Q^4 - 5r^2Q^6 - 2Q^8 \\ &- r^6Q^2\sqrt{r^2+Q^2} - r^4Q^4\sqrt{r^2+Q^2} + r^2Q^6\sqrt{r^2+Q^2} \\ &+ Q^8\sqrt{r^2+Q^2})]/[(Q^4\sqrt{r^2+Q^2} + 3r^2Q^2\sqrt{r^2+Q^2} \\ &- 2r^2Q^2 + \sqrt{r^2+Q^2}r^4 - 2r^4)^3] \end{aligned} \tag{6.43}$$

and $G_\phi = 0$.

By substituting these in the formula for the curvature K we find

$$\begin{aligned} K = [&-(-96\,Q^6 + 44\,Q^6\sqrt{r^2+Q^2} + 48\,\sqrt{r^2+Q^2}Q^4 + 12\,Q^4\sqrt{r^2+Q^2}r^2 \\ &- 124\,r^2Q^4 - 4\,r^4Q^2 + 48\,r^2Q^2\sqrt{r^2+Q^2} - 16\,\sqrt{r^2+Q^2}r^4Q^2 \\ &+ 12\,r^6 - 12\,\sqrt{r^2+Q^2}r^4)] \\ &* \left(\frac{1}{2\left(\sqrt{r^2+Q^2}r^4 + 3\,r^2Q^2\sqrt{r^2+Q^2} + \sqrt{r^2+Q^2}Q^4 - 2\,r^4 - 2\,r^2Q^2\right)\left(r^2+Q^2\right)^3}\right) \end{aligned} \tag{6.44}$$

Again, we check that this reduces to the Schwarzschild case if $Q = 0$. In this case we get

$$\begin{aligned} K &= \frac{-(12\,r^6 - 12\,\sqrt{r^2}r^4)}{2\left(\sqrt{r^2}r^4 - 2\,r^4\right)r^6} \\ &= \frac{-6(r-1)}{r^5\,(r-2)} \end{aligned} \tag{6.45}$$

which is as we have seen before in Schwarzchild space time, giving us the negative curvature everywhere in the exterior region.

Next, we see how this changes as Q grows through Q_c. When $Q < Q_c$ we see that the curvature in the exterior region is always negative. This is just like Schwarzschild space, and confirms that there are no conjugate points and so no caustics on the light cones.

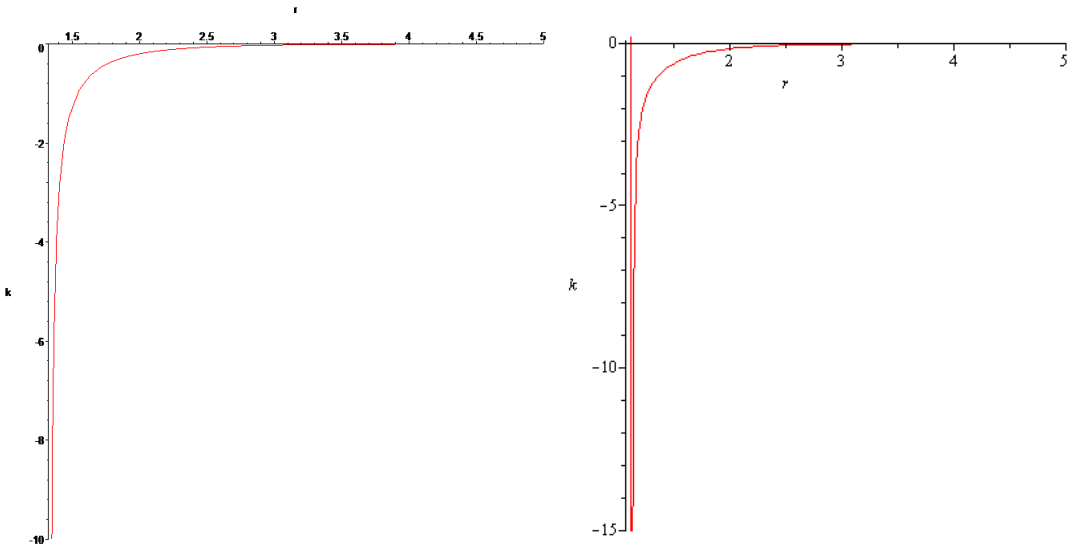

Figure 6.31: Curvature k and r when charge $Q = 0.6, 0.63$ and r start from 1.1

In the next figures we can see for Q a little bigger than Q_c there is a region of large negative curvature around $r = 0$, then positive, then finally negative (but small). This suggests that it might be interesting to see in more detail how light cones grow through the origin for values of Q in this range.

Finally, as Q increases through about 0.78 the curvature become positive in neighbourhood of the origin , and from then on we have a region of positive curvature near $r = 0$, then the curvature becomes (slightly) negative for r large enough.

In this last case we now have a space-time whose curvature behaves in a similar way to the gravitational lens space time from the first case study. We are not, then, too surprised to see that the growth of light cones is similar: conjugate points develop

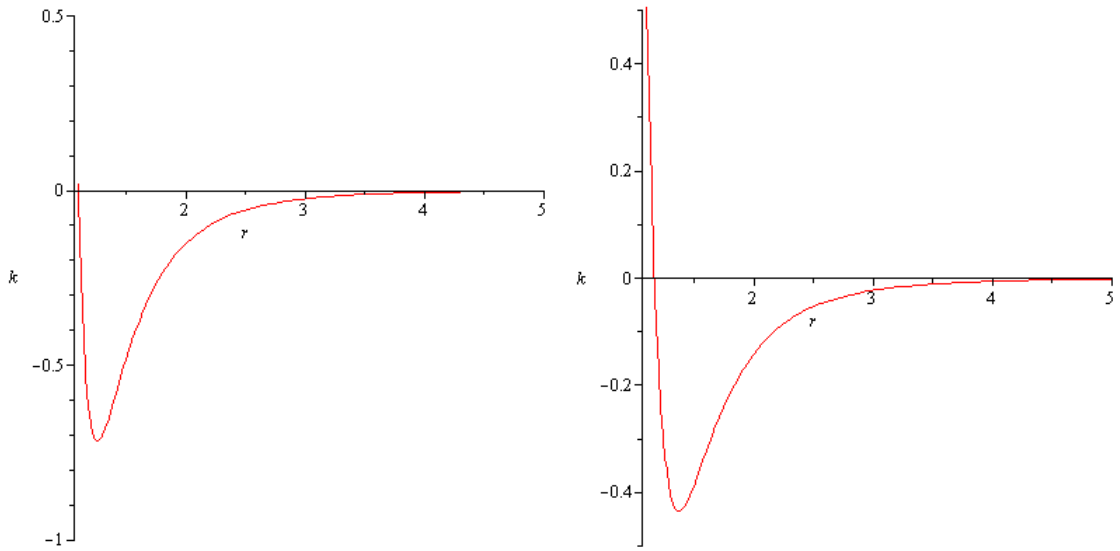

Figure 6.32: Relation between curvature k and r when charge $Q = 0.64, 0.65$ and r start from 1.1

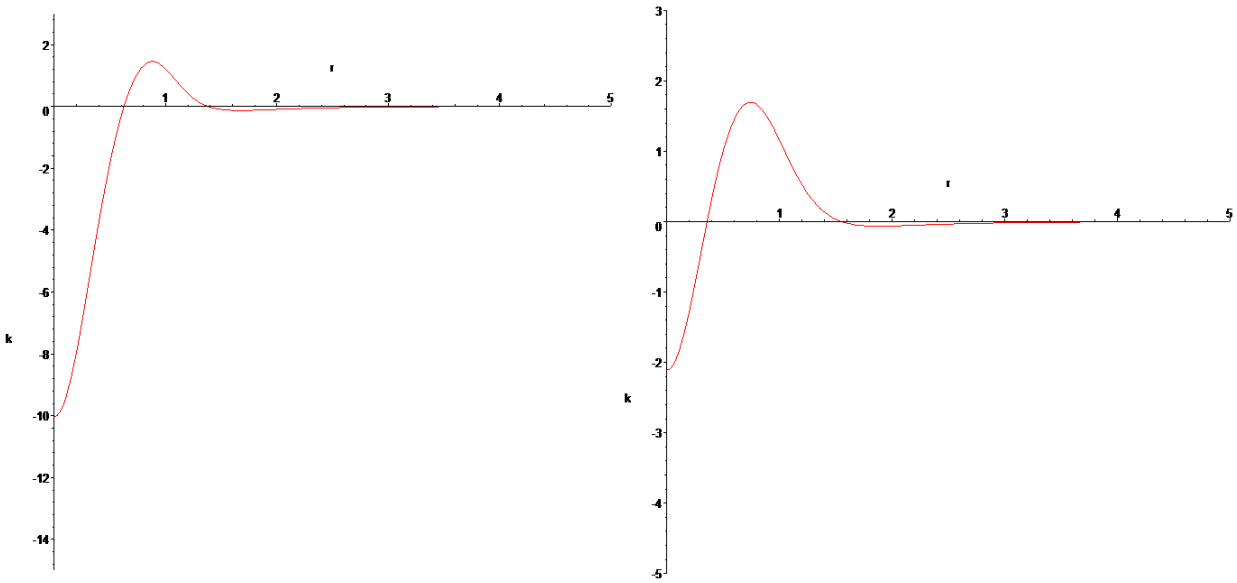

Figure 6.33: Relation between curvature k and r when charge $Q = 0.7, 0.75$

on the radial null geodesics after they pass through $r = 0$.

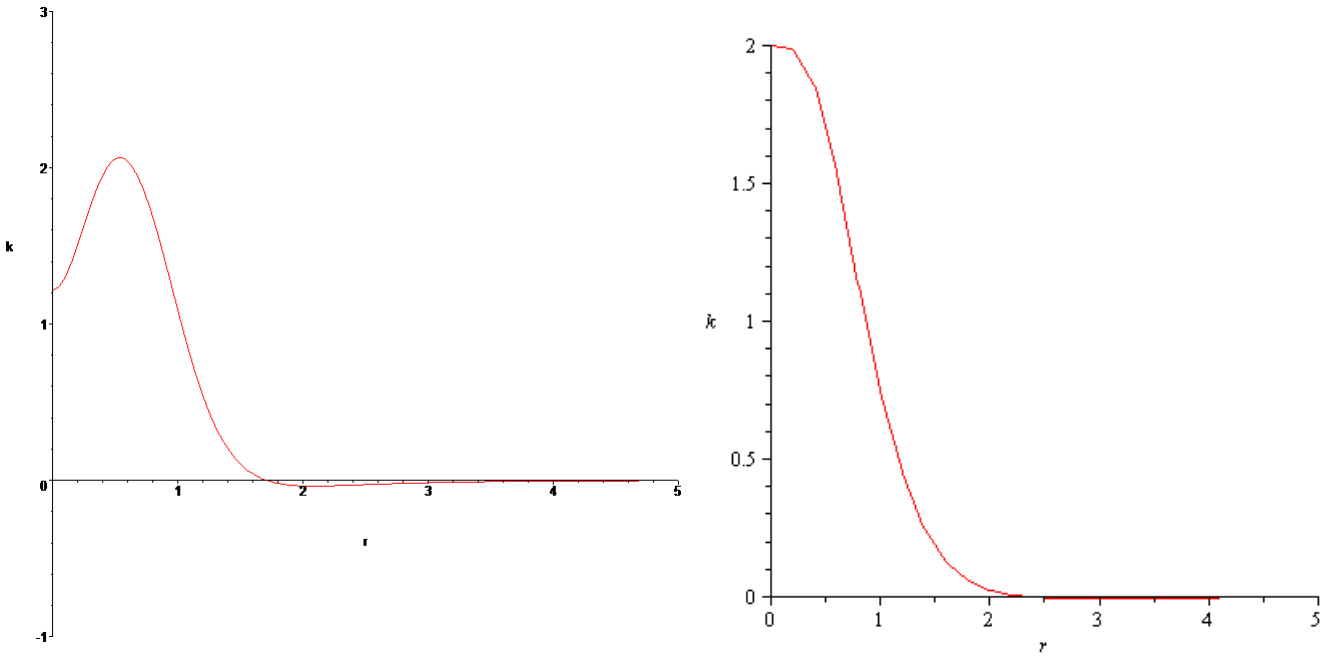

Figure 6.34: Relation between curvature k and r when charge $Q = 0.8, 1$

6.5 Case Study 4: A non-spherically symmetric gravitational lens

In this example we consider a model of space-time which is not spherically symmetric. As with the first case study, this is not a physical solution to the Einstein equations, but is chosen to illustrate the effect of a non-radially symmetry distribution of curvature centred on the origin, and to show that our approach deals with the case also. It is important to notice that in all the previous cases we were dealing with the development in the equatorial plane of light cones in a space-time with 3 spatial dimensions, and could recover the full light cone by rotating about the axis containing the origin and the initial point of the light cone. In this case, we are only considering a $(2+1)$-dimensional space-time, and the rotation used before becomes meaningless.

We will use Cartesian coordinates to describe this static space-time, which is given by $\mathbb{R}^3$ with the metric:

$$-dt^2 + (1 + e^{-x^2-y^4})dx^2 + (1 + e^{-x^2-y^4})dy^2 \tag{6.46}$$

We immediately see that none of the metric components are ever zero or infinite, so the metric is regular.

Furthermore, when $x^2 + y^4$ is large (so we consider a region far from the origin) it is easy to see that the metic is approximately

$$-dt^2 + dx^2 + dy^2 \tag{6.47}$$

i.e. the metric of Minkowski space-time, which is flat.

We therefore have an asymptotically flat, regular space-time, with its curvature concentrated near the origin.

We now have $E = 1 + e^{-x^2-y^4}$, $F = 0$ and $G = 1 + e^{-x^2-y^4}$ which we enter using `choose_metric.m` in just the same way as the spherically symmetric metrics, using the dialogue

```
>> choose_metric
Please select the metric coefficients E,F,G as functions
 of x,y so  that the metric is Edx^2+2Fdxdy+Gdy^2
E =exp(-x^2-y^4)+1
F =0
G =exp(-x^2-y^4)+1
```

This automatically sets up the geodesic equations:

$$\begin{aligned}\ddot{x} = \frac{1}{2(EG-F^2)}[&(-GE_x - FE_y + 2FF_x)\dot{x}^2 \\ &+ (-2GE_y + 2FG_x)\dot{x}\dot{y} + (-GG_x + 2GF_y + FG_y)\dot{y}^2]\end{aligned} \tag{6.48}$$

and

$$\begin{aligned}\ddot{y} = \frac{1}{2(EG-F^2)}[&(FE_x + EE_y - 2EF_x)\dot{x}^2 \\ &+ (2FE_y - 2EG_x)\dot{x}\dot{y} + (2FF_y - FG_x - EG_y)\dot{y}^2]\end{aligned} \tag{6.49}$$

In this case we obtain

$$\ddot{x} = \frac{1}{1+e^{x^2+y^4}}\left(x\dot{x}^2 - 4y^3\dot{x}\dot{y} - x\dot{y}^2\right) \tag{6.50}$$

and

$$\ddot{y} = \frac{2}{1+e^{x^2+y^4}}\left(-y^3\dot{x}^2 + x\dot{x}\dot{y} + y^3\dot{y}^2\right) \tag{6.51}$$

We can also investigate the curvature in this case, but the situation is rather more complicated.

6.5.1 Light Cones

After choosing the metric and setting up the geodesic equations, we run `wave_front_general.m` to investigate the light cones.

By choosing initial values of x and y such that $\sqrt{x^2+y^2}$ is significantly larger than 1, and t is comparatively small, we can check that the light cones develop as in Minkowski space, as shown in figures 6.35.

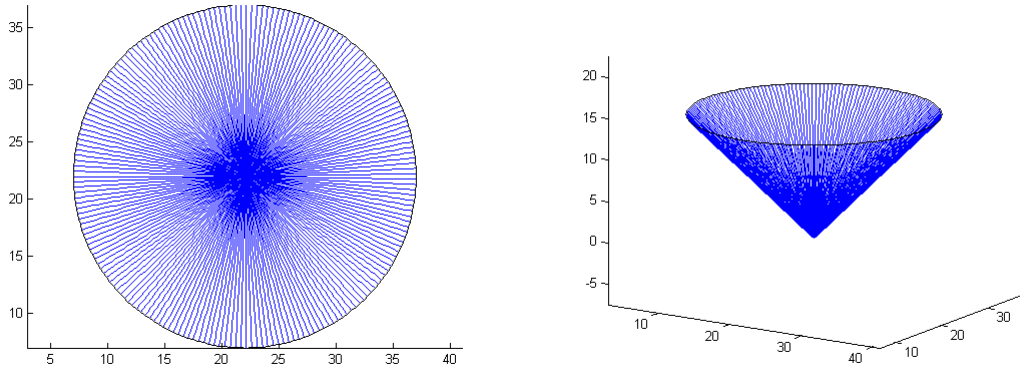

Figure 6.35: When x=22, y=22, t=15

We can also consider initial points and evolution times such that the light cone develops past the origin. These show the development of conjugate points and a caustic on the far side of the origin from the point of origin of the light cone, in a way which is qualitatively similar to our first case study.

As in the first case study, and the third case study with large enough Q, we see that the future of a point is determined by the light cone, but not every point on the boundary of the future is on the light cone: after a conjugate point, the null geodesic enters the future set.

First, we consider an initial point with $y = 0$. In this case, the light cone develops very similarly to those in the first case study.

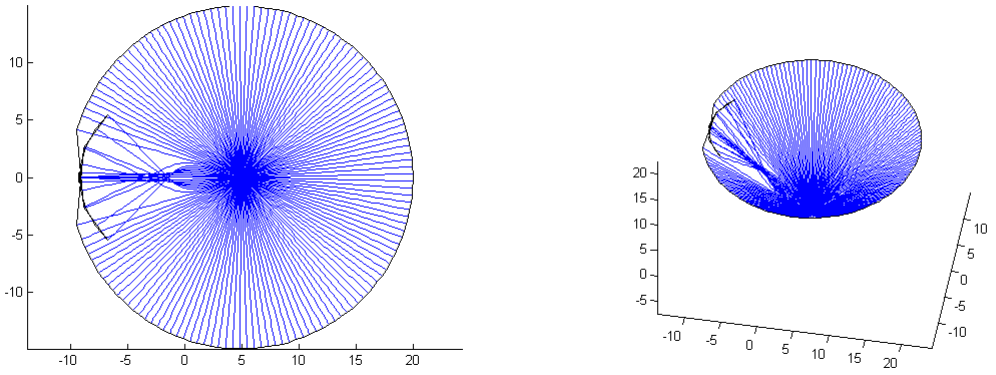

Figure 6.36: When x=5, y=0, t=15

From figures 6.37 to 6.39, we can also focus in on the part of the null cone and see the development of the caustic. The next figures with figures for $x = 5, y = 0$, with $t = 6, 8, 10$,

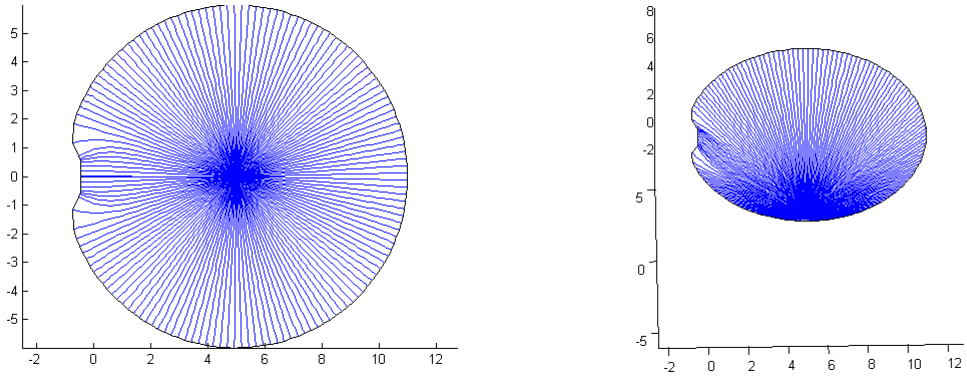

Figure 6.37: When x=5, y=0, t=6

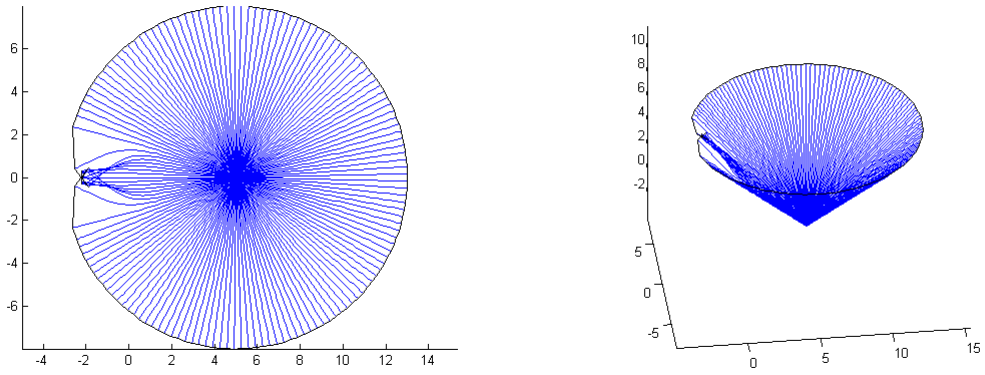

Figure 6.38: When x=5, y=0, t=8

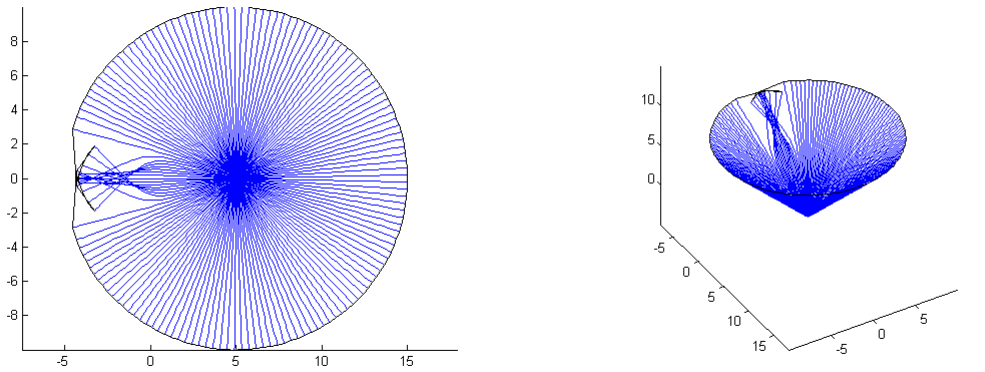

Figure 6.39: When x=5, y=0, t=10

As in previous cases, we see that this choice for the number of geodesics plotted is insufficient; and also as in previous cases, we can simply increase the number of geodesics, resulting in the figures below. The figures 6.40 to 6.43 for $x = 3, 5, 7, 9, y = 0$, with $t = 9$,

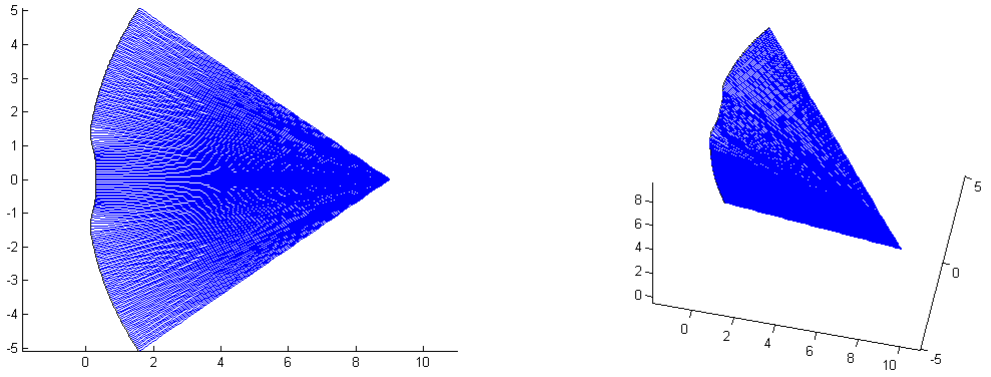

Figure 6.40: When x=9, y=0, t=9

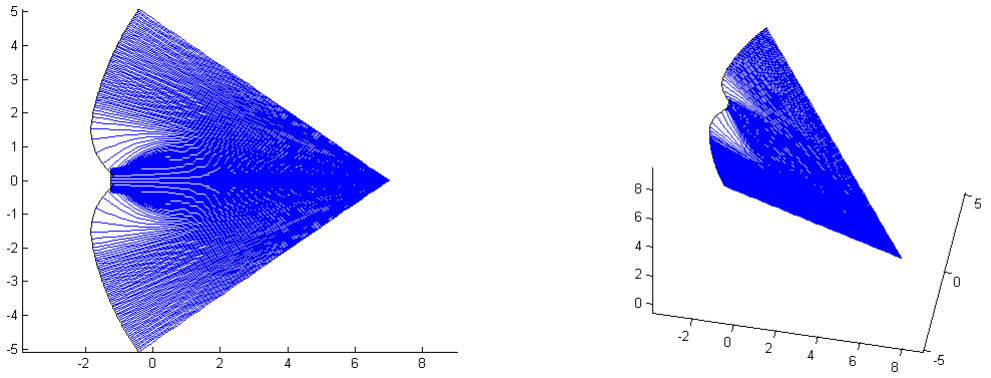

Figure 6.41: With y=0, x =7, t=9

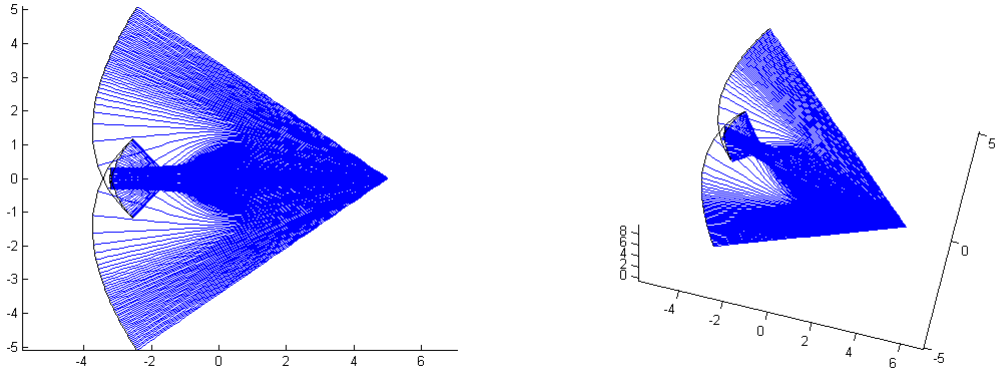

Figure 6.42: With y=0, x =5, t=9

This is a special case, as we have $y = 0$, and the metric has the x-axis as an axis of symmetry. We therefore also investigate what happens if the light cone does not start

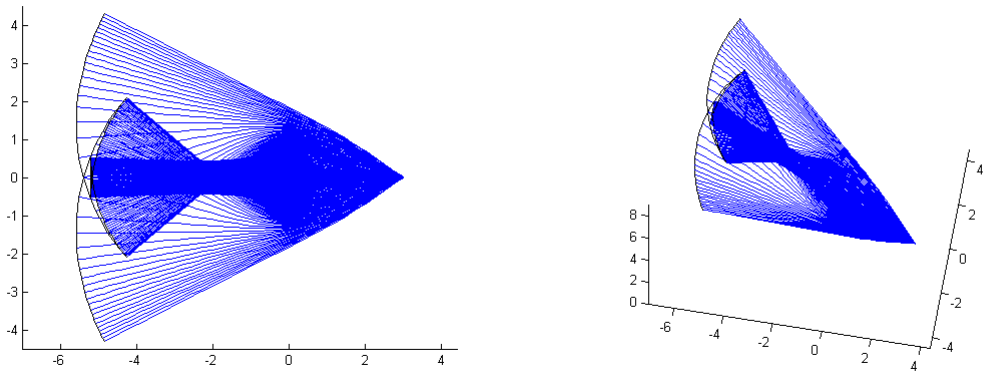

Figure 6.43: With y=0, x=3, t=9

on an axis of symmetry.

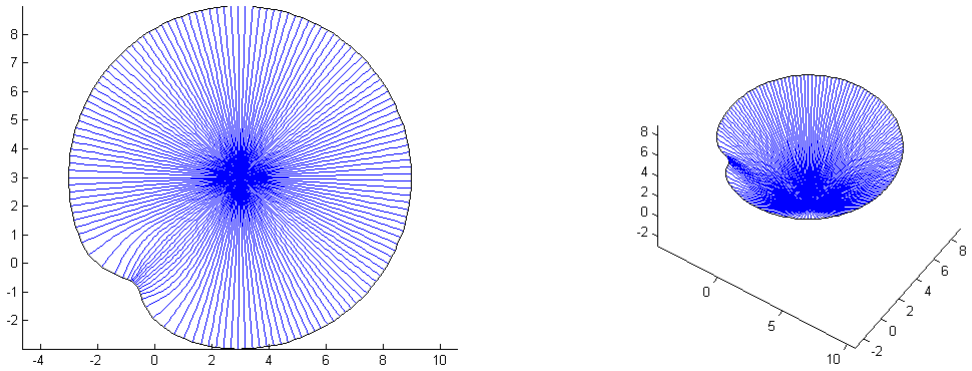

Figure 6.44: When x=3, y=3, t=6

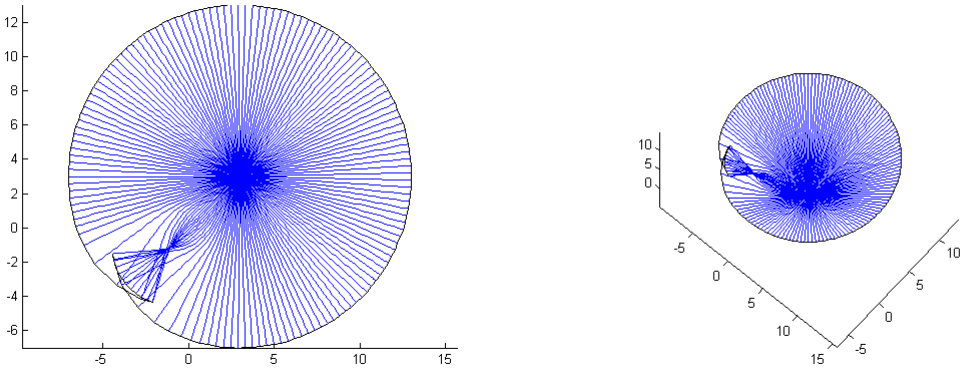

Figure 6.45: When x=y=3, t= 10

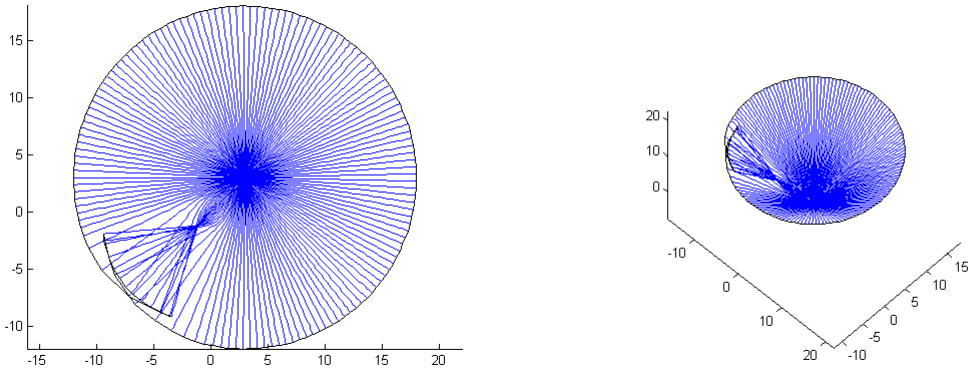

Figure 6.46: When x=y=3, t= 15

We see from these figures that the caustic on the light cone starting at $(3,3)$ has a qualitative development that is similar to the symmetric case, but is slightly different in detail.

6.5.2 Curvature

Because this metric is not radially symmetric, it is harder to analyse its behaviour than in the previous cases. However, we can see by inspection that for small x and y the curvature is positive, while for sufficiently large x and y it is negative, which suggests that the general behaviour should be similar to that of case study 1, but that the detailed structure of the light cones show be less symmetric. We consider the Gaussian curvature again. As before, we have an orthogonal coordinate system $F = 0$, so the Gaussian curvature K is still given by

$$K = (\frac{-1}{2})(EG)^{(\frac{-1}{2})}[(E_x(EG)^{(\frac{-1}{2})})_x + (G_y(EG)^{(\frac{-1}{2})})_y] \tag{6.52}$$

This time we have $E = 1 + e^{-x^2-y^4}$, $F = 0$ and $G = 1 + e^{-x^2-y^4}$, which eventually gives

$$K = -\frac{e^{x^2+y^4}\left(-6\,y^2e^{x^2+y^4} + 8\,y^6e^{x^2+y^4} + 2\,x^2e^{x^2+y^4} - e^{x^2+y^4} - 6\,y^2 - 1\right)}{\left(e^{x^2+y^4} + 1\right)^3} \tag{6.53}$$

This cannot be expressed as a function of r; however, we can still plot the curve $K = 0$ to see when it is positive and when it is negative.

This suggests that as in the first case study we will have light cones very much like those of Minkowski space as long as they stay away from the origin, but that light cones which pass through the origin will develop caustics in a similar way.

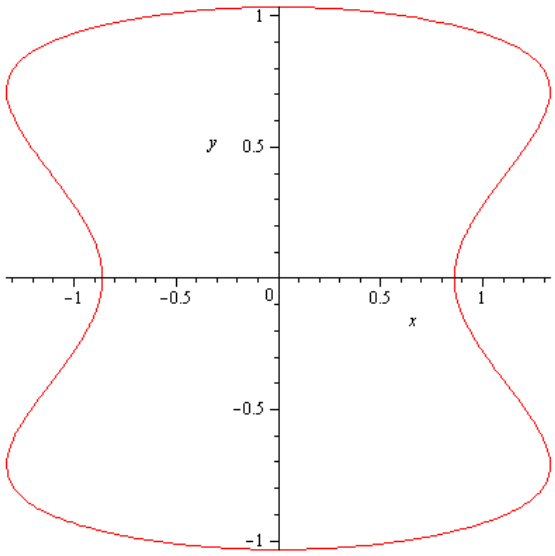

Figure 6.47: non-spherically symmetric curvature k

The resulting graph shows a roughly hourglass shaped region of positive curvature surrounding the origin, with negative curvature outside.

This confirms that the general pattern of conjugate points and caustics arising when the light cone passes through the region of positive curvature is preserved in its general structure, although the fine details depend on the shape of the region.

Chapter 7

Conclusions and Further Work

7.1 Summary and Conclusions

After providing a brief review of the relevant aspects of differential geometry, we concentrated on the development of Matlab code to assist in the visualisation of light cones in space-times of sufficiently high symmetry. Matlab was chosen because of the high quality of its numerical routines and graphical output, and also because there are free programs similar enough in structure to make the conversion of much of this work fairly straightforward, making it more widely available.

The use of conformal transformation to take a static space-time to a space-time whose metric is of the form

$$-dt^2 + g_{ab}dx^a dx^b \tag{7.1}$$

and whose null geodesics have t as affine parameter is central. This allows us to compute the null geodesics between two surfaces of constant t easily, whereas the use of the affine parameter in the original space-time would force us into additional work to know when to stop.

The first application was dedicated code for the investigation of Schwarzschild

space-time, which allowed the construction of light cones in the equatorial plane, and three-dimensional animations of the growth of the full light cone. This was then extended to allow the user to specify a metric as well as the point of origin of the light cone and the range and number of null geodesics to be considered.

The ability to choose the range and number of null geodesics used in the visualisation, and the speed of Matlab's differential equation solvers makes this a powerful interactive tool for the user to investigate aspects of the growth of light cones in (sufficiently symmetric, (2+1) dimensional) space-time. However, the user must still remain aware that coordinate distance can be substantially different from geometric distance, and take care in the interpretation of some aspects of the resulting figures.

7.2 Further Work

There are various ways in which the work described here might be extended.

First, there were various issues raised in some of the sample case studies which merit a more detailed investigation. A detailed study of the light cones in Reissner-Nordström space-time which collide with the central singularity would be interesting, as would a more careful study of the relationship between the curvature and the presence of conjugate points in the Ayon-Beato-Garcia metric.

A constraint in what has been done here is the restriction to space-times which are essentially (2+1) dimensional. Producing diagrams of the development of light cones in (3+1) dimensions, where more complicated types of caustic can develop would be desirable.

As was mentioned in Chapter 2, the geodesic equations are Hamiltonian in form. This means that they have considerable additional structure, which might be exploited in their numerical integration. It is well-known [34] that for separable Hamiltonian systems, there are symplectic numerical methods, such as the Verlet method,

which have desirable conservation properties, allowing the use of much greater time-steps without loss of accuracy. However, for non-separable Hamiltonians, the symplectic numerical integrators are generally implicit rather than implicit. It would be useful to investigate whether the gains made by using a symplectic method are more significant than the additional work required by the method being implicit.

The methods developed here should also be applicable to the development of wave-fronts in more general situations. The most obvious is the propagation of light in a material with a varying index of refraction: one could even argue that the work we have done amounts to modelling general relativistic space-times using a material with a non-constant index of refraction. But the code developed here could also be used to investigate, for example, the propagation of wave-fronts in an elastic membrane where the effective metric (or index of refraction) is determined by the density and elasticity of the membrane.

More ambitiously, one could attempt to generalise the first metric considered in Chapter 7 by having many regions of localised high curvature, and investigate the propagation of null geodesics and wave fronts in this situation: the question here is, to what extent would such a smooth geometry allow the modelling of diffusion processes?

Appendix A

Schwarzschild Matlab Code

A.1 Schwarzschild Matlab code 2-D code

```
function wave_front_s
%wave_front plots the development of the light cone from a
%user-specified point for a user-specififed amount of coordinate time.
%The function uses plane polar coordinates (r,phi)
%in the equatorial plane of Schwarzschild space.
clc
clf
hold on;
 obtain the parameters of the point and light cone.
T=input('Enter the evolution time period: ');
r=input('Enter the initial radial coordinate: ');
phi=pi/2;
% the spacelike part of the conformal Schwarzschild metric at the initial point
M=r^2/(r-2)*[1/(r-2) 0;0 r];
%initialise the directions which will be used to construct
```

```
%the light cone and the endpoints for the light cone as a vector;
infin=input('Enter the range of tangent directions you want to investigate: ');
ndirs=input('Enter the number of directions: ');
circle=linspace(infin(1),infin(2),ndirs);
%calculate the null geodesics emanating from (r,0) and
%their endpoints
% ep will be the locus of geodesic endpoints after time T
ep=[];
for theta=circle
   %express the initial vector in terms of polar coordinates
    v=[cos(theta) sin(theta)/r];
   %normalise to obtain a unit vector
    m=sqrt(v*M*v');
    v=v/m;
    %solve the geodesic starting at (r,phi) in direction theta
    [t,rphi]=ode45(@covdiff,[0,T],[r;phi;v(1);v(2)]);
    % plot the geodesic from (r,phi) with initial direction theta
    % comment this line out to plot only the locus of endpoints.
    plot3(rphi(:,1).*cos(rphi(:,2)),rphi(:,1).*sin(rphi(:,2)),t);
    %pick off the end point to plot the front at time T
    TP=rphi(length(t),:);
    TP=[TP(1),TP(2)];
    ep=[ep;[TP(1)*cos(TP(2)),TP(1)*sin(TP(2))]];
end

%plot the locus of the endpoints of the geodesics.
```

```
plot3(ep(:,1),ep(:,2),T*ones(size(ep(:,1))),'Color','black');
axis equal;
%plot the event horizon
colormap([1,0,0]);
[evX, evY, evZ]= cylinder(2, 30); evZ=evZ*T; mesh(evX,evY,evZ);
end
-----------------------------------------------
% calculate the covariant derivative of the tangent
function dy = covdiff(t,y)
  dy = zeros(4,1);
  dy(1)=y(3);
  dy(2)=y(4);
  dy(3)=(2*y(3)^2/(y(1)*(y(1)-2)))+((y(1)-3)*y(4)^2);
  dy(4)=(-2*(y(1)-3)*y(3)*y(4)/(y(1)*(y(1)-2)));
end
```

A.2 Schwarzchild Matlab code 3-D code

```
function W = wave_front_3d_s
%wave_front plots the development of the light cone from a
%user-specified point for a user-specififed amount of coordinate time
%in Schwazschild space with M=1.
%The function uses plane polar coordinates (r,phi)
%in the equatorial plane of Schwarzschild space
%and rotates the resulting curve to give the full wave front.
% clear the graphics display
clc
clf
% obtain the parameters of the point and light cone.
Ts=input('Enter the evolution time period: ');
r=input('Enter the initial radial coordinate: ');
% take phi=0 as default angular coordinate
phi=pi/2;
% calculate the conformal Schwarzschild metric at the initial point
M=r^2/(r-2)*[1/(r-2) 0;0 r];
%choose how many points to use to generate the wavefront
ndirs=input('Enter the number of geodesics to compute: ');
circle=linspace(0, 2*pi,ndirs);
%choose how many frames to have in the animation of wave
%front development
%frames=input('How many frames? ');
%calculate the null geodesics emanating from (r,0) and
%their endpoints
```

```
for k = 1:frames
  T=k*Ts/frames;
  % ep will be the locus of geodesic endpoints after time T
  ep=[];
  for theta=circle
    %express the initial vector in terms of polar coordinates
    v=[cos(theta) sin(theta)/r];
%normalise to obtain a unit vector
    m=sqrt(v*M*v');
    v=v/m;
%solve the geodesic starting at (r,phi) in direction theta
    [t,rphi]=ode45(@covdiff,[0,T],[r;phi;v(1);v(2)]);
%pick off the end point to plot the front at time T
    TP=rphi(length(t),:);
    TP=[TP(1),TP(2)];
    ep=[ep;[TP(1)*cos(TP(2)),TP(1)*sin(TP(2))]];
  end

  %build the 3d surface of revolution, with rots steps.
  x=ep(:,1);
  y=ep(:,2);
  rots=10;
  theta=linspace(0,2*pi,rots);
  X=kron(x,ones(size(theta)));
  Y=kron(y,cos(theta));
  Z=kron(y,sin(theta));
```

```
  colormap('white');
  surf(X,Y,Z);
  axis([r-Ts,r+Ts,-Ts,Ts,-Ts,Ts]);
 % axis([r-15,r+15,-15,15,-15,15]);
  axis square;
  alpha(0.7);
  W(k)=getframe;
 % movie(W(k));
end
end
-----------------------------------------------
% calculate the covariant derivative of the tangent
function dy = covdiff(t,y)
  dy = zeros(4,1);
  dy(1)=y(3);
  dy(2)=y(4);
  dy(3)=(2*y(3)^2/(y(1)*(y(1)-2)))+((y(1)-3)*y(4)^2);
  dy(4)=(-2*(y(1)-3)*y(3)*y(4)/(y(1)*(y(1)-2)));
end
```

Appendix B

General Code

B.1 Choose metric code

```
% This mfile allows the user to specify a metric, and computes
% the coefficients of the geodesic equations using the symbolic toolbox.
% Input the metric components in terms of coordinates x,y, with xd and yd
% being the first derivatives of x and y wrt the affine parameter.
syms x y xd yd
disp('Please select the metric coefficients E,F,G as functions of x,y so');
disp(' that the metric is Edx^2+2fdxdy+Gdy^2 ');
E=input('E =' );
F=input('F =' );
G=input('G =' );
% set up the metric
I=[E F; F G];
If = matlabFunction(I);
%compute the required derivatives
```

```
Ex=diff(E,x);

Ey=diff(E,y);

Fx=diff(F,x);

Fy=diff(F,y);

Gx=diff(G,x);

Gy=diff(G,y);

% construct the functions p,q such that ddx=p(x,y,dx,dy), ddy=q(x,y,dx,dy)

p= (1/(2*(E*G-F^2)))*((-G*Ex-F*Ey+2*F*Fx)*xd^2

+(- 2*G*Ey+2*F*Gx)*xd*yd+(G*Gx-2*G*Fy+F*Gy)*yd^2);

q= (1/(2*(E*G-F^2)))*((F*Ex+E*Ey-2*E*Fx)*xd^2

+(2*F*Ey-2*E*Gx)*xd*yd+(2*F*Fy-F*Gx-E*Gy)*yd^2);

xdd=matlabFunction(p);

ydd=matlabFunction(q);

%finally, make functions m-files containing all required functions.

Mf=matlabFunction(I,'vars',[x,y],'file','M');

xdd=matlabFunction(xdd,'vars', [x,y,xd,yd],'file', 'p');

ydd=matlabFunction(ydd,'vars', [x,y,xd,yd],'file', 'q');
```

B.2 Wave front general code

```
function wave_front_general
% wave_front_general calculates and displays the development of
% the light cone for a user-specified choice of cartesian or polar
% coordinates, time of evolution, initial point, range of
% directions and number of null geodesics.
% first, the user selects the background coordinate system.
test=-1;
while test~= 1 && test~=2
test= input('For cartesian coordinates enter 1
 and for polar coordinates enter 2:  ');
end
% use logical variable cartesian and polar to improve readability of code.
cartesian=test==1;polar=test==2;
% initialise graphics
clf
hold on;
axis equal;
% obtain the parameters of the initial point and light cone
T=input('Enter the evolution time period: ');
if cartesian
    x0=input('Enter the initial value of x: ');
    y0=input('Enter the initial value of y: ');
end
if polar
    x0=input('Enter the initial value of r: ');
```

```
    y0=input('Enter the initial value of phi: ');
end
%initialise the directions which will be used to construct
%the light cone and the endpoints for the light cone as a vector;
fprintf('Enter the range of tangent directions\n')
infin=input('you want to investigate in the form [start end]: ');
ndirs=input('Enter the number of directions: ');
circle=linspace(infin(1),infin(2),ndirs);
%calculate the null geodesics emanating from (r,0) and
%their endpoints
%ep will be the locus of geodesic endpoints after time T
ep=[];
 for theta=circle
   %express the initial vector in terms of the appropriate coordinates
   if cartesian v=[cos(theta),sin(theta)]; end
   if polar v=[cos(theta)*cos(y0)+sin(theta)*sin(y0),(sin(theta)*cos(y0)
   -cos(theta)*sin(y0))/x0];
    end
   %normalise to obtain a unit vector
   m=sqrt(v*M(x0,y0)*v');
   v=v/m;
   %solve the geodesic starting at (x0,y0) in direction theta
   [t,xy]=ode45(@pqode,[0,T],[x0;y0;v(1);v(2)]);
   %convert from polar to cartesian if necessary for plotting
   if polar
       xtemp=xy(:,1).*cos(xy(:,2)); ytemp=xy(:,1).*sin(xy(:,2));
```

```
        xy(:,1)=xtemp; xy(:,2)=ytemp;
   end;
   % plot the geodesic from (x0,y0) with initial direction theta
   % comment this line out to plot only the locus of endpoints.
   plot3(xy(:,1),xy(:,2),t)
   %pick off the end point to plot the front at time T
   TP=xy(length(t),:);
   ep=[ep;TP];
 end
%plot the locus of the endpoints of the geodesics.
plot3(ep(:,1),ep(:,2),T*ones(size(ep(:,1))),'Color','black');
```

Appendix C

References

Bibliography

[1] Weinberg S., *Gravitation and cosmology* , Oxford University Press, Cambridge, UK, 2010.

[2] Padmanabhan, T. *Gravitation Foundations and Frontiers*, Cambridge University Press, Cambridge, UK, 2010.

[3] Stewart, J. *Advanced General Relativity* , Cambridge University Press, Cambridge, 1993.

[4] Hobson, M. P. Lasenby, A. N.*General relativity: an introduction for physicists*, Cambridge 2006.

[5] Brickell, F. , Clark, R. S., *Differentiable Manifolds: An Introduction*, Van Nostrand Reinhold Company, 1970 .

[6] Adler,R., Bazin,M. , Schiffer M., *Introduction to general relativity*, New York, McGraw-Hill, 1975.

[7] Krishan L. Duggal, Dae Ho Jin *Null Curves and Hyper-surfaces of Semi-Riemannian Manifolds*, World Scientific 2007 .

[8] Vladimir G., Tijana T. *Complex Non-linearity: Chaos, Phase Transitions, Topology Change*, Springer- Verlag Berlin Heidelberg, 2008.

[9] Nicolaescu L. N. *Lectures on the Geometry of Manifolds*, World Scientific publishing , 1996.

[10] Plaue M., *Causality-Violating Lorentzian Manifolds Admitting a Shear-Free Timelike Flow*, Logos Verlag, Berlin, 2012.

[11] Hawking S.W. and Ellis G.F.R. *The Large Scale Structure of Space-Time*, Cambridge University Press, London, 1973.

[12] Wald R.M., *General Relativity*, University of Chicago Press, 1984.

[13] Geroch R., *General relativity from A to B* , University of Chicago, USA, 1978.

[14] Pressley A. *Elementary Differential Geometry*, Springer 2000.

[15] Penrose R., *Techniques of Differential Topology in Relativity*, University of London, 1972.

[16] Naber G.L. Geometry of Minkowski Space, Springer-Verlag, New York, 1992.

[17] Hughston K.P., *General Relativity*, Cambridge University Press, Cambridge, UK, 1994.

[18] Roberto B., Salgado. B.S., *Toward a Quantum Dynamics for Causal Sets*, State University of New York at Stony Brook, 1989.

[19] Minguzzi E., Sanchez M., *The causal hierarchy of spacetimes* in H. Baum and D. Alekseevsky (eds.), vol. *Recent developments in pseudo-Riemannian geometry, ESI Lect. Math. Phys.,* Eur. Math. Soc. Publ. House, Zurich, 2008

[20] Müller T. and Frauendiener J., *Studying null and timelike geodesics in the classroom*, Eur. J. Physics, **32** 2011, 747.

[21] Rindler W., *Special Relativity*, Clarendon Press, Oxford, UK, 1991.

[22] d'Inverno R. *Introducing Einstein's Relativity*, Clarendon Press, Oxford, UK, 1992.

[23] Taylor E.F. and Wheeler J.A. *Spacetime Physics*, San Francisco, 1992.

[24] Jerry B. Griffiths, Ji Podolsk *Exact Space-Times in Einstein's General Relativity*, Cambridge University 2009.

[25] Raychaudhuri A. K., Banerji S., Banerjee A. , *General Relativity, Astrophysics, and Cosmology*, Springer-Verlag New York 1992.

[26] Fabbri A. , *Modeling Black Hole Evaporation*, Imperial college 2005.

[27] O'Neill B. *Semi-Riemannian Geometry With Applications to Relativity*, Academic Press London 1983.

[28] Ashtekar A. , Cohen R. S., Shimony A. *Revisiting the Foundations of Relativistic Physics*, Kluwer Academic Publishers, 2003.

[29] Kuhnel W., *Differential Geometry: Curves - Surfaces - Manifolds*, Wiesbaden, 2003.

[30] Cotsakis S., Papantonopoulos E. , *Cosmological Crossroads: An Advanced Course in Mathematical, Physical*, Springer, 2001.

[31] Deza M. M., Deza E. *Dictionary of Distances*, Boulevard, Langford Lane, Kidlington, Oxford, 2006.

[32] Garćia A., Hackmann E., Kunz J., Lmmerzahl C., Macias A. *Motion of test Particles in a regular black hole space-time* , Submitted on 11 Jun 2013 (v1), last revised 5 Jul 2013 (this version, v2)).

`http://arxiv-web3.library.cornell.edu/abs/1306.2549v2 .`

[33] Gron O., Hervik S., *Einstein's General Theory of Relativity: With Modern Applications in Cosmology*, Springer Science, 2007.

[34] Hairer E. , *Geometric numerical integration illustrated by the StormerVerlet method* , Cambridge University Press, 2003.

Appendix D

Published work


JGSP **29** (2013) 53–63

JOURNAL OF
Geometry and Symmetry in Physics
ISSN 1312-5192

VISUALIZING LIGHT CONES IN SCHWARZSCHILD SPACE

TARIG ELMABROUK AND ROBERT J. LOW

Communicated by Gregory L Naber

Abstract. We present a numerical approach to the visualization of the light cones, and hence the causal structure, of exterior Schwarzschild space, taking advantage of the symmetries of Schwarzschild space and the conformal invariance of null geodesics.

doi: 10.7546/jgsp-29-2013-53-63

Figure D.1: copy of journal paper

VISUALIZING LIGHT CONES IN SCHWARZSCHILD SPACE

TARIG ELMABROUK & ROBERT J LOW

Communicated by Gregory L Naber

Abstract. We present a numerical approach to the visualization of the light cones, and hence the causal structure, of exterior Schwarzschild space, taking advantage of the symmetries of Schwarzschild space and the conformal invariance of null geodesics.

8

10

11